INFORMATION TO USERS

This manuscript has been reproduced from the microfilm master. UMI films the text directly from the original or copy submitted. Thus, some thesis and dissertation copies are in typewriter face, while others may be from any type of computer printer.

The quality of this reproduction is dependent upon the quality of the copy submitted. Broken or indistinct print, colored or poor quality illustrations and photographs, print bleedthrough, substandard margins, and improper alignment can adversely affect reproduction.

In the unlikely event that the author did not send UMI a complete manuscript and there are missing pages, these will be noted. Also, if unauthorized copyright material had to be removed, a note will indicate the deletion.

Oversize materials (e.g., maps, drawings, charts) are reproduced by sectioning the original, beginning at the upper left-hand corner and continuing from left to right in equal sections with small overlaps.

ProQuest Information and Learning
300 North Zeeb Road, Ann Arbor, MI 48106-1346 USA
800-521-0600

Université d'Ottawa • University of Ottawa

CYNO-EBV, A CYNOMOLGUS MONKEY EBV-LIKE VIRUS, AND ITS LATENT MEMBRANE PROTEIN 1 ONCOGENE

A Thesis Submitted to the
School of Graduate Studies and Research
University of Ottawa

In Partial Fulfillment for the Degree of
Doctor of Philosophy
Department of Biochemistry, Microbiology and Immunology
Faculty of Medicine

By
Sylvie Faucher

ABSTRACT

Epstein-Barr virus (EBV) and its oncogene, the latent membrane protein 1 (LMP1), are associated with many human malignancies. Likewise, EBV-like viruses have been associated with lymphomas in immunosuppressed cynomolgus monkeys. This study characterizes the biology of Cyno-EBV, a cynomolgus monkey EBV-like virus, including the structural proteins, antigenic relatedness to EBV and molecular and functional analysis of its LMP1 homologue.

Cyno-EBV infection is ubiquitous in its host species. *In vitro*, Cyno-EBV immortalized cynomolgus monkey but not human B cells. The electrophoretic profile of Cyno-EBV structural proteins was almost identical to that of EBV proteins, and cynomolgus monkey and human sera showed reciprocal reactivities for several of these proteins, including the EBV receptor binding protein gp350.

The coding region of the Cyno-EBV LMP1 gene was cloned and expressed. The sequence predicted a 588 amino acid (a.a.) protein with a 19 a.a. N-terminus, 6 transmembrane domains and a carboxy tail of 404 a.a. containing a 8-histidine cluster used as a natural protein tag in expression studies. Western blot analysis revealed a major polypeptide of 110 kDa. Cyno-EBV LMP1 contained series of repeats that shared no homology with other LMP1s. However, a proline-rich sequence $GPXXPX_6$ found within the 11 a.a.-repeats of EBV LMP1 was conserved in a non-repeat region of Cyno-EBV LMP1 and contained two Janus kinase (JAK) binding motifs PXXPXP. Cyno-EBV LMP1 harbored 4 motifs PXQXT/S, predicted to interact with TRAFs, adapter proteins of the tumor necrosis factor receptor signaling pathway, which lead to activation of the nuclear factor κB (NFκB). Cyno-EBV LMP1 shared the same ability as EBV LMP1 to

induce a NFκB driven reporter gene. An apparent increased toxicity of Cyno-EBV LMP1 for rodent Rat-1 cells impeded the establishment of LMP1 expressing cell lines whereas a reduced toxicity was observed for transiently expressing 293 cells when compared to EBV LMP1.

Cyno-EBV is structurally and antigenically closely related to EBV. Cyno-EBV LMP1 harbored several features and motifs found in EBV LMP1. New conserved sequences were reported including a histidine cluster and a proline-rich sequence encompassing two Janus kinase binding motifs. The increased numbers of TRAF motifs found in Cyno-EBV LMP1 did not result in increased ability to activate NFκB in 293 cells and as for EBV LMP1, the protein appeared to have specific cell type toxicity.

ACKNOWLEDGEMENTS

I wish to express all my gratitude to my supervisor, Dr. Kathryn E. Wright, for her constant support throughout the realization of this work. Her vision, guidance and patience have been instrumental in the success of this project. I am also deeply indebted to Francis Mandy and Michèle Bergeron, both friends and colleagues at Health Canada, who believed in me and in this work. Without their help, generosity and inestimable encouragement this work would not have been possible.

I also want to thank the members of my advisory committee, Dr Ken Dimock, Dr Eilleen Tackaberry and Dr Francis Diaz-Mitoma for their helpful directions.

I would like to thank Dr Koji Fujimoto, Dr Ken Dimock, Dr José Menezes, Dr Francis Diaz-Mitoma, Dr Fred Wang, Dr Elliott Kieff, Dr Jerry Tanner, Dr John Webb, Dr Earl Brown, and Dr Jo-Anne Dillon who provided expertise and/or reagents used in this project.

Warm thoughts to all the graduates, who sailed at my side. I was surrounded by a great crew who shared their good words and frustrations, a precious gift to keep things in perspective. Many thanks also to my colleagues at Health Canada whose friendship has brought joy and laughter throughout those years.

Close to my hearth is my family, who despite the distance, succeeded to keep me going. Their understanding and encouragement have been a source of motivation throughout this journey. I feel very privileged to be part of their lives.

With all my love.

I dedicate this thesis to the memory of Madeleine.

TABLE OF CONTENTS

ABSTRACT ii

ACKNOWLEDGEMENTS iv

TABLE OF CONTENTS v

LIST OF TABLES viii

LIST OF FIGURES AND ILLUSTRATIONS ix

INTRODUCTION 1

1. EBV
   - A. Virus structure 2
   - B. Genome organization 4
   - C. Replication 6
   - D. Lytic cycle 10
   - E. Latent cycle 13
   - F. Transforming ability 16
   - G. Association with human cancers 19
   - H. LMP1 25
     - (i) Molecular mechanisms of LMP1 interference with cell signaling 29

2. EBV-like viruses of non-human primates 38
   - A. Herpesvirus papio 38
     - (i) Antigenic and DNA homologies with EBV 39
     - (ii) Transforming and oncogenic properties 40
     - (iii) Latent genes 41
     - (iv) Herpesvirus papio LMP1 homologue 42
   - B. Cyno-EBV 43
     - (i) Antigenic and DNA homologies with EBV 44
     - (ii) Transforming and oncogenic properties 45

3. Rationale and objectives 46

MATERIALS AND METHODS

1. Cell lines and culture conditions 48

2. Virological methods
A. Preparation of virus stocks 48
B. Titration of virus stocks by transformation assays 49
C. Quantification of viral particles 50
D. Virus purification 50
E. Electronic microscopy of the shedding cell line 51

3. Immunological Assays
A. Immunofluorescence Assays 51
B. Flow cytometry analysis 52
(i) Intracellular detection of viral antigen 52
(ii) Viability studies 53

4. Protein analysis
A. SDS-PAGE 53
B. Western Blot analysis 53

5. Molecular biological methods
A. DNA and RNA isolation 54
(i) Plasmid DNA 54
(ii) Genomic DNA 56
(iii) RNA isolation 56
B. DNA manipulations and analysis
(i) Restriction and modification of DNA 56
(ii) Agarose and polyacrylamide gel electrophoresis 57
(iii) Southern analysis 58
(iv) Polymerase Chain Reaction 58
(v) Reverse Transcription 58
C. DNA sequencing 60

6. Gene Transfer and expression
A. Cell transfections
(i) Transient expression 60
(ii) Stable expression 60
B. Reporter gene assays
(i) CAT assays 62
(ii) β-galactosidase assays 63

RESULTS

1. Prevalence of Cyno-EBV infection among captive cynomolgus monkeys 64

2. Structural and antigenic analysis of Cyno-EBV 66

A. Electron microscopy of Cyno-EBV 66

B. Structural proteins of Cyno-EBV 66
C. Cynomolgus and human antibody cross-reactivities to EBV and Cyno-EBV 68
(i) Western Blot analysis of structural proteins 71
(ii) Viral lytic cycle antigens detected by IFA 76
(iii) Envelope protein gp350 and early antigen 77
(iv) Latent Membrane Protein 1 (LMP1) 80

3. Functional analysis 80

A. Transforming activity of Cyno-EBV 81
B. Cloning of EBV and Cyno-EBV LMP1 in pCR-Script™Amp SK(+) 85
C. Cloning the ends of Cyno-EBV LMP1 coding region 90
D. Nucleotide sequence of Cyno-EBV LMP1 region 93
E. Localization of Cyno-EBV LMP1 introns by RT-PCR 93
F. Predicted amino acid sequence 95
G. Expression of Cyno-EBV and EBV LMP1 in 293 cells 98
H. Induction of NFκB activity by Cyno-EBV LMP1 102
I. Toxicity of LMP1 in 293 cells 105
J. Establishment of EBV and Cyno-EBV LMP1 stable transfectants 107

DISCUSSION 111

CONCLUSION 125

REFERENCES 128

APPENDIX I 152

APPENDIX II 153

APPENDIX III 154

APPENDIX IV 155

APPENDIX V 156

APPENDIX VI 157

APPENDIX VII 158

LIST OF TABLES

	Page
TABLE 1. Lytic proteins of EBV	5
TABLE 2. Latent proteins of EBV	9
TABLE 3. Order of classification of primates	18
TABLE 4. List of primers for PCR of EBV and Cyno-EBV LMP1	59
TABLE 5. List of sequencing primers	61
TABLE 6. SDS-PAGE analysis of purified Cyno-EBV, EBV and H.papio	70
TABLE 7. Quantification of viral particles in Cyno-EBV and H. papio shedding cell line supernatants	84
TABLE 8. Induction of NFκB driven CAT activity by Cyno-EBV and EBV LMP1	104

LIST OF FIGURES AND ILLUSTRATIONS

		Page
FIGURE 1.	Diagram of an herpesvirus particle and its genome organization	3
FIGURE 2.	EBV cell cycle in B lymphocytes	7
FIGURE 3.	LMP1 cell signaling pathways	30
FIGURE 4.	Prevalence of Cyno-EBV infection among captive cynomolgus monkeys	65
FIGURE 5.	Electron micrograph of Cyno-EBV shedding cell line TsB-B6	67
FIGURE 6.	SDS-PAGE of the structural proteins of Cyno-EBV, EBV and H. papio	69
FIGURE 7.	Reactivity of cynomolgus serum antibodies with the structural proteins of Cyno-EBV	72
FIGURE 8.	Cross-reactivity of cynomolgus serum antibodies with the structural proteins of EBV and H. papio	73
FIGURE 9.	Cross-reactivity of human and cynomolgus monkey serum antibodies with EBV and Cyno-EBV structural proteins.	75
FIGURE 10.	Cross-reactivity of cynomolgus monkey serum antibodies with H. papio and EBV	78
FIGURE 11.	Cross-reactivity of EBV gp350 MAb and EA R3 MAb with Cyno-EBV	79
FIGURE 12.	Growth transforming titers of Cyno-EBV and H. papio with cynomolgus B cells	82
FIGURE 13.	Intracellular staining of Cyno-EBV and H. papio by Flow cytometry	86
FIGURE 14.	Agarose gel analysis of PCR amplified Cyno-EBV LMP1 (partial sequence)	88
FIGURE 15.	Agarose gel analysis of PCR amplified EBV LMP1 and restriction analysis of EBV LMP1 clone#29	89
FIGURE 16.	Determination of clonable size LMP1 fragments from Cyno-EBV viral DNA digests.	91

FIGURE 17.	PCR amplification of the full length Cyno-EBV LMP1 coding region.	92
FIGURE 18.	Nucleotide sequence of Cyno-EBV LMP1 region	94
FIGURE 19.	Predicted amino acid sequence of Cyno-EBV LMP1	96
FIGURE 20.	Flow cytometry detection of Cyno-EBV LMP1 and EBV LMP1 in transfected 293 cells	99
FIGURE 21.	Expression of Cyno-EBV LMP1 and EBV LMP1 in transfected 293 cells.	100
FIGURE 22.	Cellular growth and loss of cell adherence of human 293 cells transfected with Cyno-EBV LMP1/pcDNA3	106
FIGURE 23.	Viability and light scatter properties of LMP1 transfected 293 cells	108
FIGURE 24.	EBV LMP1 expression in Rat-1 stable transfectants	110
APPENDIX I	Localization of sequencing primers for Cyno-EBV LMP1	152
APPENDIX II	Kyte and Doolittle hydropathy plot of the predicted Cyno-EBV LMP1	153
APPENDIX III	Predicted amino acid sequence of Cyno-EBV LMP1 and multialignment with human and Rhesus-EBV LMP1s	154
APPENDIX IV	Predicted amino acid sequence of Cyno-EBV LMP1 and multialignment with human EBV and other EBV-like monkey viruses	155
APPENDIX V	TRAF binding motifs and their flanking sequences	156
APPENDIX VI	Conservation of the pattern $GPXXPX_6$ in human, rhesus and cynomolgus monkey LMP1s	157
APPENDIX VII	Multialignment of N-term. domains of LMP1 of Cyno-EBV, Rhesus-EBV, EBV and MyoD.	158

INTRODUCTION

1. EBV

Epstein, Achong and Barr were the first to report herpesvirus-like particles in a cell line established from a Burkitt's lymphoma biopsy (Epstein et al. 1964). This new herpesvirus was then called Epstein-Barr virus (EBV or Human Herpesvirus 4, HHV4). Only 2 types of EBV have been described to date, EBV1 and 2. They have different *in vitro* B cell transforming abilities and are associated with distinctive incidences of various types of lymphomas (Kieff 1996). These viruses have become the subject of extensive research targetted to their ability to immortalize B lymphocytes *in vitro* and their apparent association with cancer. The association of viruses with human cancers is not simple as tumors develop over a very long period and other infections or co-factors are often involved. For EBV, understanding the association with cancer presents an additional challenge since the infection is ubiquitous and the virus is present in 95% of the world population (Morgan 1995).

Throughout most of the world, primary infection with EBV usually occurs during the first years of life and is asymptomatic. In developed countries however, improved hygiene results in delayed exposure to the virus, so primary infections often occur in late childhood and early adulthood (Straus et al. 1993). In such cases, approximately 50% of newly infected children develop a condition known as infectious mononucleosis (IM) (Ring 1994). The most common symptoms of IM include sore throat, malaise, headache accompanied by lymphadenopathy, pharyngitis and fever. The illness usually resolves within weeks, and complications, such as severe hemolysis, airway obstruction or splenic rupture, are rare but have been reported (Straus et al. 1993).

In immunocompromised individuals EBV infection leads to uncontrolled growth of infected B lymphocytes and can lead to lymphoproliferative diseases and B cell lymphomas. Burkitt's lymphoma (BL), undifferentiated nasopharyngeal carcinoma (NPC) and some forms of Hodgkin's lymphoma have all been associated with EBV infection. As technology refines the viral detection assays. EBV is being linked to an increasing number of cancers thereby creating strong incentive for the development of an EBV vaccine. The need for an anti-EBV intervention as been reinforced by the more recent worldwide spread of the human immunodeficiency virus (HIV). The immunodeficiency conditions triggered by HIV infection have generated additional cases of EBV-associated neoplasms.

A. Virus structure

EBV viral particles share the typical morphology of other herpesviruses: an icosahedral capsid with a diameter of 100-110 nm. surrounded by a proteinaceous tegument and an envelope (Figure 1A). The complete virion size varies from 120 to 200 nm in diameter and the particles are often of irregular shape due to the uneven thickness of the tegument around the capsid. The nucleocapsid is composed of 162 capsomers and contains a double-stranded viral DNA associated with a dense protein core. The virion's envelope has spikes on its outer surface composed mainly of the glycoprotein gp350/220. Gp350 and gp220 are generally found in equivalent amounts. Both glycoproteins originate from the same gene but gp220 is derived from spliced RNA. Other proteins such as the gp85 and a heavily glycosylated protein of 55-80 kDa have also been described as components of the viral membrane (Morgan 1995). The major components of the capsid are 160, 47 and 28 kDa proteins and the most abundant tegument protein is

Figure 1. Diagram of an herpesvirus particle and its genome organization

A. Diagram of the major structural components of EBV. The virion is composed of an icosahedral capsid of 100-110 nm in diameter surrounded by a proteinaceous tegument and an envelope. The virion size varies from 120-200 nm in diameter. The virus carries a double-stranded DNA (172 kb) associated to a dense protein core. The virion's envelope spikes are composed mainly by the glycoprotein gp350/220. Other proteins such as the gp85, involved in viral fusion with cellular membrane and a heavily glycosylated protein of 55-80 kDa are also found in the envelope.

B. Representation of the 172 kb EBV genome with depiction of the unique short (U_S) and long (U_L) regions and internal (IR) and terminal repeats (TR). Below is a BamHI digestion map of the EBV B95-8 prototype strain genome. The letters corresponding to the various restriction fragments are used to define the ORFs (see text).

Diagrams of the genome were adapted from (Kieff 1996; Morgan 1995)

A.

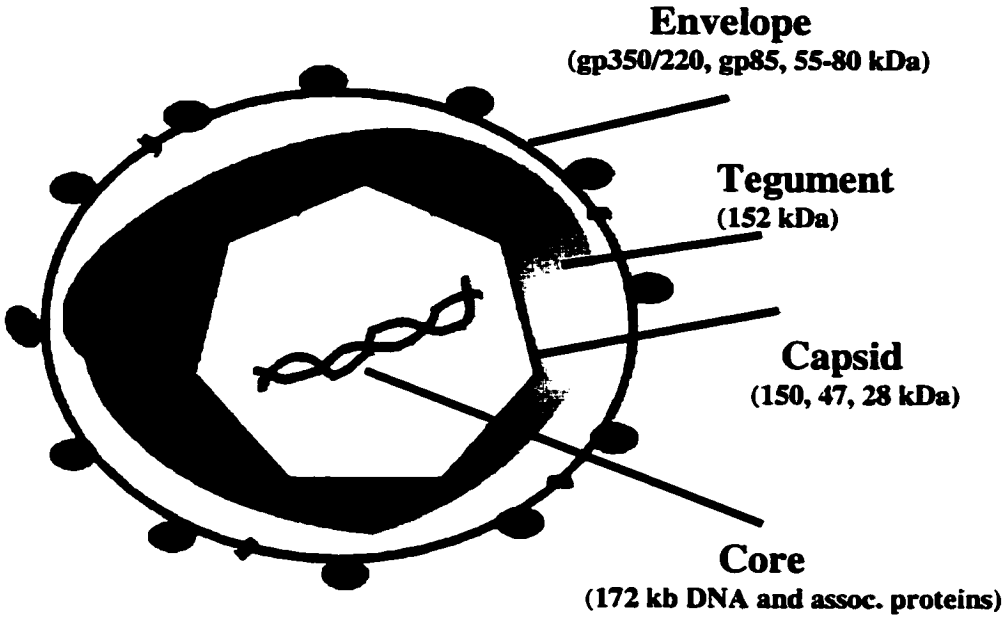
Envelope
(gp350/220, gp85, 55-80 kDa)
Tegument
(152 kDa)
Capsid
(150, 47, 28 kDa)
Core
(172 kb DNA and assoc. proteins)

B.

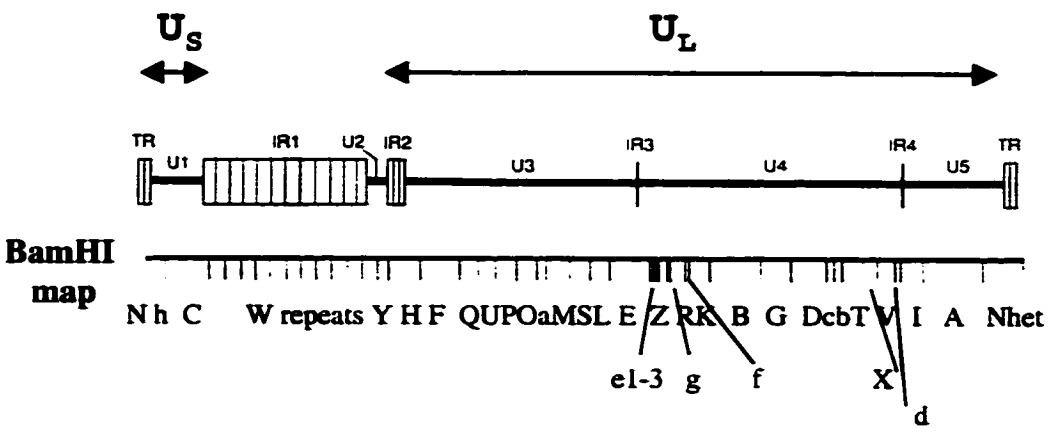
U_S
U_L
TR
U1
IR1
U2
IR2
U3
IR3
U4
IR4
U5
TR
BamHI map
N h C W repeats Y H F QUPOaMSL E Z RK B G DcbT V I A Nhet
e1-3
g
f
X
d

a 152 kDa protein (Kieff 1996). A list of known structural antigens of EBV is included in Table 1.

B. Genome organization

Twenty years after the isolation of the virus, Baer and collaborators (Baer et al. 1984) published the complete EBV genomic DNA sequence using an IM derived EBV strain B95-8 (Blacklow et al. 1971; Miller et al. 1972). The virus genome is composed of 172 282 nucleotides and contains approximately 100 open reading frames (ORFs) which encode 80 or so proteins. Since EBV DNA had been sequenced from a series of clones containing one of the 45 fragments of genomic DNA generated from digestion with the restriction enzyme BamHI, the ORFs are referred to by their corresponding BamHI fragment using a five digit code: BNLF1, then refers to the first ORF (F1) located in the BamHI fragment N. The middle letter L or R indicates the orientation, leftward or rightward, of transcription. The viral DNA (Figure 1B) contains 0,5 kbp terminal repeats (TR) at both ends that allow the genome to circularize to form an episome during replication. A succession of 3-kbp repeated sequences, called internal direct repeats (IR1), are found along the genome. These have been used to divide the genome into short and long unique domains (U_S and U_L) (Figure 1B). However, repetitive sequences are also scattered along these "unique" sequences, some of which also encode repetitive domains in viral proteins. These repetitive sequences are useful markers for EBV typing, as a given strain tends to keep the same number of reiterations through serial passage, and fresh tissue viral isolates often express differences in their repeat numbers (Kieff 1996).

TABLE 1. Lytic Proteins of EBV

Immediate early proteins	**ORF**	**M.W. (kDa)**
Z or ZEBRA	BZLF1	38
R	BRLF1	
Early proteins		
nuclear protein	BS/MLF1	44
dUTPase	*BLLF3*	*32*
alkaline exonuclease	*BGLF5*	
thymidine kinase	*BXLF1*	
DNA polymerase	BALF5	
major DNA binding protein	*BALF2*	*p135*
LMP1 lytic	BNLF1	45
bcl-2 homologue (restricted EA complex)	BHRF1	17
ribonucleotide reductase subunit	*BORF1*	*140*
ribonucleotide reductase subunit	*BaRF1*	*38*
nuclear protein	BMRF1	47
Serine/Threonine protein kinase	BGLF4	52
Late proteins		
major capsid protein	BcLF1	p150
IL10 homologue	BCRF1	~17
gB homologue (non-virion, ER assoc.)	*BALF4*	*gp110*
envelope glycoprotein	BILF2	p28 (55-80)
gH homologue	*BXLF2*	*gp85*
(fusion, virion and plasma membrane)		
basic core protein by homol. to VZV	BXRF2	
CD21 ligand (virion/plasma membrane)	BLLF1	340/220
gp42	BZLF2	42 and 38
gL homologue	*BKRF2*	*25*
tegument or membrane protein	BNRF1	140
virion and plasma membrane protein	BDLF3	gp35/42 (100-150)
capsid protein	BDRF1	40
capsid protein	BFRF3	21 (23/18)

Proteins in italics were identified by homology with Herpes Simplex Virus
Compiled from (Chen et al. 2000; Dawson et al. 1998; Kurilla et al. 1995; Li et al. 1995; Mackett et al. 1990; Morgan 1995; Nolan and Morgan 1995; Oba and Hutt-Fletcher 1988; Pulford et al. 1995; Sanchez-Pinel et al. 1991; Serio et al. 1997; Tanner et al. 1997)

C. Replication

EBV transmission occurs via the oral route and its main target cells in the oropharynx are epithelial cells and infiltrating B lymphocytes, where the virus sustains a productive infection and sheds in the oral cavity. This shedding fulfills EBV's need for horizontal transmission. After replication in the oropharynx, the virus spreads to the draining lymph nodes through circulating B cells. In the circulation, EBV is found only in B lymphocytes. During the acute phase of infection, at least 1 in 10^4 circulating B lymphocytes, are EBV infected. These infected B cells have the capacity to spontaneously proliferate *in vitro*. Immunocompetent individuals control this proliferation of EBV infected B cells but never clear the virus. The viral reservoir of EBV is long lived memory B lymphocytes (Babcock et al. 1998; Miyashita et al. 1997). In healthy EBV carriers, less than 1 in 10^5 or 10^6 peripheral B lymphocytes are EBV infected (Kieff 1996; Straus et al. 1993) and in these cells, the virus is mainly latent, that is, it expresses only a limited number of its proteins and does not replicate or generate viral progeny. For years B cells and epithelial cells were thought to be the only tissue for EBV infection. However, in rare cases, EBV is detected in T cells and in some T cell lymphomas therefore indicating that the virus is not strictly targetted to B/epithelial cells (Gaffey and Weiss 1992; Suzushima et al. 1995).

At this time it is not clear if B cells or epithelial cells are the earliest target cells at the onset of infection (Rickinson and Kieff 1996). Virus entry into cells is best understood for B cells (Figure 2). The virus enters B cells via interaction of its major envelope protein gp350/220 with cellular CD21, the C3d complement receptor followed

Figure 2. EBV cell cycle in B lymphocytes

The virus enters B cells via interaction of its major envelope protein gp350/220 with cellular CD21, the C3d complement receptor followed by internalization of the viral particles into cytoplasmic vesicles. The virus and vesicle membranes then fuse, a phenomenon involving viral gp85, leading to the release of the nucleocapsid and tegument into the cell cytoplasm. Once in the cytoplasm, the tegument proteins are shed as the capsid migrates toward the nucleus, a process thought to involve the cytoskeleton. The viral DNA is then translocated to the nucleus where transcription and replication occur. Once in the nucleus, both ends of the linear viral DNA join to form an episome which is replicated and passed on to daughter cells. From there, the virus proceeds toward the generation of new viral particles (lytic infection) or latent infection. In latent infection, viral particles are not formed and the virus only expresses a limited number of its genes.

Data in this diagram were derived from (Griffiths and Rottier 1992; Kasamatsu and Nakanishi 1998; Kieff 1996; Li et al. 1997)

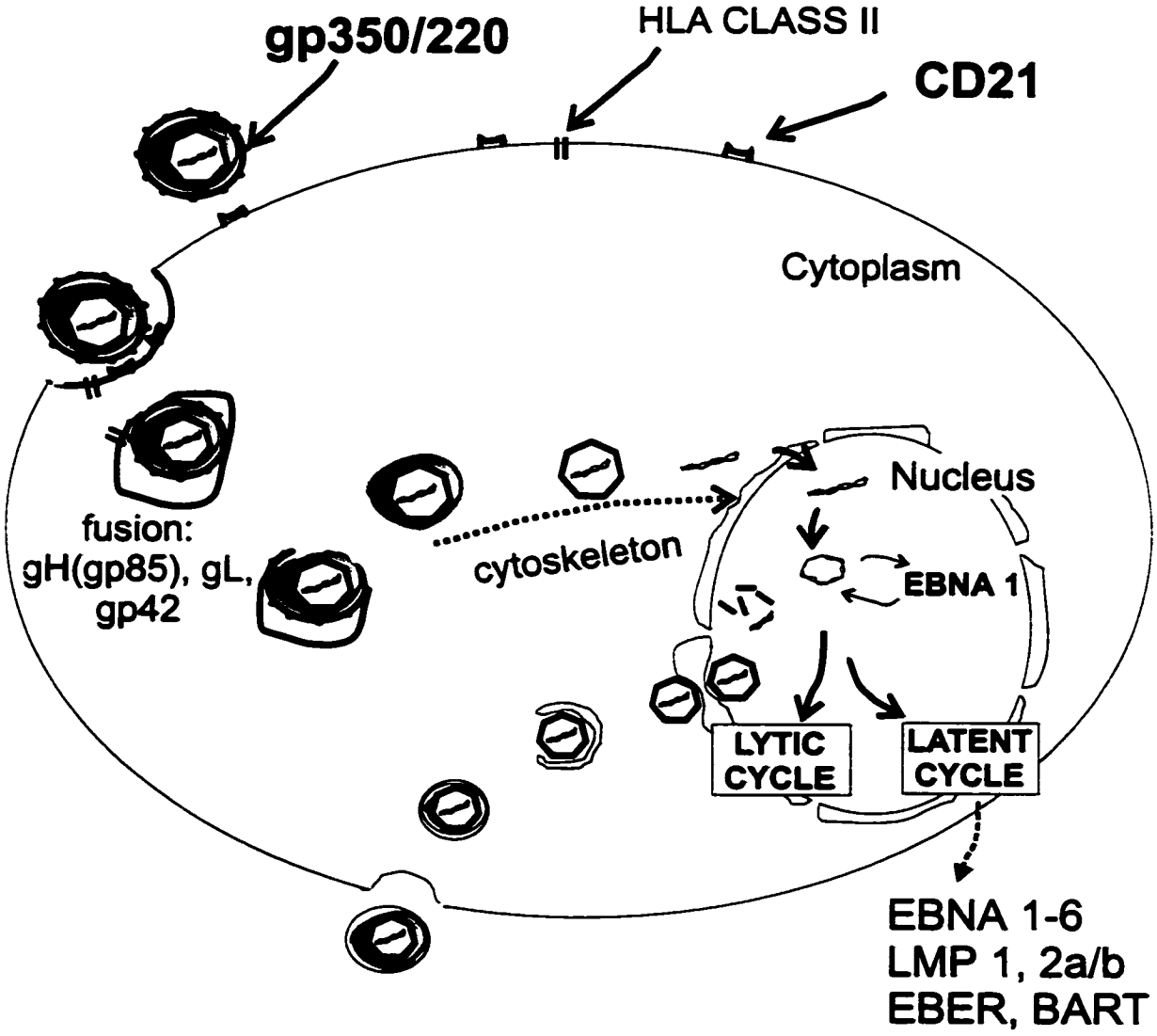
gp350/220
HLA CLASS II
CD21
Cytoplasm
Nucleus
fusion:
gH(gp85), gL,
gp42
cytoskeleton
EBNA 1
LYTIC
CYCLE
LATENT
CYCLE
EBNA 1-6
LMP 1, 2a/b
EBER, BART

by internalization of the viral particles into cytoplasmic vesicles. The virus and vesicle membranes then fuse, a phenomenon involving viral gp85, leading to the release of the nucleocapsid and tegument into the cell cytoplasm. Infection of epithelial cells has been documented but the mechanism of entry remains a subject of debate. CD21 expression has been demonstrated in epithelial cell lines but the demonstration of CD21 expression on normal eptithelial cells has been difficult due to the presence of contaminating B lymphocytes in the tissue (Rickinson and Kieff 1996). Several mechanisms of entry into epithelial cells have been proposed and include binding to epithelial cell CD21, cell-to-cell fusion with infiltrating B cells (Imai et al. 1998) and interaction with polymeric IgA receptors (antibody assisted entry) (Sixbey and Yao 1992; Sugden 1992). Once in the cytoplasm the tegument proteins are shed as the capsid migrates toward the nucleus. The viral DNA is then translocated to the nucleus where transcription and replication occur. The cytoskeleton is likely to be involved in the transport of the capsid to the nucleus as a disorganized microtubule network prevents transport to the nucleus (Kasamatsu and Nakanishi 1998). Shortly after entry into the nucleus, both ends of the linear viral DNA join to form an episome which is maintained, replicates and is passed on to daughter cells. The episome is formed before or as the earliest viral genes are expressed (Kieff 1996). From there the virus has two options, it can proceed toward the generation of new viral particles (lytic infection) or it can restrict its gene expression to only a special set of proteins, called the latent proteins (Table 1 and 2). In latent infection, viral particles are not formed as the virus only expresses a limited number of its genes. The latent genes are unique to EBV; no such proteins are found in other herpesvirus. One of these, called

TABLE 2. Latent Proteins of EBV

Protein	ORF	M.W. (kDa)
Latent Cycle		
EBNA1	BKRF1	65-85
EBNA2	B W/Y/H RF1	86
EBNA3 (EBNA3a)	BERF1, BLRF3	140-157
EBNA4 (EBNA3b)	BERF2a/b	148-180
EBNA5 (EBNA LP)	BW spliced	46
EBNA6 (EBNA3c)	BERF3/4	160
LMP1	BNLF1	58-63
LMP2a	BNLF2a/b	53
LMP2b	BNLF2b	

Compiled from (Kieff 1996; Morgan 1995; Ricksten et al. 1988)

EBNA1 is essential and sufficient for viral episome maintenance and replication. The selection of the latent or lytic cycle appears to be determined by cellular transcription factors (Miller 1990; Schwarzmann et al. 1998).

D. Lytic cycle

Although both B lymphocytes and epithelial cells can sustain lytic infection, the epithelial cells are thought to be responsible for the shedding of EBV in the oral cavity. Circulating B cells had been associated mainly with latent infection. However recently, oropharyngeal infiltrating B cells were shown to contain lytic viral antigens suggesting that these cells could also contribute to shedding of viral progeny (Tao et al. 1995).

There is no epithelial cell culture system available that allows the study of lytic infection in these cells, so lytic infection has been studied by inducing the lytic cycle in latently EBV infected B cells (Rickinson and Kieff 1996). This can be done using stimulation of the cells with a chemical such as phorbol ester. This induction is likely to act through the activation of protein kinase C. A second approach to lytic cycle induction involves the infection of the latently EBV infected cell line, RAJI, with the growth transformation deficient EBV strain, P3HR1 (Menezes et al. 1975). RAJI is a Burkitt's lymphoma derived cell line harboring an EBV genome with at least two deletions preventing viral replication and late gene expression, while P3HR1 is missing the EBNA2 and part of the EBNA 5 gene. P3HR1 infected RAJI cells proceed to the lytic cycle.

During productive infection, immediate early viral genes are the first to be expressed and do not require the synthesis of new proteins. The products of the BZLF1, BRLF1 and BI'LF4 ORFs constitute immediate early genes. They encode proteins that

act as transactivators for the early genes. BZLF1 also acts as a switch from latency to lytic cycle (Grogan et al. 1987) and might favor this transition by downregulating the latent protein EBNA Cp promoter (see below). These immediate early proteins upregulate the expression of other genes by binding to specific DNA sequences, called responsive elements, usually located upstream of the gene to be activated. A second domain of the transactivator, called the transactivating domain, is then responsible for bringing the transcription machinery into the proximity of the gene to be transcribed. Early genes are a set of viral genes expressed shortly after the immediate early genes and their expression is independent of viral DNA synthesis. Some of the described early genes are BHLF1, BHRF1, BSMLF1, BALF2 as well as a series of early RNAs within the DR and DL regions. A total of approximately 30 mRNA species are believed to constitute the pool of early genes. Many of those encode for enzymes involved in viral DNA replication (Table 1).

The next event is DNA replication. In lytic infection, the number of viral episomes first increases then viral DNA replication appears to occur in the form of large linear concatemers. These undergo cleavage before packaging into nucleocapsids (Kieff 1996). The last genes to be expressed are the late genes and their expression is clearly affected when viral DNA synthesis is blocked. Another 30 or so (Hummel and Kieff 1982; 1982) mRNAs have been described as late genes, many of which code for structural proteins (Morgan 1995). Among them the best characterized is the viral receptor, gp350/220, encoded by the BLLF1a/1b ORF. The transcript possesses an alternative initiation site located downstream of the first one and which generates the smaller form of the protein. Gp85, encoded by the BXLF2 ORF is the homologue of

HSV-1 gH, a protein involved in the cell-virus fusion process along with gL (Kieff 1996). The EBV homologue of HSV-1 gL is a 25 kDa glycoprotein encoded by the ORF BKRF2. The gp85/gp25 complex associates with a third glycoprotein, the BZLF2 gp42, recently described as an important protein in the fusion of EBV to B cells (Wang and Hutt-Fletcher 1998). A 110 kDa glycoprotein is encoded by the ORF BALF4 and represents the homolog of HSV-1 gB. Gp110 is not found in the virion and is associated with the endoplasmic reticulum in infected cells. The product of the BILF2 ORF, a 55-80 kDa glycoprotein, is found in purified preparations of EBV. The BDLF3 ORF, a 100-150 kDa glycoprotein, is recognized by serum antibodies of normal EBV seropositive individuals (Nolan and Morgan 1995). A 140 kDa protein, probably encoded by the BNRF1 ORF, was identified and may be part of the virion tegument (Kieff 1996). The major nucleocapsid protein is a 150kDa protein, encoded by the ORF BcLF1.

Beside the lytic genes, two latent genes, LMP1 and EBNA1, are also expressed during lytic infection (Kieff 1996). The presence of EBNA1 is not surprising in view of its role in maintenance and replication of the episomal DNA. The LMP1 gene, expressed as a 63 kDa protein in latently infected cells, is also translated from a second initiation site during lytic infection. The second start site, located between the fourth and the fifth transmembrane domains, gives rise to a 45 kDa protein, whose function in lytic infection is unknown.

To assemble new virions, the newly synthesized capsid constituents are assembled in the nucleus and newly formed capsids bud from the nuclear membrane (Kasamatsu and Nakanishi 1998). It has been postulated that the viral particles first bud from the nucleus inner membrane and then fuse with the outer membrane, a process that

would release the naked capsids into the cytoplasm (Griffiths and Rottier 1992). A later envelopment would take place in the region of the Golgi complex.

E. Latent cycle

In B cells, EBV infection is mostly latent and recent reports suggest that memory B cells are the actual site of the virus persistence (Babcock et al. 1998; Miyashita et al. 1997). These B cells, as a result of viral gene expression, have acquired the ability to spontaneously proliferate, and can divide indefinitely *in vitro*. This B cell immortalization feature has been instrumental in providing continuous cell lines for the study of numerous other viral systems. *In vivo*, this cell proliferation is kept under control by the individual's cellular immune system. However, EBV life long persistence is possible because of restricted viral gene expression thereby escaping surveillance from the immune system. Only 10-12 genes out the 80 or so contained in the EBV genome are considered to be "latency genes". Six of these encode nuclear antigens (EBNA1, 2, 3a, 3b, 3c, LP also called EBNA 1 to 6) and 2 encode the 3 latent membrane proteins LMP (LMP-1, 2a and 2b). The LMP2 proteins, formerly called terminal proteins 1 and 2, are encoded by the same gene but LMP2a possesses one additional exon. Other genes are transcribed into RNA without translation to a final protein. Two of these code for 2 short RNAs (EBER1 and EBER2) and others located in the BamHI A region generate RNA transcripts one of which appears to be translated to the protein, RK-BARF0 (Fries et al. 1997).

One of the functions of EBNA1 is to enable replication of the episomal DNA by binding to a 1.8 kbp region called the episomal origin of replication, OriP. EBV DNA forms an episome shortly after entering the cell nucleus and rarely integrates into cellular

DNA. The episomal form is also efficiently passed on to daughter cells through interaction of EBNA1 with the cell chromosomes (Lee et al. 1999; Mackey and Sugden 1997; Morgan 1995). EBNA1 is unique among EBV encoded proteins in that it does not induce cytotoxic T cell responses and thereby remains invisible even in immunocompetent individuals (Levitskaya et al. 1997). EBNA2 is essential for growth transformation of B cells as illustrated by the fact that the EBNA2 mutant strain P3HR1 cannot immortalize B cells *in vitro*. EBNA 2 also acts in the transactivation of both cellular and viral genes. CD23, a B-cell activation marker expressed shortly after antigen or mitogen stimulation of B cells (Wang et al. 1987a), as well as LMP1 and 2 expression are driven by EBNA2 binding to the cellular DNA-binding protein CBF1. The latter transactivator upregulates gene expression through binding to CBF1 responsive elements located in transcription regulatory regions of CD23 and LMP genes. Among the EBNA3s, EBNA3C (EBNA6) also contributes to the upregulation of cellular gene expression, in this instance, CD21, the EBV cellular receptor. EBNA3A and EBNA3C (EBNA3 and 6) were shown to be essential for B cell growth transformation whereas EBNA3B (EBNA4) appeared not to be (Kieff 1996). EBNA LP (or EBNA5) seems also to have a role in B cell growth transformation by upregulating cellular growth factors as reported by Mannick et al. (1991) who showed that cultures of B cells transformed by an EBV recombinant expressing a mutated form of EBNA LP required the presence of feeder cells for growth. This protein has also been shown to form complexes with the tumor suppressor molecule p53 and Rb thereby suggesting a role in transformation through alteration of p53 and Rb functions. However such a role is unclear as others reported that this interaction was indirect and mediated via heat-shock proteins (Neil et

al. 1997). The genes encoding EBNA LP, as well as EBNA 2, 3A, 3B and 3C differ in type 1 and type 2 EBV which have different abilities to transform B cells *in vitro*. The EBER transcripts are small uncapped and non-polyadenylated RNAs of 167 and 172 bp in length. Their function is unclear but their association with polyribosomes and the ribosomal protein L22 suggest a role in the translation process (Greifenegger et al. 1998).

The last group of latent proteins is not restricted to nuclear expression. LMP1 is found in the plasma membrane and has been shown to co-localize with vimentin suggesting an association with the cell cytoskeleton (Liebowitz et al. 1987). Transfection studies have shown that LMP1 induces the expression of various cellular genes including, B cell activation markers (CD21, CD23), adhesion molecules (CD54, LFA-1, LFA-3) (Peng and Lundgren 1993; Wang et al. 1990b) as well as bcl2 and vimentin (Birkenbach et al. 1989; Henderson et al. 1991) (see below). It is unique among all the latent genes since on its own, it induces growth transformation and tumorigenic properties in rodent fibroblasts. LMP2s, like LMP1, form patches in the plasma membrane and interfere with B-cell receptor signaling pathways through interaction with protein kinases (Kieff 1996). LMP2A also interacts with protein kinases in epithelial cells although different protein kinases are affected in epithelium (Csk kinases) and B cells (Src kinases) (Scholle et al. 1999).

In EBV associated tumors and transformed B cells, 3 types of viral latency have been defined according to the viral genes expressed. Latency III is characterized by the expression of the 6 EBNA proteins under the control of the promoter Wp/Cp, expression of LMP1, 2a and 2b as well as two untranslated RNA transcripts EBER1/2 and the RNA transcripts from the BamHI A. This pattern of expression is typical of lymphoblastoid

cell lines and is also found during the acute phase of infection in individuals with infectious mononucleosis (IM). Such cells are cleared by the individual immune response. In latency II, the promoters Wp/Cp are inactivated through methylation (Paulson and Speck 1999) and the expression of the EBNAs is shutdown with the exception of EBNA1. Another promoter, Qp, which is protected from methylation, then controls EBNA1. Qp driven EBNA1 results in a 5' truncated form of EBNA1 transcripts. Other genes expressed in latency II are the LMPs, EBERs and BamHI A transcripts. This pattern is found in nasopharyngeal carcinoma cells and also in EBV positive Hodgkin's Disease (HD) Reed-Sternberg (HRS) cells. Latency I, characteristic of Burkitt's lymphoma cells, is defined as cells expressing only EBNA1, under the Qp promoter, the EBER and BamHI A transcripts with their encoded protein, RK-BARF0, but not the LMPs. Recently, latently infected B cells of healthy EBV carriers were shown to consistently express LMP2a mRNA (Miyashita et al. 1997) and Qp driven EBNA1 (Rickinson and Kieff 1996). A new nomenclature has been proposed to include this new latency pattern (Thorley-Lawson et al. 1996). Growth latency would include the previously named latencies II/III whereas latency alone would correspond to the viral pattern seen in resting B cells. These patterns are distinguished by the presence or absence of growth promoting genes such as LMP1 and EBNA2 (found in type II/III but absent in resting B cells) rather than on specific viral gene expression. The type I latency would fall in a different category called EBNA1-only latency.

F. Transforming ability

In vitro, EBV has growth transforming ability for normal human B lymphocytes leading to continuous proliferation of the cells or immortalization. These lymphoblastoid

cell lines are polyclonal, clone poorly in agarose and do not induce tumors when injected s.c. into nude mice. The cells are diploid and do not show abnormal karyotype. This is contrasting with cells derived from Burkitt's lymphoma, which are monoclonal, clone well in agarose, are tumorigenic in nude mice and carry a translocated c-myc gene (Ernberg et al. 1983).

For many years, EBV was thought to transform lymphocytes from New World monkeys (Platyrrhine monkeys) and apes but not from Old World monkeys (Catarrhine monkeys) (Table 3). Extensive studies of non-human primate lymphocyte transformation by EBV conducted by Ishida and Yamamoto (1987) showed that lymphocytes from some species of the Old World monkeys could actually be transformed by the EBV strain B95-8. B cells from almost all species of Colobinae tested (5/6, from 2 genera) were transformed by EBV whereas cells from only one species (Patas monkeys) out of the 16 Cercopithecinae species tested were transformed. Lymphocytes from all ape species (5) tested but none of the New World monkeys (7 species) and prosimians (3 species) were transformed. Others have also demonstrated the ability of EBV to transform lymphocytes from gibbons (apes) (Werner et al. 1972). The results of Ishida and Yamamoto (1987) on the inability of EBV to transform lymphocytes of New World monkeys have been contradicted by several other groups who have demonstrated the transformation of lymphocytes from squirrel, tamarins, cebus and owl monkeys by EBV (Ablashi et al. 1979; Deinhardt et al. 1974; Falk et al. 1974; Miller et al. 1972).

Table 3. Order of classification of primates

Suborder Prosimii ("early" or pre-monkeys)
Prosimians
Lemuriforms: Lemurs, Indris, and Aye-aye
Lorisiforms : Pottos, Galagos and Lorises (Bushbabies)
Suborder Anthropoidea ("human-like")
Anthropoids

New World Monkeys (Platyrrhines)	
Families / Genus and Species	Common Names
Callitrichidae	
Callithrix spp.	Marmosets
Saguinus spp.	Tamarins
Cebuella pygmaea	Pygmy marmoset
Cebidae	
Aotus spp.	Owl monkeys
Saimiri spp.	Squirrel monkeys
Cebus spp.	Capuchin monkeys
Ateles spp.	Spider monkeys

Old World Monkeys (Catarrhines)	
Families / Genus and Species	Common Names
Cercopithecidae	
Cercopithecinae	
Cercopithecus spp. (Guenons)	African green monkeys
Erythrocebus Patas	Patas monkeys
Cercocebus spp.	Mangabeys
Macaca spp. (Macaques)	
M. fascicularis group	Cynomolgus, rhesus and Japanese monkey
Papio spp. (Baboons)	Hamadryas baboons
Colobinae	
Colobus spp.	Colobus monkeys
Presbytis spp.	Langurs or leaf monkeys

Apes	
Families / Genus and Species	Common Names
Hylobatidae	
Hylobates spp.	Gibbons and Siamangs
Pongidae : Great Apes	
Pongo pygmaeus	Orangutan
Pan spp.	Chimpanzees
Gorilla gorilla	Gorilla

compiled from (Whitney 1995)

G. Association with human cancers

In vivo, lymphomas occurring in immunosuppressed individuals constitute the best examples of the oncogenic potential of EBV in humans. X-linked lymphoproliferating syndrome (XLP) results from a rare form of immunodeficiency linked to chromosome X in young boys. In these boys, EBV infection leads to a fatal IM-like disease, which results in 75% mortality a few weeks after primary infection. The proliferating cells are mostly lymphoblastoid of B cell origin and express EBNA1, EBNA2 and LMP1, a type III latency pattern. Patients treated with immunosuppressive drugs can also suffer from EBV associated lymphoma or organ failure due to infiltrating B lymphoma cells resulting in death. In others, death ensues after tissue destruction from invasive phagocytic cells (Rickinson and Kieff 1996).

Non-Hodgkin's lymphomas (NHL) are a common form of lymphomas (up to 50% of all malignancies) in individuals with inherited immune deficiencies (Mueller 1999). In organ transplant recipients, NHL and skin or lip cancer are the most frequent tumors resulting from iatrogenic immunosuppression. The use of stronger immunosuppresive regimens has lead to increased cases of these lymphomas particularly in bone marrow, heart, lung and liver transplantations. More than 90% of post-transplant NHL are EBV positive (Mueller 1999). The tumors show a B-cell phenotype and are usually of type III latency.

AIDS-associated lymphomas are similar to post-transplant lymphomas as they develop late in the course of HIV infection when the individual is severely immunosuppressed. EBV has been shown in 75-80% of lymphomas and type I and III viral latency patterns have been reported. Interestingly, EBV-2 was demonstrated in

several of these lymphomas supporting an earlier observation of a higher incidence of EBV-2 infection in HIV infected individuals (Rickinson and Kieff 1996). NHL and Hodgkin's diseases are among the AIDS-associated malignancies. All HD tumors in AIDS patients are EBV positive whereas, in contrast to NHLs from post-transplant recipients, only 50% of NHLs in AIDS patients harbor the EBV genome.

Burkitt's lymphoma (BL) is endemic in equatorial Africa and New Guinea with a rate of 5-10 cases/100 000/year during the first 15 years of life. Tumors of endemic BL are characterized by the presence of small noncleaved cells and gene translocations in close proximity to the c-myc locus on chromosome 8 and either the immunoglobulin heavy chain locus on chromosome 14 (seen in 80% of the cases) or one of the light chain loci on chromosomes 2 or 22. In these cells, the c-myc encoded transcription factor is under the control of an immunoglobulin promoter and therefore, no longer down-regulated in resting B cells. The constitutive expression of c-myc promotes uncontrolled cell growth (Klein 1994). A strong association of EBV with endemic BL was revealed by the detection of EBV DNA in virtually all tumors examined to date with viral gene expression limited to EBNA1. The geographical distribution of endemic BL suggested the involvement of co-factors. Malaria has been associated with the development of BL. Some have proposed that the polyclonal stimulation of B cells along with T cell suppression seen in malaria infected individuals may contribute to uncontrolled EBV growth and a higher incidence of gene mutation. Other factors linked to regional diets or remedies have also been questioned as some of them can induce EBV lytic infection (Morgan 1995). EBV association with sporadic cases of BL and AIDS associated BL is

not as consistent as for endemic cases, there EBV is found in 15-85% and 30-40% of tumors respectively.

Nasopharyngeal carcinoma (NPC) represents a major health problem with 80 000 new cases annually (Morgan 1995). The most common form of NPC are tumors with poorly differentiated or undifferentiated (UNPC) cells, called respectively WHO II and WHOIII subtypes. These UNPC are sometimes mistaken for lymphomas but can be distinguished using antibodies to cytokeratin (Gaffey and Weiss 1992). These tumors occur mainly in Southern China, Mediterranean Africa and are also found in Inuit populations. A strong association with EBV has been shown in these NPC as all confirmed tumors harbor the EBV genome (Gaffey and Weiss 1992). The presence of EBV DNA supported the association that was made earlier from elevated EBV antibody levels in individuals with NPC. The high incidence of NPC in specific geographical locations has brought forward the possibility of a viral association with enviromental factors in the development of NPC. The consumption of salted fish during childhood has been associated with an increased risk of NPC in Chinese populations (Morgan 1995). This virus-environment association has been supported by recent reports (Li et al. 1997; Liu et al. 1998) showing that nude mice transplanted with B95-8 infected nasopharyngeal mucosa and treated with phorbol ester developed lymphoma and carcinoma. A less common form of NPC found mainly in Europe and North America and classified as a well-differentiated tumor (WHO I subtype), demonstrated a poor association with EBV (Rickinson and Kieff 1996).

In the Western world, Hodgkin's Disease (HD) is the most common malignant lymphoma. HD tumors are characterized by the presence of sparsely distributed large

cells. These cells are either mono- or multi- nucleated and are referred as Hodgkin (H) or Reed-Sternberg cells (RS) respectively. HRS cells normally constitute less than 1 % of the cells in the tumors. The surrounding cells are apparently non-malignant T and B lymphocytes, histiocytes, eosinophils and neutrophils. Classical HD comprises 3 types of tumor, nodular sclerosis, mixed cellularity and lymphocyte depleted (Kuppers and Rajewsky 1998). The first two are tumors populated mainly by T lymphocytes. HRS cells in classical HD often express the activation markers CD15 and CD30 but lack B cell lineage markers such as CD20. Lymphocyte predominant (LP) HD tumors are considered as a separate type with tumors infiltrated mainly by B lymphocytes. As opposed to classical HD. HRS cells of LP tumors express B cell lineage markers. The absence of lineage markers and the low frequency of HRS cells in HD have delayed the elucidation of their cellular origin and clonality (Kuppers and Rajewsky 1998). However, results of immunoglobulin gene rearrangement and EBV genome analysis demonstrated that HRS cells are derived from a single cell that originated from lymph node germinal centre B cells (GC). Overall, 40 to 50% of classical HD tumors carry the EBV genome (Masucci 1993) and this frequency varies with the HD types and geographic locations (Kuppers and Rajewsky 1998). In these tumors, EBV gene expression is limited to LMP1 and 2, and EBNA1 (Santon et al. 1998).

The presence of the EBV genome in T cells in some cases of infectious mononucleosis and chronic EBV infection (Kikuta et al. 1988; Mori et al. 1992; Tokunaga et al. 1993) has pointed toward a wider EBV cellular tropism than was first believed. The presence of CD21 on immature thymocytes (Watry et al. 1991) and some circulating T cells (Fischer et al. 1991) or an uncharacterized mechanism, constitute

potential ports of EBV entry into T cells. Cases of T cell lymphomas occurring in HIV-infected individuals afflicted with oral hairy leukoplakia lesions suggested that T cells infiltrating sites of EBV replication might be targets for EBV infection (Rickinson and Kieff 1996). So far, at least 3 types of T cell lymphomas have been shown to harbor EBV EBER transcripts (Rickinson and Kieff 1996). Biopsies from nasal tumors in cases of lethal midline granuloma revealed the clonality of the EBV genome in the T cell tumors (Minarovits et al. 1994). The presence of a single EBV clone in a given tumor indicates that the virus was present early in the lymphoma development and therefore may have contributed to its formation.

Induction of tumors in nonhuman primates by EBV has been investigated in view of establishing an animal model suitable for the development of a preventive or therapeutic anti-neoplasm vaccine for EBV. Several authors have reported the induction of lymphoproliferative diseases by EBV in the cottontop tamarins (or crested tamarins, *Saguinus oedipus*). Sporadic reports on the induction of lymphoproliferative diseases in other New World monkeys have also been published but remain isolated cases (Rabin 1985). In spite of the low level of persistent infection and the lack of oral transmission of EBV, the tamarin animal model has been used to test most experimental vaccines to date (Morgan 1995). Protection of gp350 vaccinated cotton-top tamarins from tumorigenic doses of EBV has been demonstrated (Epstein et al. 1985; Finerty et al. 1992). The common marmosets (*Callithrix jacchus*) are also susceptible to EBV infection, however the infection does not result in lymphoproliferative diseases (Farrell et al. 1997). The animals develop an infectious mononucleosis like syndrome preventable through vaccination with recombinant gp350 (Cox et al. 1998; Emini et al. 1986; 1989;

Wedderburn et al. 1984). More recently, severe combined immunodeficiency (SCID) mice have been described as an alternative model to study the interaction of EBV and B cells *in vivo*. These animals lack mature B and T cells and develop tumors upon injection of B lymphocytes from EBV-seropositive donors. These tumors express all the latent genes characteristic of latency III (Rickinson and Kieff 1996; Veronesi et al. 1994). However, SCID mice are not a model for EBV infection and consequently can not be used for testing vaccines aimed at preventing infection (Morgan 1995).

The persistence of EBV DNA and expression of some latent genes in tumor biopsies are distinctive features of malignancies with suspected viral etiology (Masucci 1993). Tumors associated with EBV generally take several years (up to 60 years) to develop and many of them are monoclonal, thereby they originate from the transformation of a single cell. These two observations combined with the fact that only a small proportion of EBV infected individuals will suffer from cancer suggests that EBV infection may be essential but is not sufficient per se for initiating a tumor. So EBV infection along with host and/or environmental factors is likely to be intimately linked to development of malignancies. A deficient immune response as well as tumor cell escape from immune surveillance or from natural programmed cell death (apoptosis) are major ways leading to host invasion by the transformed cells (Dragovich et al. 1998; Masucci 1993).

The studies of cell transformation by EBV have delineated several EBV genes as well as cellular proteins involved in the transformation process. *In vitro* B lymphocyte transformation requires only 6 of the 12 set of genes normally expressed in B-lymphoblastoid cells. These are EBNA1, EBNA2, EBNA 3A, EBNA 3C, EBNA LP,

and LMP1 whereas the transcripts EBER, BARTs, EBNA 3B, LMP2A and 2B are dispensable. The recent reports of LMP1 interaction with cellular activation and apoptosis signaling pathways have emphasized its potential role in oncogenesis.

H. LMP1

LMP1 is the only EBV protein that by itself can transform rodent fibroblasts and consequently has earned the title of the EBV oncogene. Wang et al. (1985) showed that the Rat-1 fibroblast cell line transfected with LMP1 DNA lost their contact inhibition and frequently grew piled up as opposed to the flat foci phenotype seen in control cells. The formation of cell foci in soft-agar cultures confirmed the anchorage independent growth of the LMP1-Rat1 cells. Moreover, the tumorigenicity of LMP1 expressing cells was demonstrated by the induction of tumors in nude mice injected (s.c.) with LMP1-Rat1 cells. Baichwal and Sugden (1988) reported further support for these observations by transfection of Balb 3T3 fibroblasts with LMP1. LMP1-3T3 cells also developed anchorage independent growth and induced tumors in nude mice. Moorthy and Thorley-Lawson (1993) assessed the loss of contact inhibition in Rat1 cells transfected with a mutated form of LMP1 and reported that all three major domains of LMP1 (N-, C-terminal and transmembrane) were required for transformation of rodent cells (Wang et al. 1988b). The effect of LMP1 expressed in transgenic mice support the role of LMP1 in cell transformation and oncogenesis. Transgenic mice expressing a LMP1 transgene targetted to the epidermis were shown to suffer from hyperplasia and overexpression of keratin (Wilson et al. 1990). More recently, a transgene of LMP1 expressed in B cells under the control of the Ig heavy chain promoter was associated with lymphomas in

transgenic mice. The incidence of lymphomas in these animals reached 42% over 18 months of the study (Kulwichit et al. 1998).

In vitro, the expression of LMP1 has been shown to affect the growth pattern of the human keratinocyte cell line RHEK-1 by disrupting the characteristic tight organization of the cultures and inducing the formation of multilayered bundles and foci (Fahraeus et al. 1990). LMP1 was shown to interact with vimentin intermediate filaments and this interaction might contribute to the phenotypic changes in transformed cells (Liebowitz et al. 1987). Intermediate filaments extend from the plasma membrane to the nucleus and alteration in their composition may alter chromatin organization and gene expression contributing to the development of oncogenesis (Holth et al. 1998). In human B cells, LMP1 has been shown to induce the expression of markers of cell activation CD23 and CD40, as well as several adhesion molecules, ICAM-1 (CD54), LFA-1 and LFA-3 (Peng and Lundgren 1993; Wang et al. 1988a; Wang et al. 1990b) and vimentin (Birkenbach et al. 1989). These phenotypic changes are reminiscent of antigen activated B cells. In epithelial cells, LMP1 induces expression of the receptor for the epidermal growth factor (EGFR) (Miller et al. 1995; 1998). LMP1 can also protect cells from apoptosis. Anti-apoptotic genes, such as *bcl*-2, *mcl*-1, *bfl*-1 and A20 were all shown to be upregulated by LMP1 (D'Souza et al. 2000; Fries et al. 1996; Henderson et al. 1991; Wang et al. 1996) and their involvement in cell survival depends on the cell type. In B cells, bcl-2 but not A20 is upregulated and protects cells from apoptosis, whereas in epithelial cells, A20 has been shown to protect against the p53 tumor suppressor-mediated apoptosis (Fries et al. 1996). More recently, the product of the *bfl*-1 gene, a homologue of bcl-2, that also suppresses p53-induced apoptosis, appeared to be involved

in survival of B cell lines but not in T or epithelial cell lines (D'Souza et al. 2000). The prevention of apoptosis by LMP1 may therefore be a contributing factor to the development of HD tumors. In normal individuals only GC B cells that acquire high affinity antibodies for a given antigen survive whereas B cells with low affinity or those losing their ability to produce antibody are eliminated by apoptosis. One scenario for the role of EBV in the development of HRS cells relies on the presence of LMP1 in GC B cells. LMP1 might prevent apoptosis of non-functional B cells therefore contributing to the accumulation of B cells with highly mutated DNA. These cells would then have an increased risk of oncogenic transformation leading to the development of HRS cell clones (Kuppers and Rajewsky 1998).

In contrast to functions of LMP1 that prolong cell life, other reports suggest that LMP1 may be toxic or promote apoptosis. This dual function of LMP1 appears to be dependent on cell type as well as conditions under which the protein is expressed. Studies of Hammerschmidt et al. (1989) on LMP1 expression in human B cells and rodent cells revealed that LMP1 was cytotoxic when expressed at high levels. This effect was linked to the N-terminal domain of LMP1 as the toxicity was lost when the N-terminal domain was truncated. In addition, Eliopoulos et al. (1996) demonstrated that transient expression of LMP1 in the Rat-1 fibroblast cell line, resulted in inhibition of cellular growth. In this instance, the inhibitory effect was associated with the first functional site (CTAR1) located in the protein carboxy terminus (see below). In the intestinal epithelial cell line 407, expression of LMP1 was shown to enhance TNFα-induced apoptosis and this effect was associated with the presence of at least one of the functional sites CTAR1 and CTAR2 (see below) (Kawanishi 2000).

The LMP1 protein is a 62-65 kDa integral membrane protein expressed in the plasma membrane of latently infected cells. It possesses six 20-22 a.a. transmembrane domains bridged by short hydrophilic sequences, a short 24 a.a. N-terminus and long carboxy tail of approximately 200 a.a. Two sites of phosphorylation have been reported in the carboxy tail of LMP1, one at Serine 313 and the other at Threonine 324 (Moorthy and Thorley-Lawson 1993). Both residues appeared to be phosphorylated at a ratio of 6:1 (Moorthy and Thorley-Lawson 1992). The protein forms aggregates in the plasma membrane with both C-terminal and N-terminal domains oriented on the cytoplasmic side (Liebowitz et al. 1986). Two short introns (78 and 76 nt) are located in the region of the gene encoding the transmembrane domains. The protein is encoded by the BNLF1 ORF, which yields two known transcripts (2.5 and 2.25 kb) regulated from two promoter regions: EDL1, located at position –72 from the start site and EDL1a, located in the first intron. The latter controls a N-truncated form of LMP1 from a second start site located at Met-129. This truncated LMP1 has a Mr of 45 kDa and has been called lytic LMP1 because of its upregulation in lytically infected cells (Hudson et al. 1985). Erickson and Martin (1997) reported the presence of the lytic form in viral particles and suggested a role of the lytic LMP1 in the early events of infection or in the lytic phase of the virus. However, others have reported the absence of the lytic form in lytically infected cell lines (Rowe et al. 1987) and strains of EBV lacking the second initiation codon (Torii et al. 1998) have been reported as well, therefore favoring a non essential function for this shorter protein.

A specific form of LMP1 containing a 30 bp deletion in the distal carboxy domain was first described in EBV strain CAO, a nude mouse propagated Chinese NPC isolate,

as well as in Taiwanese NPC tumors (Chiang et al. 1999; Kingma et al. 1996). This 10 a.a. deletion (res. 346-355), has since been reported in other types of EBV neoplasms, such as HD, NHL, and T cell lymphomas. The deleted LMP1 is not restricted to neoplasms since it has also been shown in healthy EBV carriers. However, when tested for tumorigenicity in rodents, the deleted LMP1 demonstrated a higher incidence of tumor formation in SCID and nude mice (Chen et al. 1992; Hu et al. 1991). A comparative analysis of nasopharyngeal tissues from post-mortem normal carriers versus neoplastic patients demonstrated that the deleted LMP1 was prevalent in 91% (21/23 cases) of nasal NK/T cell lymphomas and in 63% (7/19) of normal nasal tissues, indicating a higher frequency of the non-deleted form of LMP1 in normal tissues (Chiang et al. 1999).

i) Molecular mechanisms of LMP1 interference with cell signaling

The mechanism by which LMP1 alters cell growth, phenotype, survival and death is being unraveled in part by the demonstration of its interaction with three important cellular signaling pathways: the NFκB, the c-Jun amino-terminal kinase (JNK) and the Mitogen Activated Protein (MAP) kinase p38 signal transduction pathways (Figure 3) (Eliopoulos et al. 1999; Huen et al. 1995; Mitchell and Sugden 1995). These pathways are normally triggered by cellular stresses or inflammatory cytokines. For example, TNFα and IL1β lead to activation of transcription factors, such as NFκB and Activation Protein 1 (AP-1) which upregulate several genes that ultimately engage or prevent apoptosis.

Figure 3. LMP1 cell signaling pathways

LMP1 aggregates in the cell membrane through interaction of its transmembrane domains. In the carboxy tail of LMP1, two functional domains have been described, the Carboxyl Terminal Activating Region 1 and 2 (CTAR1 and CTAR2). CTAR1 is located within the first 45 a.a. of the membrane proximal region and binds several members of the Tumor Necrosis Factor Receptor (TNFR) Associated Factors (TRAFs), TRAF1, 3, 5 and to a lesser extent TRAF 2 through a motif PXQXT (TRAF binding motif). TRAF1, 2 and 5 have been associated with NFκB activation. Their binding to CTAR1 triggers the NFκB Inducing Kinase (NIK) which in turn activates the IκB Kinases (IKKα/IKKβ). The IKKs phosphorylate the Inhibitor κB (IκB) which results in its ubiquitination and degradation by the 26S proteasome. Upon degradation of the IκBs, the Nuclear Factor κB (NFκB), so far sequestered in the cell cytoplasm through its binding to IκBs, migrates to the cell nucleus where it binds to κB sites and activates several genes involved in cellular growth.

CTAR2 does not bind TRAFs but associated with death domain proteins such as the TNFR Associated Death Domain protein (TRADD) and the Receptor-Interacting Protein (RIP). TRADD than recruits TRAF2 which then binds to NIK and Mitogen Activated Protein Kinases (MAPK) upstream kinases, MAPKKKs and MAPKKKKs resulting in NFκB and MAPK activation. The MAPKs JNK and p38 upregulate members of the transcription factor family AP-1, Jun and ATF2 respectively, which then activate cellular genes involved in cell growth and survival.

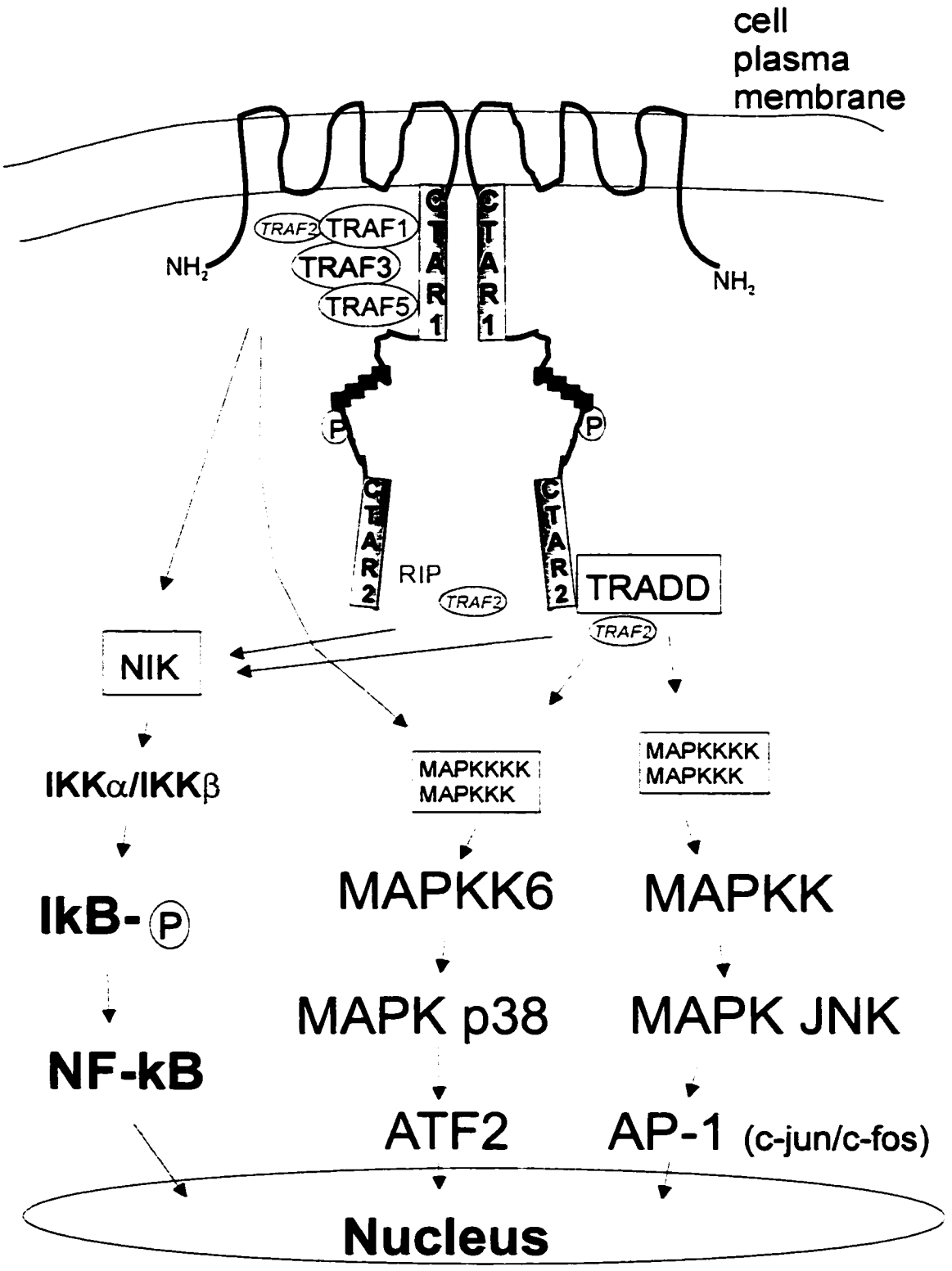
cell
plasma
membrane
NH2
NH2
TRAF2
TRAF1
TRAF3
TRAF5
CTAR1
CTAR1
P
P
CTAR2
CTAR2
RIP
TRAF2
TRADD
TRAF2
NIK
IKKα/IKKβ
IkB-P
NF-kB
MAPKKKK
MAPKKK
MAPKKKK
MAPKKK
MAPKK6
MAPKK
MAPK p38
MAPK JNK
ATF2
AP-1 (c-jun/c-fos)
Nucleus

The NFκB prototype is an heterodimer composed of NFKB1 (p50) and Rel A (p65). NFKB2 (p52), c-Rel, RelA and RelB constitute the other four members of the NFκB family (reviewed by (Mercurio and Manning 1999)). The NFκB dimer is found in the cell cytoplasm in association with a third subunit, the inhibitor κBs (IκBs). IκB members identified to date include IκBα, IκBβ, IκBε, Bcl3, NFKB1 (p105) and NFKB2 (p100). These latter two IκBs require proteolytic cleavage to generate the transcriptionally active NFκB factors NFKB1 (p50) and NFKB (p52). Phosphorylation of the IκBs is controlled by the IκB kinase, a polypeptide complex composed by the three polypeptides IKKα/IKKβ/IKKγ. This phosphorylation leads to the ubiquitination and degradation of IκBs by the 26S proteasome (Zandi et al. 1998). The activation of IKKs constitutes the key regulatory step in the NFκB pathway and as such, IKKs are themselves regulated by the upstream kinase, NFκB Inducing Kinase (NIK), a member of the MAPKKK family (see below) (Karin 1999). The free NFκB is then translocated to the nucleus where it binds to κB binding sites of specific genes and activates their transcription. In concert with other transcription factors, NFκB regulates the expression of a wide spectrum of cellular genes including immunoreceptors such as CD40, a member of the Tumor Necrosis Factor Receptor (TNFR) superfamily, adhesion molecules (such as ICAM1), cytokines, growth and transcription factors (Baeuerle and Baichwal 1997). The outcome of the signal is cell specific and depends on the stimulus as well as the cellular context. Dysregulation of NFκB results in alterations of cell receptor expression, requirement for growth factors and resistance to cell killing, all of which have been associated with tumorogenecity (Mercurio and Manning 1999).

Incidentally, constitutive nuclear expression of NFκB has been associated with several forms of cancer, including Hodgkin's lymphoma (Krappmann et al. 1999). The NFκB pathway confers resistance to TNF-induced cell killing by upregulating the expression of anti-apoptotic proteins such as the superoxide dismutase and A20. More recently other proteins were added to this list; the inhibitor of apoptosis (IAP) proteins, c-IAP1 and c-IAP2, the Tumor Necrosis Factor Receptor (TNFR) associated factors TRAF1 and TRAF2 (Wang et al. 1998) (see below) and an unspliced protein from the immediate-early response gene IEX-1 (Wu et al. 1998). Wang et al. (1998) have proposed that c-IAP1 and c-IAP2 interact with TRAF1 and TRAF2 leading to the inhibition of caspase 8, an upstream member of the caspase cascade committing the cell to apoptosis.

The JNKs (c-Jun N-terminal kinases, also referred to as stress-activated protein kinases, SAPKs) along with the MAP p38 kinases belong to the Mitogen-Activated Protein Kinase (MAPK) family. Contrary to other MAPKs such as the External-stimuli Regulated Kinases (ERKs), both JNKs and p38 MAPKs signaling pathway are preferentially triggered from inflammatory cytokines and cellular stresses, including withdrawal of growth factors (Ichijo 1999). The signal is transmitted to the nucleus through the sequential phosphorylation of a series of MAPKs (Dhanasekaran 1998). A typical phosphorylation chain reaction is operated by a MAPK kinase kinase (MAPKKK) which phosphorylates, and by doing so, activates a MAPK kinase (MAPKK) which in turn, phosphorylates and activates the MAPK JNK or p38. More recently, several MAPKKKKs have also been identified as potential activators of the MAPKKKs (Ichijo 1999). The activated JNK and p38 MAP kinases then regulate the transcription factor c-Jun and ATF2 respectively. This activation favors the formation of the heterodimer c-

Jun/c-Fos, members of the transcription factor family AP-1, which then activates a wide spectrum of cellular genes (Kieser et al. 1997). Activation of the JNK and MAP 38 kinase pathways often result in apoptosis, however this outcome varies largely depending on cell type or cellular environment (Leppa and Bohmann 1999). In B cells, the ligation of BCMA (B Cell Maturation protein), a novel TNFR family member, triggers the activation of the JNK/p38 as well as the NFκB pathways and has been shown to protect cells from apoptosis induced by B cell receptor ligation (Hatzoglou et al. 2000; Laabi and Strasser 2000).

Signal transmission from the cell surface inflammatory cytokine receptors to the cytoplasmic signaling pathways is conveyed by additional proteins, called adapter proteins, which couple the cell surface receptor signal to upstream kinases of signaling pathways. Receptors from the TNF superfamily share only 20-25% degree of homology at the protein level but they all express extracellular cysteine rich regions that enable them to form multimeric complexes essential to their activation (Baker and Reddy 1998). One common feature to all TNFRs is their role in regulation of cell viability (Ware et al. 1998). In this regard, they can be divided into subgroups; one that promotes apoptosis and the other that protects cells from apoptosis. TNFR1 (p55), Fas (CD95) and the Death Receptor 3 (DR3), also called death receptors, are members of the first group. These receptors all possess an intracellular DD through which they bind other DD containing adapter proteins such as TRADD (TNFR-Associated Death Domain protein), FADD (Fas-Associated Death Domain protein) and RIP (Receptor Interaction Protein).

The death receptor Fas binds to FADD (or MORT-1) (Boldin et al. 1995; Chinnaiyan et al. 1995) which then recruits the pro-caspase 8 (or FLICE). Both FADD

and the pro-caspase 8 interact through their respective "death effector domain" (or Caspase Recruitment Domain, CARD). The oligomerization of pro-caspase 8 leads to its proteolytic cleavage and activation. The activated caspase 8 then activates other pro-caspases, such as pro-caspase 9, ultimately leading the cell to apoptosis (Baker and Reddy 1998). A similar scenario happens upon TNFR1 ligation by TNFα. In this case however, TNFR1 interacts with FADD via binding to TRADD, a 34 kDa DD protein. This interaction also lead to activation of pro-caspase 8 (Hsu et al. 1995). Signaling from the TNFR1/TRADD has also been associated with cell survival through its interaction with the DD of the Receptor-Interacting Protein (RIP) and the adapter protein TRAF2 (see below). RIP is a 74 kD DD protein that also contains a kinase-like domain. It has been suggested that TNFR1-activated RIP triggers the NFκB pathway through phosphorylation of the IKK upstream kinase, NIK (Hsu et al. 1996).

TRAF2 appears to play a role in TNF-induced activation of NFκB, JNK and p38 pathways. TRAF2 is one of the six TRAFs (TRAF1 to TRAF6) first described for their association with the TNFR family member, TNFRII (p75) (Rothe et al. 1994). Along with CD40 and CD30, TNFRII is associated with cell survival signaling. In contrast to TNFRI and Fas, these receptors do not possess DDs but bind directly to TRAFs via their cytoplasmic TRAF binding motif (Rothe et al. 1994). Overexpression of TRAF 2, 5 and 6 leads to activation of JNK and NFκB pathways but not TRAF 1, 3 and 4 (Arch et al. 1998). TRAFs are 409-567 a.a. proteins that shared a conserved C-terminal TRAF domain. All TRAFs, except TRAF1, also harbor an N-terminal ring finger and several zinc finger motifs which are reminiscent of other transcription factors (Baker and Reddy 1998). TRAF2 is believed to activate NFκB through binding to NIK, which results in the

activation of IKKs and release of free NFκB (Malinin et al. 1997). JNK and p38 activation is mediated through interaction of TRAF2 with MAPKKKs (MEKK1, ASK1) and MAPKKKKs (reviewed by (Ichijo 1999)). It appears that other TRAFs are also implicated in TNF-induced NFκB since TRAF2 deficient murine cells fail to activate JNK but demonstrate NFκB activity (Yeh et al. 1997). TRAF6 was shown to be involved in CD40, IL1 and LPS induced NFκB but did not affect TNF-induced NFκB (Ichijo 1999).

LMP1 has been shown to interfere with the signaling from the TNFR superfamily members through interaction with DD and TRAF adapter proteins (Brodeur et al. 1997; Devergne et al. 1996; 1998; Eliopoulos et al. 1999; Izumi and Kieff 1997; Izumi et al. 1999; Mosialos et al. 1995; Sandberg et al. 1997). LMP1 interacts with these adapters via two domains located in its carboxy tail called CTAR1 and CTAR2 (Carboxyl-Terminal Activation Regions 1 and 2). Mosialos et al. (1995) first reported the 44 a.a. CTAR1 domain proximal to the transmembrane region (a.a. 186 to 231). This region also known as TES1, Transformation Effector Site 1 (Izumi et al. 1999), contains a conserved TRAF binding motif $P^{204}xQ^{206}xT^{208}/S$ (B95-8). TRAF1, 2, 3 and 5 were all shown to bind to LMP1 but TRAF2 appears to associate only weakly (Brodeur et al. 1997; Devergne et al. 1996; Kaye et al. 1996; Mosialos et al. 1995; Sandberg et al. 1997). The binding of TRAFs to LMP1 CTAR1 domain mimics the TNFRII-, and CD40-TRAF interaction. The second domain, CTAR2 (or TES2), encompasses the last 35 a.a at the carboxy-terminus (pos. 351-386) and interacts with TRADD (Eliopoulos et al. 1999; Izumi and Kieff 1997; Izumi et al. 1999). Through its CTAR2 domain, LMP1 behaves like TNFRI with binding to TRADD/TRAF2 and TRADD/RIP (see above).

EBV recombinants expressing a truncated form of LMP1 that contains only the first 231 a.a. (MS231), therefore harboring CTAR1 but not CTAR2, were shown to support transformation of B cells (Kaye et al. 1999). However, the efficiency of the MS231 recombinants to generate long term growth of transformed B cells was dependent on initial viral titer and cell culture density (Kaye et al. 1999) suggesting a role for CTAR2 in cell growth at low density. Both LMP1 functional sites are known to induce NFκB activity although CTAR1 is a much weaker NFκB activator than CTAR2. CTAR1 and CTAR2 mediate 30% and 70% of the LMP1-induced NFκB activity respectively (Huen et al. 1995; Mosialos et al. 1995). NFκB activation by LMP1 has been associated with an increase of IκBα phosphorylation and degradation (Herrero et al. 1995). Signaling through CTAR2 also activates the JNK protein kinase and results in phosphorylation of c-Jun (Eliopoulos et al. 1999). Mutational analysis at the LMP1 C-terminus revealed that residues P^{379}, Q^{381}, S^{383} and T^{384} within the CTAR2 domain appear to be important in the induction of the JNK activity (Eliopoulos et al. 1999). More recently, Eliopoulos et al. (1999) demonstrated that LMP1 initiates the p38 MAPK cascade leading to the activation of the transcription factor ATF2. TRAF6 has recently been shown to be important in the signaling events leading to p38 MAPK activation (Schultheiss et al. 2001). Mutational analysis showed that both functional domains of LMP1 engaged the p38 MAPK pathway. Moreover, specific inhibition of p38 using the anti-inflammatory drug SB203580 resulted in the reduced expression of LMP1-induced IL6 and IL8, hence suggesting a role for the p38 signaling cascade in LMP1-induced cellular growth (Tanner and Menezes 1994; Tosato et al. 1993).

As LMP1 transduces signals via the NFκB, JNK and the MAPK p38 pathways in ways similar to TNFR family members, it has been proposed that LMP1 acts as a constitutive CD40 receptor (Floettmann et al. 1998). LMP1 would act independently from ligand binding and form spontaneous oligomers through interaction of its transmembrane domains. LMP1 expression in B cells, epithelial cells or carcinoma cell lines was reported to show similar effects on cell phenotype as CD40 ligation, including upregulation of ICAM1 (CD54), proliferation, differentiation or apoptosis (Eliopoulos et al. 1996; 1997; Zimber-Strobl et al. 1996). Uchida et al. (1999) (Eliopoulos et al. 1997; Zimber-Strobl et al. 1996) showed partial restoration of CD40 functions in CD40 deficient mice transgenic for LMP1. In these animals, LMP1, under the control of an immunoglobulin promoter/enhancer, induced extrafollicular B cell activation and differentiation as well as immunoglobulin class switching. However, in contrast to CD40, LMP1 expression did not restore the ability of B cells to enter the germinal center pathway, a site essential for antibody affinity maturation and formation of memory B cells. In contrast to B cells, CD40 expression on primary epithelial cells and various carcinoma cell lines is associated with growth inhibition and apoptosis. In this cellular context, LMP1 once more simulated the CD40 receptor by inducing cell growth inhibition when transiently expressed in Rat-1 fibroblasts (Eliopoulos et al. 1996). This effect relied on an intact LMP1 TRAF binding motif and might implicate TRAF3 binding (Eliopoulos et al. 1996). The similitude between CD40 and LMP1 signaling has recently been challenged by Floettmann (1998) when signaling from both proteins were compared in the T cell line Jurkat. Despite similar levels of NFκB activity, ligation of CD40 on transfected Jurkat cells failed to induce ICAM1 expression in contrast to the upregulation

observed in LMP1 transfected cells. It was argued that the difference might partly be due to difference in TRAF binding, since CD40 binds only TRAF2 and 3 (Floettmann et al. 1998).

2. EBV-like viruses of non-human primates

Because of the limitations of the available EBV animal models, non-human primates and their endogenous EBV-like viruses might represent a better approach to understand EBV pathogenesis and oncogenesis. Ishida and Yamamoto (1987) tested for the presence of cross-reactive EBV antibodies in 42 species of non-human primates. All apes, Old World monkeys and 2 of the 7 New World monkeys species harbored antibodies that recognized EBV. None of the prosimians had anti-EBV reactive antibodies. EBV-like viruses have been isolated in apes from chimpanzees, gorillas and orangutans and among the Old World monkeys, from baboons (*Papio hamadryas, P. cynocephalus and P. anubis*), macaques (*Macaca mulatta*/rhesus monkeys, *M. fascicularis*/cynomolgus monkeys, *M. arctoides*/stumptailed macaques) and African green monkeys (*Cercopithecus aethiops*/vervets) (Bocker et al. 1980; Djatchenko et al. 1976; Falk et al. 1976; Fujimoto et al. 1990; Gerber et al. 1977; Heberling et al. 1981; Neubauer et al. 1979; Rangan et al. 1986; Rasheed et al. 1977; Voevodin et al. 1985).

A. Herpesvirus papio

Among all non-human primate EBV-like viruses, herpesvirus papio (H. papio) has been the best studied. One group reported the development of several lymphoblastoid cell lines from two species of baboons (*Papio cynocephalus* and *P. hamadryas*) (Gerber et al. 1977). Two cell lines *P. cynocephalus* (BA65, BA72) and 3

from *P. hamadryas* (BA99, BA100 and BA105) were established from the spontaneous transformation of PBMC of healthy H. papio seropositive animals. Several other lymphoblastoid cell lines originated from spontaneous transformation of lymphocytes from tissues of animals with lymphoproliferative diseases (Agrba et al. 1975; Djatchenko et al. 1976; Falk et al. 1976; Kokosha et al. 1977). These cell lines include, 594S, isolated from the spleen of a female baboon (*P. hamadrya*) diagnosed with lymphoreticular hyperplasia (Rabin et al. 1977), KMPG-1 derived from the bone marrow of an hamadryas baboon with malignant lymphoma (Agrba et al. 1975) and 3 cell lines, 8CB-1, 13CB-1 and 26CB-1, isolated from the spleen of a lymphomatous hamadryas baboon from a captive colony (Falk et al. 1976).

(i) Antigenic and DNA homologies with EBV

All the baboon cell lines were of B cell phenotype and cross-reacted with human sera specific for EBV VCA, EA and some EBNA+ sera. Specifically, human and baboon sera recognized EBV P3HR-1 as well as baboon 594S and KMPG-1 cells. Ranges from 1 to 5% VCA positive cells were detected in both baboon cell lines. Some baboon sera reacted with EA in RAJI cells superinfected with P3HR-1 virus while human EA+ sera stained the baboon 594S cells (Rabin et al. 1977). The baboon cell lines, 8CB-1, 13CB-1 and 26CB-1, were recognized by human VCA+ sera (Falk et al. 1976).

Reassociation kinetic studies with ^{3}H-DNA of EBV P3HR-1 strain revealed that the baboon herpesvirus DNA shared approximately 40% homology with the human virus (Falk et al. 1976). The colinearity of herpesvirus papio and EBV was demonstrated by Heller and Kieff (1981) by probing digested herpesvirus papio DNA with EBV DNA fragments. Only 2 regions of herpesvirus papio failed to hybridize with EBV fragments,

the BamHI E region and the terminal repeats region and its adjacent unique sequence. The size of H. papio genome estimated from the sum of the size of its restriction fragments was 110 – 114 x 10^6 daltons, very similar to EBV, 115 x 10^6 daltons when estimated by the same approach (Heller et al. 1981). The similar organisation of both viruses opened the door to the possibility of recombination between EBV and H. papio. Functional complementation between H. papio and EBV was investigated by Roubal et al. (1983) using superinfection of Raji cells with both H. papio (594S-F9) and UV-irradiated EBV (P3HR-1). The dual infection induced an increased number of EA positive cells compared to infection with P3HR-1 alone.

(ii) Transforming and oncogenic properties

Because of the poor release of viral particles from some of these baboon cell lines, investigators have used irradiated baboon cells as a source of virus in growth transformation assays. Using co-cultures of PBL and X-irradiated baboon 13CB-1 cells. Falk et al. (1977) showed that H. papio transformed lymphocytes from tamarins but not cells from squirrel monkeys or humans. Cell free preparations of herpesvirus papio produced by three other cell lines (KMPG1, 594S, BA72) were shown to transform macaque, baboon, ape and occasionally, human lymphocytes (Gerber et al. 1977; Rabin et al. 1977). The transformation of human cord blood lymphocytes was inconsistent and occurred at a lower frequency and a slower rate than with EBV.

In 1967, an outbreak of lymphoproliferative diseases was noted at the Sukhumi baboon colony (Sukhumi, Georgia) and correlated with the inoculation of animals with human leukemic tissues. The cases were observed only in inoculated animals or in animals in contact with them and were absent in a group of baboons kept separated from

the main colony. The death rate reached 20 monkeys/year. Most tumors were of B cell phenotype but T cell as well as non-lymphoid tumors were also observed. Cultures of tumorigenic tissues from lymphomatous baboons often led to the isolation of H. papio (frequency of 36%) however other types of virus such as type C retrovirus, foamyvirus, cytomegalovirus and STLV-I like virus have also been reported obscuring the identity of the virus associated with the tumors (Schatzl et al. 1993). Viral particles detected in tumorigenic tissues by electron microscopy were herpesvirus and type C retrovirus (Rabin 1985). Moreover, they reported the identification of two subtypes for each virus. Serologic studies conducted in the diseased and the healthy groups pointed to an association between anti-H. papio antibodies and disease whereas no serologic pattern was detected with type C retrovirus and cytomegalovirus antibodies. Experimental attempts to induce tumors with H. papio were done in baboons (*P. cynocephalus*), cottontop tamarins and rhesus monkeys with cell-free preparations of virus from the BA72 cell line. None of the animals developed tumors (Gerber et al. 1977) but another group did report the induction of lymphoproliferative disease in adult but not newborn cottontop tamarins using an isolate of H. papio derived from a lymphomatous baboon (Deinhardt et al. 1978). Lapin et al. (1993) showed the induction of lymphomas in rabbits inoculated with 594 SF cell line.

(iii) Latent genes

The first attempts to demonstrate the reactivity of EBV human sera to nuclear antigens (latent proteins) of H. papio failed due the poor sensitivity of the assay (an anticomplement immunofluorescence assay, ACIF) but the newer acid-fixed nuclear binding assay (AFNB) developed by Ohno et al. (Ohno et al. 1977) allowed detection of

EBNA-like antigen in H. papio cell lines. Both baboon and human sera reacted to H. papio EBNA-like proteins (Ohno et al. 1978; Rabin et al. 1980) in this assay and by Western blot, where 2 nuclear antigens were identified, one of 74 and another of 103 kDa (called HUPNA-1 and -2) (Dillner et al. 1987). One of the HUPNA-2 reactive baboon sera also bound to EBNA 2 of EBV. Even with evidence of shared EBNA-2 epitopes, both viruses remain quite divergent at the DNA level. Ling and colleagues (1993) have cloned and sequenced the EBNA 2 gene from H. papio and reported a global 35-37% amino acid identity with EBV EBNA 2. However, the two proteins contained conserved CBF1 binding domains vital to the transactivation function of EBNA 2 (Ling and Hayward 1995). The LMP2A homologue of H. papio was shown also to contain a conserved functional domain described for EBV LMP2A (Franken et al. 1995). The baboon LMP2A protein has conserved tyrosine kinase interaction motifs, 12 transmembrane domains as well as 2 promoter CBF1 binding regions important for EBNA-2 induced transactivation. In addition to conservation of functional domains in latent genes, the H. papio Qp promoter region was shown to be 86% homologous to the EBV promoter (Fuentes-Panana et al. 1999). The H. papio Cp promoter, active in B lymphoblastoid cell lines (latency III), showed a 64% conservation at the nucleotide level when compared to EBV Cp region (Fuentes-Panana et al. 1999).

(iv) Herpesvirus papio LMP1 homologue

Franken et al. (1996) reported the partial sequence of H. papio LMP1 gene with the omission of the nucleotides coding for the N-terminus and the first and part of the second transmembrane domains. The predicted protein (approx. 445 a.a.) was slightly larger than EBV LMP1 (386 a.a.) and considerably shorter than its counterpart isolated

from a rhesus monkey virus (588 a.a.) (Rangan et al. 1986). The transmembrane domains were very well conserved among all 3 proteins with 44% identity. Eight TRAF binding motifs P(X)Q(X)T were found within the carboxy tail of H. papio LMP1, with the last one located at the carboxy terminus. Binding studies using *in vitro* translated TRAF3 showed that at least 5 of these motifs interacted with the TNF receptor binding factor. The Rhesus-EBV LMP1 possessed 6 of these motifs with 3 of them shown to bind TRAF3. Induction of NFκB activity by LMP1 proteins from both monkey viruses was demonstrated in human 293 cells using a NFκB driven CAT-reporter assay system. Levels of CAT activity in cells transfected with H. papio or Rhesus-EBV LMP1 were similar to levels induced by EBV LMP1. The TNF responsive gene ICAM1 was tested for expression in co-transfection studies. Both LMP1s induced ICAM1 expression in DG75 cells, an EBV-negative human B-lymphoma cell line, to levels comparable as those observed with EBV LMP1.

B. Cyno-EBV

Over the past 18 years, several cell lines derived from healthy or lymphomatous cynomolgus monkeys were shown to contain herpesvirus-like particles. Heberling et al. (1981) were the first to report the establishment of a virus positive cynomolgus B lymphoblastoid cell line from an inguinal tumor in a monkey treated with cyclosporin A. Herpesvirus-like particles were detected in 3-5% of the cells by electron microscopy but were never further characterized.

Fujimoto et al. (1990) also established a B-lymphoblastoid cell line (TsB) from a lymph node of a healthy cynomolgus monkey immunized with chick collagen in complete Freund's adjuvant. Electron microscopic examinations revealed the presence

of herpesvirus like particles in 20-30% of the TsB cells. The virus was called Cyno-EBV. Another EBV-like virus, named Si-IIA-EBV, was reported in a cynomolgus monkey cell line derived from a co-culture of an HTLV-II-infected human T cell line (HTLV-IIA) and normal cynomolgus leukocytes (Miyamoto et al. 1990). The Si-IIA cell line was shown to contain HTLV-II as well as EBV-like particles although the latter were rarely detectable (Hayashi et al. 1995). Two other cell lines established from tumorigenic cynomolgus monkeys were shown to contain herpesvirus-like particles. Li et al. (1994) have proposed the name herpesvirus macaca fascicularis I (HVMFI) for this tumor derived virus.

A colony of 206 captive cynomolgus monkeys were shown to have all seroconverted to the cynomolgus EBV-like virus by one year of age (Fujimoto and Honjo 1991). The presence of maternal antibodies in infant monkeys was demonstrated by a decline in the proportion of infant monkeys harboring antibodies to Cyno-EBV during the first 4 to 6 months. The proportion of seropositive infant monkeys increased rapidly thereafter and reached 100% at one year of age (Fujimoto and Honjo 1991). In the wild, a serological survey of 250 cynomolgus monkeys from Thailand showed that 96.4% of individuals had antibodies to the EBV VCA (Ishida and Varavudhi 1992).

(i) Antigenic and DNA homologies with EBV

Cyno-EBV has been shown to share antigenic epitopes with EBV. Sera to EBV nuclear antigen as well as an anti-VCA monoclonal antibody (MAB817) cross-reacted with Cyno-EBV cells (Fujimoto et al. 1990). At the DNA level, all tumor DNA derived from SIV-infected cynomolgus monkeys cross-hybridized with a 3.1 kb BamHI W probe from the long internal repeat (IR1) region of EBV (Li et al. 1994). All tumors but one

were positive when stained with human anti-EBNA and all were recognized by the anti-EBNA2 MAb PE-2 (Feichtinger et al. 1992). However tumor tissues showed no reactivity with two preparations of anti-LMP1 MAbs (Li et al. 1993). DNA from tumor tissues and a tumor derived cell line cross-hybridized with EBV EBNA1 and EBNA2 probes but not with a LMP1 probe, although hybridization with LMP1 was demonstrated when low stringency hybridization conditions were used (Li et al. 1994). The Si-IIA-EBV characterized by Ino et al. (1997) was amplified by PCR and sequence analysis showed 82% nucleotide homology within the EBV IR1 (BamHIW region) and BRRF1 sequences. The same BamHIW sequence showed 92% homology with the corresponding HVMF1 sequence.

(ii) Transforming and oncogenic properties

Supernatant from the cynomolgus B lymphoblastoid cell line described by Heberling et al. (1981) was shown to transform peripheral blood lymphocytes from baboon (*Papio cynocephalus*) and cynomolgus monkeys but failed to transform human blood lymphocytes. Cell free supernatant from the TsB lymphoblastoid cell line transformed peripheral lymphocytes from cynomolgus, rhesus and Japanese (*Macaca fuscata*) monkeys but not from humans, baboons (anubis baboons), African green monkeys (*Cercopithecus aethiops*), squirrel monkeys (*Saimiri sciureus*) or moustached tamarins (*Saguinus mustax*) (Fujimoto et al. 1990).

The incidence of tumors in healthy cynomolgus monkeys is very low (2-3 /1000 individuals) and is most commonly composed of malignant lymphomas (Feichtinger et al. 1990; McClure 1973). A high incidence of lymphomas, up to 38%, was reported in immunosuppressed cynomolgus monkeys infected with the simian immunodeficiency

virus (SIV) and all these lymphomas were associated with herpesvirus-like particles (Li et al. 1993). Direct demonstration of the oncogenic properties of cynomolgus EBV-like viruses was shown in experimental infection of rabbits with the Si-IIA cell line and the Ts-B6 virus preparation described by Fujimoto et al. (1990). Hayashi et al. (1994; 1995) reported the induction of malignant lymphomas in 70-77% of rabbits inoculated i.v. with different preparations of the Si-IIA virus. Rabbits also developed antibodies cross-reacting to EBV VCA. Most lymphomas were of T-cell origin and all harbored the EBV small RNA transcript EBER-1 as shown by *in situ* hybridization. Rabbits infected with Si-IIA or Cyno-EBV by oral spray also developed tumors, antibodies cross-reacting to EBV VCA and EBV related DNA was isolated from their peripheral leukocytes (Chen et al. 1997). PCR and in situ hybridization from the tumor tissues revealed the presence of EBER-1 and EBV related DNA. None of the rabbits infected with EBV B95-8 developed malignant lymphomas (Chen et al. 1997; Koirala et al. 1997).

3. RATIONALE AND OBJECTIVES

Animal models for the study of EBV infection pathogenesis and its role in oncogenesis are still lacking. Given the high incidence of herpesvirus associated lymphomas observed in immunosuppressed cynomolgus monkeys it appears that these primates might serve as a good animal model for studying the role of EBV-like viruses in tumor production. However, apart from the association with lymphomas, very little is known about cynomolgus monkey EBV–like herpesviruses. As the LMP1 latency protein of EBV-like viruses is the only viral protein with the ability to transform rodent fibroblasts *in vitro*, this protein is the focus of much recent research.

The hypothesis formulated based on these observations was that the LMP1 protein of the Cyno-EBV virus, associated with a high incidence of tumors in immunosuppressed monkeys, would harbor conserved domains important for LMP1 function in tumorigenesis and may show differences in functions that play a role in immortalization and tumor production. Conservation of specific motif among tumor associated LMP1s from human viruses and LMP1 of Cyno-EBV might help define novel functional domain or structural features important for LMP1 function.

There were two general objectives of this research, the first dealing with structural characterization of Cyno-EBV, and the second focusing more specifically on the molecular characterization of Cyno-EBV LMP1 and some of its functions.

1) To characterize Cyno-EBV with regard to
   a) Prevalence in captive cynomolgus monkeys.
   b) Structural proteins, antigenic homology of its constituents with EBV and another EBV-like virus.
2) To clone, sequence and express the Cyno-EBV LMP1 protein for molecular analysis and study of some of its functions.
   a) Cloning and sequencing the entire coding region of Cyno-EBV LMP1 and analysis at the molecular level.
   b) Measurement of NFκB activation in human 293 cells transiently expressing Cyno-EBV LMP1 and assessment of Cyno-EBV LMP1 transforming ability in rodent fibroblast cell lines.

MATERIALS AND METHODS

1. Cell lines and culture conditions

The Cyno-EBV shedding cell line TsB-B-6 was a generous gift from Dr. Koji Fujimoto (1990). The EBV-shedding cell line B95-8 was obtained from ATCC. The Herpesvirus papio (H. papio) shedding cell line S594 (Falk et al. 1976; Rabin et al. 1977) was a donation from Dr. Norman Letvin (Harvard Medical School, New England Regional Primate Research Centre, Southborough, MA). The cells were cultured at 37° C in a humidified 5% CO_2 atmosphere in RPMI 1640 (Gibco/BRL Life Technologies) supplemented with 7% (v/v) FBS, 2.5 g/L of sodium bicarbonate, 100 U/mL of penicillin and 0,1 mg/mL of streptomycin. The cultures were split ½ to $^1/_{10}$ every 5 to 7 days depending on growth. Rat-1 cells, NIH3T3 and 293 cells were provided by Dr. Janet Jackson (Scripps Research Institute), Dr Douglas Gray (University of Ottawa) and Dr. Ken Dimock (University of Ottawa) respectively. These cells were maintained in Dulbecco's Minimal Essential Medium (DMEM) supplemented with 10% (v/v) FBS, 100 U/mL of penicillin and 0,1 mg/mL of streptomycin. The cultures were split $^1/_{10}$ every 3 days.

2. Virological methods

A. Preparation of virus stocks Infectious virus was obtained from cell-free supernatant of 10 to 12 day-old cultures of virus shedding cell lines. For each virus, the cell suspension was pelleted at 2500 rpm (Sorvall GLC-2B, Dupont Inc., Mississauga, ON) for 30 min. The supernatant was harvested, passed through a 0,45 μm filter and kept

at 4° C for short-term storage. Concentrated stocks of virus (100X) were prepared by centrifugation at 10,000 rpm (Sorvall RC70, rotor AH629) for 2.5 hours and resuspension in a small volume of RPMI. These stocks were stored at –80° C.

B. Titration of virus stocks by transformation assays

Cynomolgus monkey blood was kindly provided by Dr. Jocelyn Fournier (Health Canada, Tunney's Pasture, Ottawa). Peripheral blood mononuclear cells (PBMC) were isolated by spinning 5 mL of fresh EDTA-blood at 2300 rpm (Sorvall GLC-2B, Dupont Inc., Mississauga, ON) for 10 min. without brake. The plasma was harvested and stored at -80° C. The buffy coat was harvested and diluted to a final volume of 2 mL with RPMI. An aliquot of 50 µL of Red-Out™ (Robbins Scientific Corp., Sunnyvale, CA), a murine monoclonal antibody to human red blood cells, was added and the suspension was incubated for 5 min. The suspension was diluted to 8 mL final with RPMI and overlayed on 5 mL of Ficoll-Paque (Pharmacia). The preparation was spun at 2200 rpm for 30 min. without brake. The PBMC layer was harvested and washed twice in 10 mL of RPMI at 300g for 10 min. The cells were resuspended in 1 mL of RPMI and counted with Gentian Blue or Trypan Blue. The transformation of cynomolgus PBMC was carried out according to Miller and Lipman, 1973. Cynomolgus monkey PBMC were resuspended at 8 X 10^5/mL in RPMI supplemented with 10% (v/v) FCS, 100 U/mL of penicillin and 0,1 mg/mL of streptomycin. 8 X 10^4 cells/well were distributed (0,1 mL/well) in a 96-round bottomed well plate. An equal volume of serial dilutions of virus containing supernatant (Cyno-EBV or H. papio) was added to 7 to 18 replicate wells. The cultures were fed twice a week by replacing half the medium. Growth transformation was monitored at 4 to 6 weeks from time of infection by counting

the numbers of wells harboring growing cells. Cell clumping, medium acidification and cell proliferation were criteria used to determine growth transformation. A transforming $titer_{50}$ was determined as the dilution of virus containing supernatant generating the transformation of 50% of cultures.

C. Quantification of viral particles

Viral particles were quantified by negative staining electron microscopy using a method described by Monroe and Brandt (1970) with the following modifications. A 5X concentrated preparation of H. papio (20 µL) was mixed with 5 µL of 97 nm bead suspension (Sigma Polystyrene #LB-1) at 2.4 X 10^{10}/mL. For Cyno-EBV supernatant, 5 µL of unconcentrated supernatant were mixed with an equal volume of beads at 2.4 X 10^{10}/mL. A volume of 5 µL was added to a Formvar-carbon coated grid and allowed to sit for 1 min. The grid was drained with a filter paper and 5 µL of 1% uranyl acetate were added for 10 sec. and drained. The grids were dried overnight and analysed by electron microscopy. The following formula was used to relate the viral particle (VP) counts to the bead counts: VP/mL = [(beads/mL) (VP counted per unit area)/beads counted per unit area] X (1/sample dilution)

D. Virus purification

Virus purification was done according to Dolyniuk et al. (1976) with the following modifications. Concentrated viral stocks (100X) were purified on 2 consecutive continuous sucrose gradient (20%-60% (w/v)) at 20 000 rpm (Sorvall RC70, SW28) for 1 hour at 4° C. At the end and in between gradients, the virus band was harvested, washed in PBS at 12 000 rpm for 2.5 hours and resuspended in 0.5-1.0 mL of PBS.

E. Electron microscopy of the shedding cell line

Cyno-EBV shedding cells were fixed in 1,25% (v/v) glutaraldehyde and 1% (w/v) paraformaldehyde in 0,1 M sodium phosphate pH 7,3. Cell pellets were then sent to the Animal Division Research Institute (Agriculture Canada, Ottawa) for embedding and examination. Thin sections were stained with lead citrate/uranyl acetate and analysed by electron microscopy at a magnification of 40,000X.

3. Immunological assays

S12 monoclonal antibody specific to EBV LMP1 was a generous gift from Dr. Elliott Kieff (Brigham & Women's Hospital, Boston, MA). R3 MAb was a donation from Dr. José Menezes (Ste-Justine Hospital, Montreal, QC), the anti-gp350 MAb was obtained from Dr. Jerry Tanner (CHEO Research Institute, Ottawa, ON), and human EBV VCA positive sera were donated by Dr. F. Diaz-Mitoma (Virology, CHEO Research Institute, Ottawa, ON). The CS1-4 MAb mix, the EBNA 1 MAb and the Anti-HIS6 MAb were obtained from DAKO, DAKO and Clontech respectively.

A. Immunofluorescence assays

Cyno-EBV, H. papio or EBV shedding cell lines were washed twice in PBS and resuspended at 2-4 X 10^6/mL. An aliquot of 10 µL was applied to each well of a 12-well slide, and let dry for at least 1 hour at room temperature. The slides were fixed for 5 min. in ice-cold acetone. The slides were stored at -20° C until analysis. Thawed slides were blocked for 45 min. at 37° C in a humid chamber using 20 µL/well of 10% goat serum diluted in PBS. The blocking solution was removed by aspiration and 20 µL of the first antibody (Cynomolgus monkey sera were used at 1/20 or 1/40, MAb gp350 hybridoma

culture supernatant was used undiluted or ½, MAb R3 ascitic fluid was used at 1/250) diluted in 10% (v/v) goat serum/PBS were added per well. The slides were incubated for 1 hour at 37 °C in a humid chamber, then washed 3 X 5 min. in PBS. The secondary antibody, 20 µL of rabbit anti-monkey IgG-FITC (Sigma) or goat anti-mouse IgG-FITC (Cappel), diluted 1/160 and 1/100 respectively in 3% BSA/PBS was added and incubated at 37° C for 30 min. in a humid chamber. The slides were washed 3 X 5 min. in PBS and counterstained with 0.01 % (w/v) of Evan's blue. The slides were mounted in glycerol:PBS (9:1) pH 8.6 and examined by epifluorescence microscopy.

B. Flow cytometry analysis

(i) Intracellular detection of viral antigen : Cells (5 X 10^5) were resuspended in 0.1 mL of PBS containing 3% (v/v) FBS (PBS-FBS) and permeabilized using the Ortho PermeaFix™ (Ortho Diagnostic Systems, Inc., Markham, ON) solution according to the manufacturer's instructions. A volume of 0.5 mL of Ortho PermeaFix™ was added to the cell suspension and incubated at R.T. for 40 min. The cells were washed in 2 mL of PBS-FBS at 300g for 6 min. The cell pellet was then resuspended in 2 mL of PBS-FBS and incubated 10 min. at R.T. The cells were pelleted and resuspended in 20 µL of PBS-FBS. An equal volume of the first antibody (MAb hybridoma supernatant or diluted sera 1/40) was added and the suspension was incubated for 30 min. at R.T. The cells were washed in 3 mL of PBS-FBS at 350g for 5 min. Goat anti-mouse IgG-FITC (Cappel Organon Teknika) or rabbit anti-monkey IgG-FITC (1/400 final) was added (40 µL) and incubated for 20 min. at R.T. The cells were washed as above and resuspended in 0,4 mL of PBS at 4° C. The cells were analysed on an EPICS XL (Beckman-Coulter) with excitation at 488 nm and emission collected in the FL1 channel.

(ii) Viability studies : Human embryonic kidney cells 293 (a confluent T75 flask) were detached by trypsinization using 0,05% trypsin-0,02% EDTA (Gibco/BRL Life Technologies) in PBS and washed in 4 mL of PBS. The cells were resuspended in 0,5 mL of cold PBS and 1 µL of propidium iodide (2 mg/mL) was added. The cells were incubated on ice for 5 min. and analysed immediately on an EPICS XL (Beckman-Coulter).

4. Protein analysis

A. SDS-PAGE

The viral structural proteins were analysed according to Laemmli (1970) on a 8% (w/v) polyacrylamide gel. Eighty to 100 µg of purified virus preparation were mixed with reducing sample buffer (2% (w/v) SDS, 2% (v/v) β-mercaptoethanol [2-ME], 20% (v/v) glycerol, 100 mM Tris pH 6.8, 0.2% (w/v) bromophenol blue) and boiled for 5 min. Samples were subjected to electrophoresis at 30 mA. The gel was stained with a solution of 0,114% (w/v) Coomassie blue (Bio-Rad), 0,0214% (w/v) Bismarck Brown (Sigma), 40% (v/v) methanol and 7% (v/v) acetic acid solution for 45 min., then destained in 20% (v/v) methanol and 7% (v/v) acetic acid solution until clear background. Wide range molecular weight markers (Sigma) were used as standards for the determination of apparent molecular weight (M_r). Calculations of M_r were done by hand according to Weber and Osborn (1969).

B. Western Blot analysis

A total of 50-70 µg of proteins/lane were resolved by SDS-PAGE on an 8% acrylamide gel. The proteins were transferred to an Immobilon-P membrane (Millipore)

according to Towbin at al. (1979). The membrane was blocked with 3% BSA (w/v) in TBS (10 mM Tris-Cl, pH 7,5, 150 mM NaCl) for 1 hour at R.T. and washed twice for 5 min. in TBS-Tween/Triton (20 mM Tris-Cl, pH 7,5, 500 mM NaCl, 0,05% (v/v) Tween 20, 0,2% (v/v) Triton X-100) and once in TBS for 5 min. The membrane was incubated in the first antibody solution, anti-HIS6 MAb (diluted 1/500 in 3% BSA/TBS) or undiluted cell culture supernatant containing the S12 MAb for 3 hours at R.T. or overnight at 4° C. For Western blots of viral structural proteins, the membrane was incubated with polyclonal sera diluted 1/25 in 3% BSA/TBS and incubated for 2 hours at R.T. The membrane was washed twice for 10 min. in TBS-Tween/Triton and once in TBS for 10 min. Goat anti-mouse IgG conjugated to alkaline phosphatase (diluted $^{1}/_{750}$, Bio-Rad) or Protein-A conjugated to alkaline phosphatase (diluted $^{1}/_{1500}$) in 3% BSA/TBS was added and incubated for 1 hour at R.T. The membrane was washed 4 times in TBS-Tween/Triton and once in TBS. The membrane was stained with 66 µL of Nitroblue tetrazolium chloride (NBT, Sigma) and 33 µL of 5-bromo-4-chloro-3-indolyl phosphate (BCIP, Sigma) diluted in 100 mM Tris, 100 mM NaCl, 5 mM $MgCl_2$ pH 9.5.

5. Molecular biological methods

A. DNA and RNA isolation

(i) Plasmid DNA

a) Vectors : The expression vector pcDNA3 (Invitrogen Corp.) as well as pCR-Script™Amp SK(+) (Stratagene, CA), pGEM-7Zf(+) (Promega Corp.) and pSV-beta-galactosidase vector (Promega Corp.) were all obtained from commercial sources. The NFκB-CAT construct, NFκB-pBLCAT2, a vector containing 3 NFκB responsive

elements upstream of a thymidine kinase promoter driven chloramphenicol acetyl transferase (CAT) gene (Luckow and Schutz 1987) was developed by George Mosialos and was donated by Fred Wang (Brigham and Women's Hospital, Harvard Medical School).

b) Plasmid DNA preparation : Mini-preparations: Mini-preparation of plasmid DNA were prepared according to Sambrook et al. (1989). **Midi-preparations:** DNA preparations from 100 mL of bacterial suspension were prepared by alkali lysis using a DNA isolation kit according to manufacturer's instructions (Quiagen).

c) Transformations : Electroporation : DNA resuspended in 2 μL of water. was electroporated into electrocompetent DH5α bacteria (20 μL) using the BRL Cell-Porator Electroporation System and cuvettes (Gibco/BRL Life Technologies) or the Bio-Rad Electroporator and cuvettes (Bio-Rad). The BRL Cell-Porator settings were at 400V, 330 μF, and low Ω on the cell porator and at 4 kΩ on the voltage booster. Settings on the Bio-Rad electroporator were at 2.5 kV, 25μF, 200 Ω. Electroporated bacteria were recovered and grown on Luria Bertani medium (LB)-ampicillin agar plates according to Sambrook et al. (1989). **Heat shock transformations :** Transformation by heat shock was done using supercompetent Epicurian Coli XL1-Blue MRF' Kan cells from Stratagene. The cells were thawed and mixed with 2 μL of DNA in the presence of 25 mM β-mercaptoethanol. The reaction was incubated on ice for 30 min. and then at 42° C for 45 sec. The reaction was chilled on ice for 2 min. and cells were grown in SOC (2% (w/v) bacto-tryptone, 0.5% (w/v) bacto-yeast extract, 0.05% (w/v) NaCl, 2.5 mM KCl, 10 mM $MgCl_2$, 10 mM $MgSO_4$, 20 mM glucose) for 1 hour at 37°C before plating on LB-ampicillin agar plates containing 80 μg/mL of 5-bromo-4-chloro-3-indolyl-β-D-

galactoside (X-gal, BRL/Gibco) and 80 μg/mL of isopropylthio- β -D-galactoside (IPTG, BRL/Gibco).

(ii) Genomic DNA

Virus containing supernatant was concentrated as described above and the concentrated preparation (0.2 mL of a 200 to 1000X) was clarified by centrifugation on a 4 mL cushion of 20% sucrose/PBS at 25 000 rpm (Beckman rotor 50.1W) for 1.5 hour at 4° C. The viral pellet was digested in 300 μL of 10 mM Tris, 10 mM EDTA solution containing 200 μg/mL of Proteinase K (BRL/Gibco) and 1 % (w/v) Sarkosyl (Sigma). The solution was incubated at 56° C for 1.5 hour. The DNA was extracted 2 to 3 times with an equal volume of phenol:chloroform as described by Sambrook et al. (1989) and resuspended in 30-50 μL of 10 mM Tris and 1 mM EDTA.

(iii) RNA isolation

Total cellular RNA was isolated from 2 confluent T25 flasks of HEK 293 cells, approximately 5-7 X 10^6 cells, by guanidine hypochloride lysis and adsorption on glass fibers using the Boehringer Mannheim High Pure RNA Isolation kit according to the manufacturer's instructions (Vogelstein and Gillespie 1979).

B. DNA manipulations and analysis

(i) Restriction and modification of DNA

Restriction endonucleases and DNA modifying enzymes were obtained from Pharmacia, New England Biolabs (Mississauga, ON) or Boehringer Mannheim.

a) Restriction: Typically, plasmid DNA (0.5-2 μg/20 μL) was digested in the presence of 5-10 units of enzyme for 1-3 hrs as recommended by the manufacturers. For the digestion of genomic DNA, spermidine was added to give a final concentration of 10

mM and the reaction was digested overnight. The restricted genomic DNA was then extracted using the GlassMax DNA purification kit (Gibco/BRL Life Technologies) according to the manufacturer instructions.

b) Ligations: DNA ligations were done using an insert to vector molar ratio of 5:1. The reactions were done in a final volume of 20 µL of OnePhorAll buffer (Pharmacia) containing 1 mM ATP and 4 Weiss units of T4 DNA ligase (Pharmacia). The reaction was incubated overnight at 10-14° C. The DNA was then precipitated with ethanol (Sambrook et al. 1989). The ligation of blunt-ended PCR products was done using the Stratagene pCR-Script™Amp SK(+) cloning kit. The PCR product (450 ng) was mixed with 10 ng of vector (insert: vector molar ratio, 40 : 1), 0.5 mM ATP, 4 units of T4 DNA ligase, 5 units of *Srf I* restriction enzyme in 16 µL of supplied reaction buffer. The reaction was incubated at R.T. for 2 hours and inactivated at 65° C for 10 min.

c) Generation of blunt ended DNA: Blunt-ended PCR products were produced using the cloned *Pfu* DNA polymerase (Stratagene). The DNA (450 ng) was mixed with 0,5 units of enzyme and 0,8 mM of dNTP in the buffer and at temperature recommended by the manufacturer.

(ii) Agarose and polyacrylamide gel electrophoresis

DNA was analysed by gel electrophoresis in 0,8% (w/v) agarose in 0.5X Tris-borate buffer (TBE, 45mM Tris-borate, 1 mM EDTA). The DNA samples were mixed with 6X loading buffer (Sambrook et al. 1989) and the electrophoresis was done at 80V for 45 min. The gel was stained for 15 min. in a fresh solution of ethidium bromide (0,5 µg/mL in H_2O) and visualized under a 302 nm ultraviolet light. Electrophoresis of DNA

in polyacrylamide gels was done with the BioRad Mini-gel apparatus using a 15% (w/v) polyacrylamide gel in 1X TBE buffer (89 mM Tris-borate, 2 mM EDTA) containing 0,75 mg/mL of ammonium persulfate and 0,5 µL/mL of TEMED 10% (v/v). The electrophoresis was conducted at 7.5 V/cm for 2 hours. The sample preparation and gel staining were done as for the agarose gel.

(iii) Southern analysis

Southern blot analyses were carried out according to Fregeau et al. (1995). ^{32}P-labeled probes were generated from a SmaI/NotI fragment of the LMP1 clone #28.

(iv) Polymerase chain reaction (PCR)

The LMP1 region was amplified from genomic DNA by PCR using the primer pairs listed in Table 4. and Taq polymerase (MBI Fermentas) using reagents supplied by the manufacturer. The thermoprofile consisted of one cycle at 95° C. 7 min.; 35 cycles at 95° C. 1 min., 55° C. 2 min., 72° C. 2 min.; and one cycle at 95° C. 1 min., 55° C. 4 min., 72° C. 8 min.

(v) Reverse Transcription

The cDNA synthesis was done using 1/10 of the total RNA (5 µL) prepared from ~6 X 10^6 LMP1 transfected cells. The reaction contained 200 ng of the Cyno-EBV primer LMP3' (2 µL), 4 µL of 5X reaction buffer, 2 µL of DTT 0.1 M, 0.8µL of dNTP (10 mM) and 1 µL (200 units) of M-MuLV reverse transcriptase (Gibco/BRL Life Technologies). The reaction was incubated at R.T. for 10 min. and then overnight at 37° C. The cDNA was then amplified by PCR as described above. Amplicons were gel purified and eluted from agarose using the GlassMax DNA purification kit (Gibco/BRL Life Technologies).

TABLE 4. List of primers for PCR of EBV and Cyno-EBV LMP1

Primer names	Descriptions	Length (nt)	Position *	Sequence (5'→3')	Amplicon length (nt)
LMP1-F	Primers flanking the coding region of EBV LMP1 (use to generate EBV clone #29)	20	169495 - 169514	CTT TCC TCA ACT GCC TTG CT	1566
LMP1-R		20	167949 - 167968	AGG GCT GGG TAA AGG TGT CT	
EBVLMP5'	Primers flanking the coding region of EBV LMP1 with protruding KpnI and Not I sites **(shown in bold)**	32	169495- 169514	**CAC ACA GGT ACC** CTT TCC TCA ACT GCC TTG CT	1566
EBVLMP3'		34	167949- 167968	**CAC ACA GCG GCC GC**A GGG CTG GGT AAA GGT GTC T	
LMP1F2	Primers within the coding region of Cyno-EBV LMP1 (use to generate Cyno clone #28)	18	81 - 98	CCT GCT CCT CCT CGT GGC	1848
LMP1R2		20	1910 - 1929	TAG TAG CTG ATC TGG ATT GG	
LMP5'	Primers flanking the coding region of Cyno-EBV LMP1 with protruding KpnI and Not I sites **(shown in bold)**	33	-24 - -4	**CAC ACA GGT ACC** GCA CAC CAG CAG CAC ACC AGC	1987
LMP3'		35	1943 - 1963	**CAC ACA GCG GCC GC**G GAA GGA AAA CTT CAC GAG CG	

* nucleotide positions of LMP1-F and LMP1-R are from EBV B95-8 DNA as per Baer et al. (1984), all other primer positions are from the Cyno-EBV LMP1 gene region where +1 corresponds to the first nucleotide of the start codon.

C. DNA sequencing

The plasmid DNA was precipitated with PEG by adding 9 µL of NaCl 5 M and 60 µL of PEG 13% (w/v) to 50 µL of DNA in water. The DNA was incubated at 4° C for 1 hr and spun at 13 000g for 20 min. at 4° C. The pellet was rinsed with 200 µL of cold 70% (v/v) ethanol and dried under vacuum. The DNA was resuspended in 20 µL of water. The DNA was sequenced by dye-dideoxytermination method using the oligonucleotides listed in Table 5, at the University of Ottawa Biotechnology Institute.

6. Gene transfer and expression

A. Cell transfections

(i) Transient expression : Human kidney cells 293 were transfected using the calcium chloride procedure (Sambrook et al. 1989). Cells were split to give about 40% confluency the next day and fresh medium was added 2-6 hours prior to the transfection. The efficiency of transfection was monitored by inclusion of a β-galactosidase vector in the transfection mix. A DNA precipitate was formed by adding a solution of 2.5M $CaCl_2$ dropwise (20 drops, over 1 min.) to a mix of 5 µg of LMP1/pcDNA3 DNA and 3 µg of β-galactosidase vector DNA (pSV-beta-Galactosidase Control Vector, Promega Corp.) in 250 µL of HBS, pH 7.05-7.11 (140 mM NaCl, 5 mM KCl, 0.75 mM $Na_2HPO_4 \cdot 2H_2O$, 6 mM dextrose, 25 mM HEPES). The solution was vortexed for 5 seconds. The reaction was incubated at R.T. for 20 min. and half of it was added per well of a 6-well plate. The cells were harvested 16 to 48 hours later.

(ii) Stable expression : Cells were transfected as for transient expression. Two days after transfection, the cells were plated in 10 cm petri dishes and selected in

TABLE 5. List of sequencing primers

Primer names	Orientation	Length (nt)	Position *	Sequence (5'→3')
Clone #28 (81....1929)				
M13+ (-21)	forward	18		TGT AAA ACG ACG GCC AGT
M13-	reverse	18		CAG GAA ACA GCT ATG ACC
LMP3R	forward	18	318....335	CCA TCC CTG ACT ACG CTC
LMP4R	forward	17	630....646	TCG CTG TCA TGC TAC AC
LMP3F	reverse	17	1668....1684	TCC GCC TCC TTC GCT GG
LMP4F	reverse	16	1336....1351	GTG AGG CGC ATG AGT G
Clone #6 (-956....1736)				
SP6	forward	18		ATT TAG GTG ACA CTA TAG
LMPupst	forward	20	-784....-765	CTC CCG CCA CCA AAT GTC CC
LMPupst2	forward	21	-369....-349	CTA TAA TCG CGG TTC ACA TGC
T7	reverse			
LMP5R	reverse	18	1432....1449	TGG ACT GGT TGT GGT AGG
LMP7R	reverse	18	1293....1310	CAT CTC CTC CGT TTT CAC
Clone #8 (1737...>2019)				
T7	forward	20		TAA TAC GAC TCA CTA TAG GG

* nucleotide positions of M13, SP6 and T7 in corresponding vectors, all other primer positions are from the Cyno-EBV LMP1 gene region where +1 correspond to the first nucleotide of the start codon.

presence of 600 μg/mL of geneticin (G418, Sigma) 24 hrs post-plating. This drug concentration was determined empirically from a titration experiment on cultures of untransfected Rat-1 cells using two-fold concentrations of G418 over a range of 200 μg/mL to 1600 μg/mL. Transfected cells were screened for the presence of distinct colony growth. Colonies were picked 5 to 6 days after selection and transferred to individual wells of a 24-well plate. Cells were then screened for protein expression by flow cytometry as described in section 3B.

B. Reporter gene assays

(i) CAT assays

The LMP1 transfected 293 cells were harvested 16 to 20 hours post-transfection by scraping. The cells were washed in 1 mL of 40 mM Tris-HCl, pH 7.5, 1 mM EDTA, 150 mM NaCl and spun at 6000 rpm for 3 min. The pellets were resuspended in 50 μL of FT buffer (25 mM sucrose, 10 mM Tris-HCl pH 7.4, 10 mM EDTA, 0.1 M KH_2PO_4 pH 7.2, 0,15 M NaCl) and lysed by 5-6 freeze-thaw cycles. The lysates were spun at 13 000 rpm for 10 min. at 4° C and the supernatants were transferred to new tubes. Aliquots from the same cell lysate were used for monitoring the CAT and β-galactosidase activity. Aliquots of 0.5 to 5 μL were tested for CAT activity according to Sambrook at al. (1989). To 2 μL of lysate were added 91 μL of water, 37 μL of 1 M Tris-HCl pH 7.5, 20 μL of a fresh 4 mM solution of Acetyl-CoA (Sigma) and 1 μL of ^{14}C-chloramphenicol (Amersham). The reaction was incubated for 1 hour at 37° C and the acetylated chloramphenicol products were extracted with 1 mL of ethyl acetate. The samples were dried under vacuum and resuspended in 10 μL of ethyl acetate. The samples were analysed by thin layer chromatography (0,25 mm Silica gel) using chloroform:methanol

as the mobile phase. The silica plate was revealed using a phosphorimager (Molecular Dynamic Storm).

(ii) β-galactosidase assays

The β-galactosidase (β -gal) assay was done as described by Sambrook et al. (1989). An aliquot of 10 to 40 μL of cell lysate was mixed with the enzyme buffer (60 mM $Na_2HPO_4 \cdot 7H_2O$, 40 mM $NaH_2PO_4 \cdot H_2O$, 10 mM KCl, 1 mM $MgSO_4 \cdot 7H_2O$, 50 mM β-mercaptoethanol, pH 7.0) to a final volume of 200 μL. Forty μL of a 4 mg/mL solution of o-Nitrophenyl- β -D-galactopyranoside (ONPG, Sigma) were added and the reaction was incubated at 30° C for 30min. to 1 hour. The reaction was stopped by the addition of 100 μL of Na_2CO_3 and the optical density was read at 420 nm. Protein concentrations of 2 μL of lysate were determined using the Bio-Rad reagents. The samples were read against a BSA standard solution. The calculation of the relative β-gal activity was done using the following equation:

$$\frac{(\text{Absorbance}_{420nm} / 0.0045)}{[\text{reaction time (min.)} \times \text{protein concentration } (\mu g/\mu L) \times \text{volume of cell lysate } (\mu L)]}$$

RESULTS

Little is known about the cynomolgus EBV-like virus other than its association with lymphomas in immunosuppressed monkeys. Here, two approaches were undertaken to characterize an isolate of Cyno-EBV derived from a lymphoblastoid cell line established from a healthy cynomolgus monkey lymph node (Fujimoto et al. 1990). First, a general study of the virus prevalence in captive monkeys and its structural and antigenic relatedness to EBV was carried out. The second part of this work was focussed on the *in vitro* transforming activity of Cyno-EBV, specifically addressing structural and functional characterization of the LMP1 oncogene homologue.

1. Prevalence of Cyno-EBV infection among captive cynomolgus monkeys

The prevalence of Cyno-EBV infection in cynomolgus monkeys is expected to reach 100% in the adult population with seroconversion occurring during the first year of age (Fujimoto and Honjo 1991). Here, adult monkeys and monkeys under one year of age, from a colony held at Health Canada facilities, were tested to ascertain the ubiquitous nature of the infection in that adult population and the time of seroconversion. Plasma from 40 adult female and 40, 5.5 to 9 month-old cynomolgus monkeys were tested for the presence of antibodies to Cyno-EBV by immunofluorescence assays using acetone fixed Cyno-EBV shedding cells. Consistent with other reports (Fujimoto and Honjo 1991), all adult females tested (plasma diluted 1/20) carried antibodies to Cyno-EBV. Among the young monkeys, 65% of the 18 females and 62% of the 22 males tested were seropositives (Figure 4) at a plasma dilution of 1/20. This dilution was

Figure 4. Prevalence of Cyno-EBV infection among captive cynomolgus monkeys

Sera from 40 adult female and 40 young (5,5 to 9 month-old) cynomolgus monkeys from Health Canada's colony were tested for reactivity with Cyno-EBV by indirect immunofluorescence. The sera were diluted 1/20 and tested for reactivity with acetone fixed Cyno-EBV shedding cells (TsB-B6). Bound antibodies were revealed with anti-monkey IgG-FITC and slides were examined by fluorescence microscopy. Cells stained with anti-monkey IgG-FITC in the absence of a primary serum were negative.

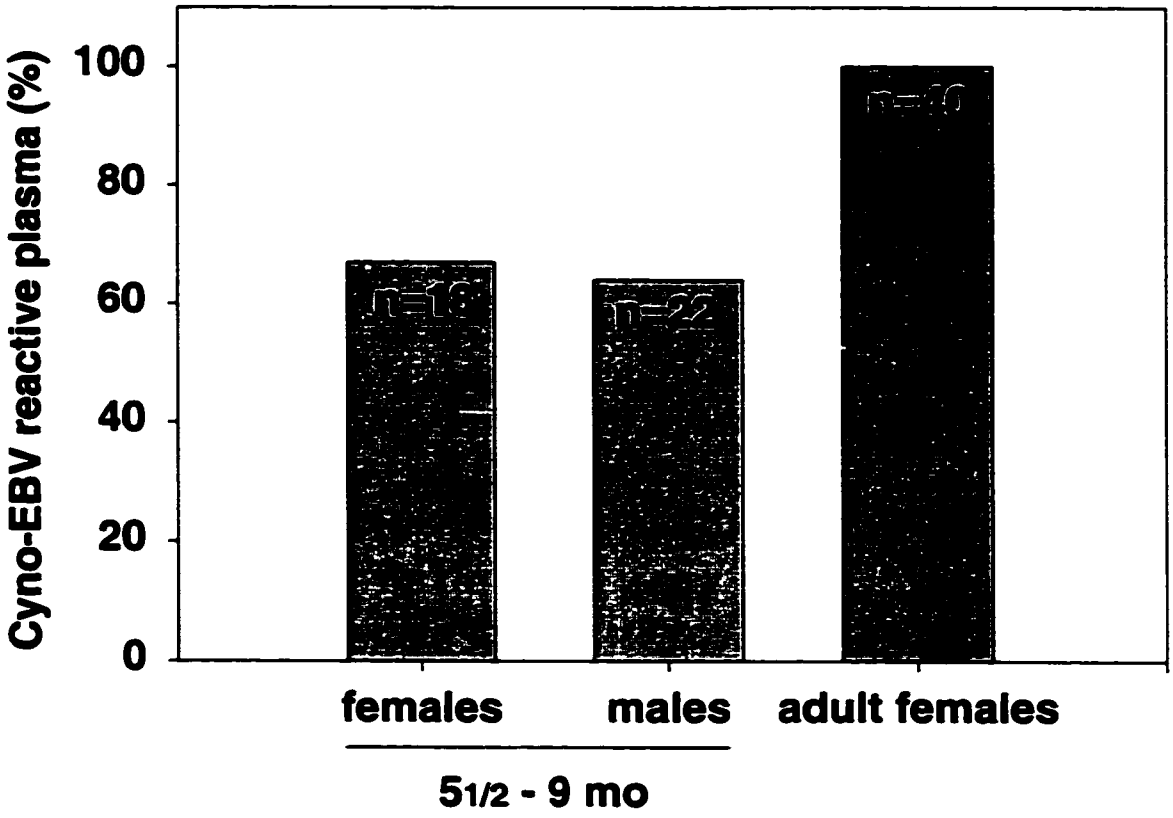
Cyno-EBV reactive plasma (%)
100
80
60
40
20
0
females
males
adult females
5 1/2 - 9 mo

established from the results of a preliminary titration done on cynomolgus monkey sera diluted from 1/10 to 1/80. Seropositivity was determined at 1/20, since a strong fluorescence signal was clearly detected for some sera whereas others remained negative over the entire dilution range. No uninfected cynomolgus monkey cell lines were available for testing specificity of these sera. Among the young monkeys tested, the seropositivity did not correlate with a specific age.

2. Structural and antigenic analysis of Cyno-EBV

A. Electron microscopy of Cyno-EBV

To verify that the shedding cell line used to generate the virus used in these studies was infected with herpesvirus, electron microscopy was undertaken. Electron microscopic observations of the Cyno-EBV shedding cell line (TsB-B6) showed the typical herpesvirus like structure of Cyno-EBV particles (Figure 5). Three mature viral particles were observed in cytoplasmic vacuoles (denoted by * on Figure 5). They contained a dense core and a capsid of approximately 100 nm in diameter surrounded by an asymmetric tegument. Their diameter varied from 130 to 160 nm depending on the thickness of the tegument. Several immature viral particles consisting of solely light core nucleocapsids could also be seen in the cellular space surrounding the vacuoles with some of them revealing the typical icosadeltahedral shape of herpesvirus capsids (denoted by ** on Figure 5).

B. Structural proteins of Cyno-EBV

Studies of the structural proteins of EBV particles have been reported by Dolyniuk et al. (1976). Eighteen proteins (range of 28-290 kDa) were associated with

Figure 5. Electron micrograph of Cyno-EBV shedding cell line TsB-B6

Thin sections of the cynomolgus monkey cell line TsB-B6 were stained with lead citrate/uranyl acetate and examined by electron microscopy at a magnification of 40 000 X. The 3 mature viral particles (denoted by *) shown here have a diameter of 100-140 nm and harbor the typical herpesvirus like structure. The viral core, capsid and tegument are indicated with arrows. Two immature viral particles are denoted by **.

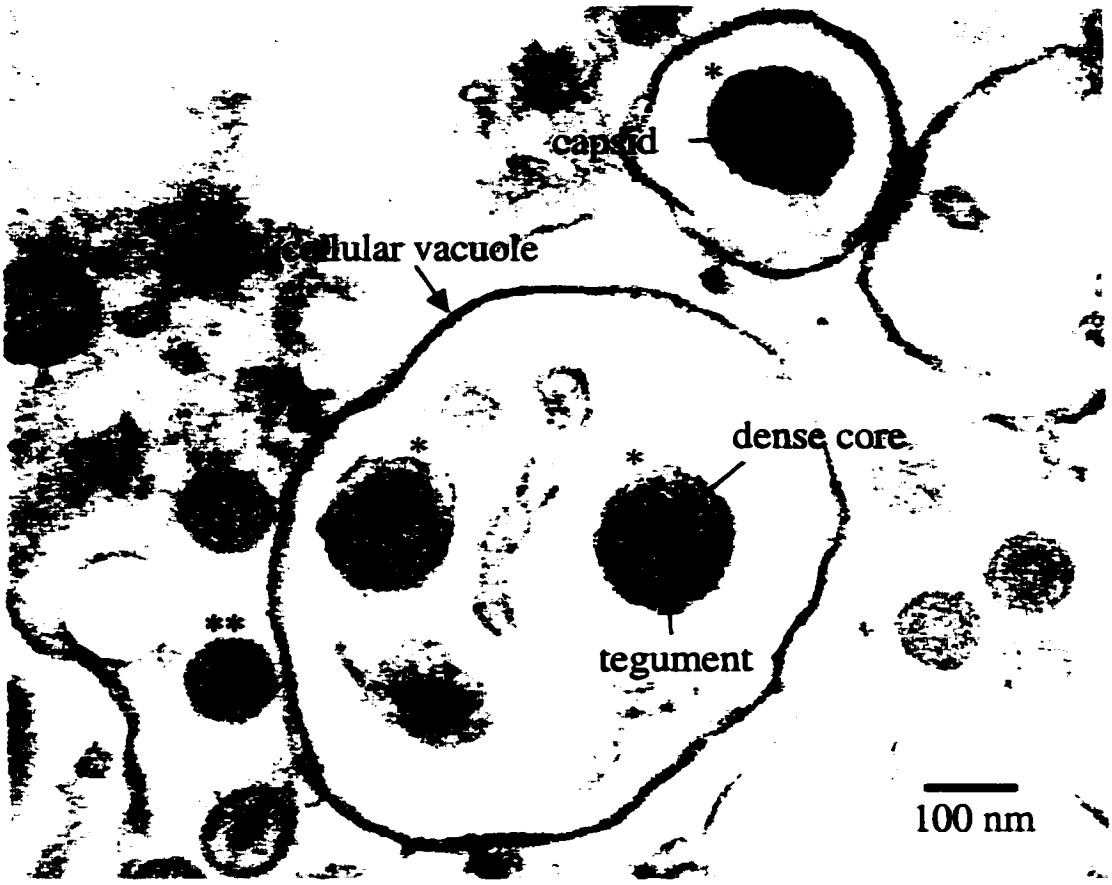
capsid
cellular vacuole
dense core
tegument
100 nm

purified virions when revealed by Coomassie blue staining. Analysis of the electrophoretic profile of purified virion constituents from EBV, H. papio and Cyno-EBV was undertaken to assess and compare the structural polypeptide profiles of all 3 viruses. Cyno-EBV, EBV and H. papio viral particles were purified from 500 to 900 mL of cell free supernatant as described in Materials and Methods. Approximately 80 μg of total proteins from purified virion preparations were analysed on a 10% polyacrylamide gel and stained with a Coomassie Blue/Bismarck Brown solution (Figure 6). Cyno-EBV and EBV shared very similar electrophoretic profiles whereas the protein profile of H. papio was unique, composed of polypeptides with apparent M_r distinct from EBV and Cyno-EBV. A total of 35-37 polypeptides were detected in Cyno-EBV and EBV preparations from which 17 were major components (shown in bold in Table 6). Among them, 15 migrated to identical positions on the gel. Three major polypeptides from Cyno-EBV: 91-92, 53-54 and 39 kDa, co-migrated with polypeptides of H. papio. Two major polypeptides from H. papio migrating at 145 and 152 kDa were also found in the Cyno-EBV but constituted only minor components of the preparation. Even though these preparations were derived from purified virions, the presence of cellular contaminants is unavoidable as cellular proteins are incorporated in viral membranes during the budding process.

C. Cynomolgus and human antibody cross-reactivities to EBV and Cyno-EBV

Antigenic homologies among the EBV and EBV-like viruses have been reported for the antigens of the lytic cycle, but the latent cycle proteins have shown very weak or no antigenic homologies (Ohno et al. 1977; Rabin et al. 1980). To assess the antigenic

Figure 6. SDS-PAGE of the structural proteins of Cyno-EBV, EBV and H. papio

Approximately 80 μg of purified virion proteins from Cyno-EBV, EBV and H. papio were analysed by SDS-PAGE on a 8 % polyacrylamide gel under reducing conditions. The gel was stained with a Coomassie Blue/Bismarck Brown solution. Wide range molecular weight markers are indicated on the left. The arrow indicates the migration front.

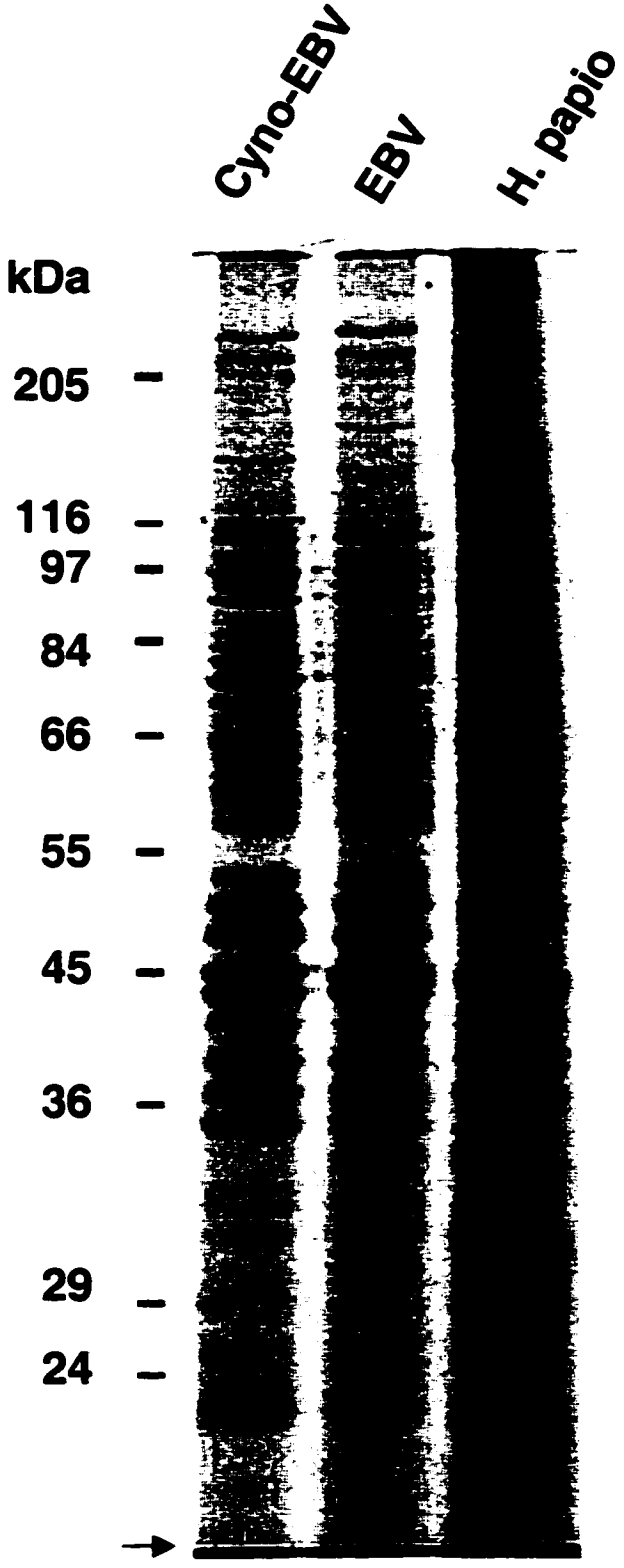
Cyno-EBV
EBV
H. papio
kDa
205
116
97
84
66
55
45
36
29
24

TABLE 6. SDS-PAGE Analysis of Purified Cyno-EBV, EBV and H. papio

Cyno-EBV	EBV	H. papio
(kDa)		
	245.2	
241.5		
	227.5	
220.8		
	171.1	
151.8		**151.8**
145.2		**145.2**
126.9		
	125.0	
121.3		
	119.5	**119.5**
116.0		
112.5	**112.5**	
106.0	106.0	
		104.4
	101.3	
94.7-96.0	**95.3**	94.7
	94.0	
93.4		
90.8-92.0	**90.8**	**90.8-93.4**
86.6		
84.2	**83.7**	
82.5	**82.0**	
		80.8
	78.7	
78.1-79.7		
76.5	76.5-77.6	**77.6**
75.0		72.9-75.0
	74.0	
71.9	**71.0-71.9**	**70.0-71.9**

Cyno-EBV	EBV	H. papio
(kDa)		
69.5	70.0	
67.6	**67.6**	68.1
65.8	65.8	65.8
64.0	64.0	
		63.2
62.3		
	61.4	
57.0		57.4
56.2		
53.2-53.9	**53.2**	**52.5-54.3**
50.4-51.4	**50.4**	
47.0-47.7	**46.7-47.4**	**46.1-47.4**
45.1-46.1	**45.1-45.8**	
43.6	**43.3**	43.3-44.5
41.6	41.3	
40.7	**40.4**	40.0-41.6
38.5-39.1	**38.3**	**38.3-39.1**
36.2-37.2	**36.5**	
	34.3	**33.6-34.5**
	31.6	
30.5	30.1	**29.3-30.5**
		26.4-27.2
		24.0-24.7
22.1-22.4	22.1	
		20.9-21.5
		18.3-18.5

closeness of Cyno-EBV to EBV and H. papio, EBV positive sera from humans and Cyno-EBV positive sera from cynomolgus monkeys were tested for ability to bind heterologous viral proteins by Western blot and immunofluorescence. As well, a limited number of monoclonal antibodies specific for EBV proteins were tested for their ability to recognize Cyno-EBV.

(i) Western blot analysis of structural proteins

Sera from cynomolgus monkeys shown to be reactive or non-reactive to Cyno-EBV shedding cells by IFA were tested for reactivity with purified preparations of Cyno-EBV by Western blot (Figure 7). Weak reactivities were observed for sera shown to be negative by IFA (sera #34, 36, 39, 41, 74) when compared to IFA positive sera (sera #1, 4, 9, 21, 38, 46, 56, 68). Five of these sera, # 1, 4, 21, 56 and 68, reacted to a total of 12 polypeptides ranging from 40 to 240 kDa (indicated by arrows to the right), and were selected, based on their broad reactivity, for use in cross-reactivity studies with EBV and H. papio. For these assays, purified preparations of Cyno-EBV, H. papio and EBV were resolved by SDS-PAGE and transferred to Immobilon-P membrane. The immobilized viral antigens were reacted with the pool of 5 cynomolgus sera (Figure 8). Several strongly reactive polypeptides (shown by the arrows to the right) were detected with the purified viral preparations of Cyno-EBV (lane 2). These polypeptides varied in size from 18 kDa to 250 kDa and corresponded to polypeptides observed in purified virus (Figure 6, Table 6). The pooled sera also showed strong cross-reactivity to purified preparations of H. papio and EBV (Figure 8, lane 3 and 4). Cynomolgus monkey serum antibodies recognized nine H. papio proteins ranging from 18 to 104 kDa. The unique migration profile of H. papio structural proteins shown by the electrophoretic pattern in Figure 6

Figure 7. Reactivity of cynomolgus serum antibodies with the structural proteins of Cyno-EBV

Cyno-EBV structural proteins were resolved by SDS-PAGE 7.5% and transferred to Immobilon membranes. They were reacted with cynomolgus monkey sera (1/25) for 2 hours at R.T. The sera were previously tested by indirect immunofluorescence assay (IFA) using the Cyno-EBV shedding cell line Ts-B6 and were grouped into IFA negative (5 sera) and positive (8 sera). Bound antibodies were detected with Protein-A-alkaline phosphatase (1/1500) for 1 hour at R.T. and the membrane was revealed using the substrate NBT/BCIP. Reactive polypeptides are shown by arrows on the right. Molecular weight markers and the migration front (shown by the arrow) are indicated on the left.

Note: The 5 sera marked by an asterisk were pooled and used in subsequent cross-reactivity studies with EBV and *H. papio*.

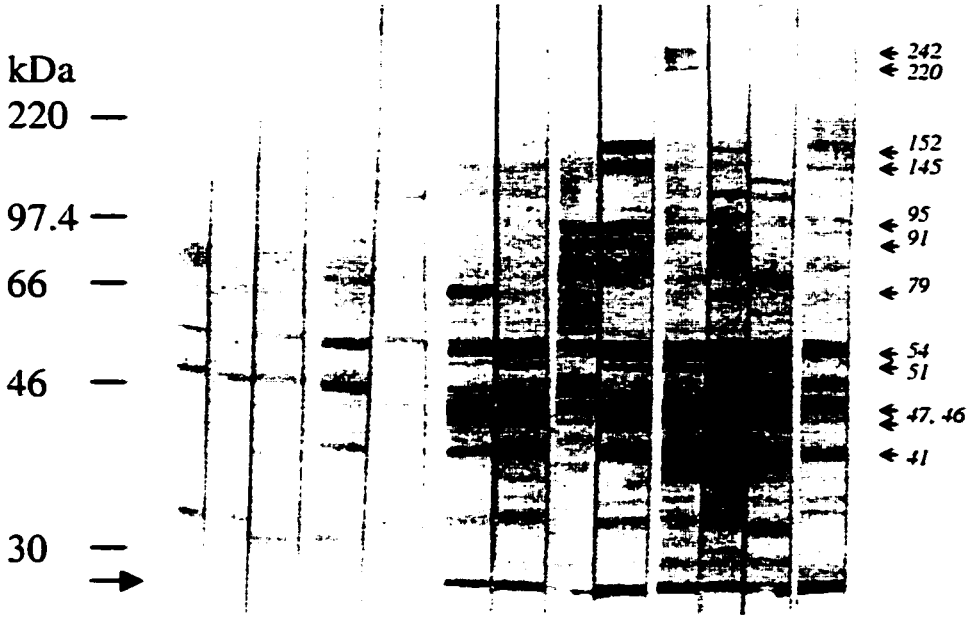
kDa
220
97.4
66
46
30
242
220
152
145
95
91
79
54
51
47, 46
41
Sera# 34 36 39 41 74 38 46 56* 9 21*1*4*68*
IFA negative
IFA positive

Figure 8. Cross-reactivity of cynomolgus serum antibodies with the structural proteins of EBV and H. papio

Cyno-EBV, H. papio and EBV structural proteins were resolved by SDS-PAGE 7.5% (A) and 12% (B) and transferred to Immobilon membranes. They were reacted with a pool of 5 Cyno-EBV positive cynomolgus monkey sera (1/25) for 2 hours at R.T. Bound antibodies were detected with Protein-A-alkaline phosphatase (1/1500) for 1 hour at R.T. and the membrane was revealed using the substrate NBT/BCIP. The arrows heads indicate the migration front. Arrows on the right show the major polypeptides recognized by the sera.

Lane 1: Uninfected Cynomolgus monkey peripheral blood mononuclear cells
Lane 2: purified Cyno-EBV
Lane 3: purified H. papio
Lane 4: purified EBV B95-8

A

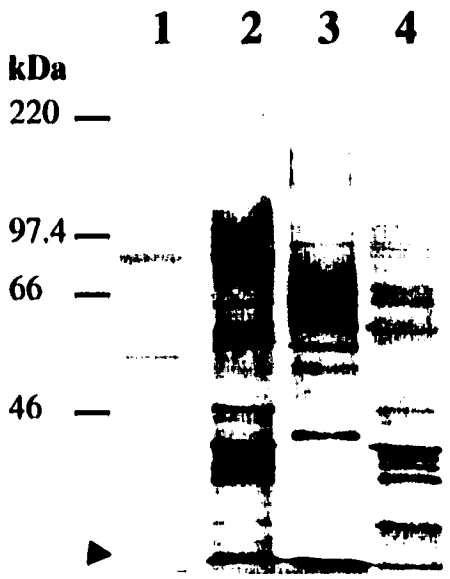
1
2
3
4
kDa
220
97.4
66
46

B

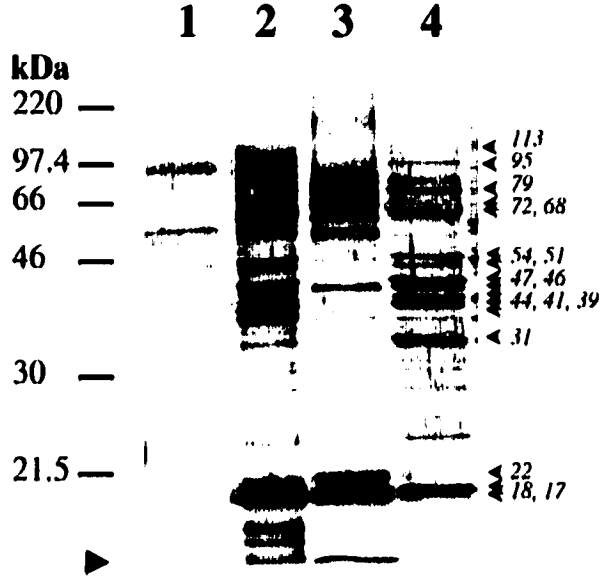
1
2
3
4
kDa
220
97.4
66
46
30
21.5
113
95
79
72, 68
54, 51
47, 46
44, 41, 39
31
22
18, 17

was also revealed here, as cross-reactive antibodies recognized polypeptides of different apparent molecular weights than observed for Cyno-EBV (lane 3). The EBV proteins recognized by the pooled cynomolgus monkey sera co-migrated with proteins of Cyno-EBV (lane 2 and 4). Although the identity of these polypeptides cannot be established with certainty from these studies, some of the strongly reactive polypeptides shared the apparent molecular weight of known structural components of EBV (see Table 1). Polypeptides of 18 and 46-47 kDa migrated closely to 2 EBV capsid proteins reported to have apparent molecular weight of 18 and 40 kDa (Morgan 1995; Serio et al. 1997). Two proteins of 38 and 42 kDa found in the EBV gH/gL complex (Li et al. 1995) might be represented by the 41 and 44 kDa polypeptides, and the 3 EBV envelope glycoproteins migrating at 55-80 kDa, 85 and 100-150 kDa, might correspond to the 79, 91-95 and the 113 kDa polypeptides. Uninfected cynomolgus peripheral blood mononuclear cells showed little reactivity with the pooled sera (lane 1).

Further evidence of the co-migrating pattern of EBV and Cyno-EBV polypeptides was shown when individual sera from 5 cynomolgus monkeys were tested for ability to recognize purified EBV (Figure 9). Individual sera detected polypeptides varying in size from 41 to 152 kDa (shown by the arrows to the right). These polypeptides were major constituent of virions as indicated by comparison with the electrophoretic profile of purified viral preparations (Figure 6 and Table 6). Among the 5 cynomolgus sera tested, sera #1 demonstrated the most reactivity for EBV proteins with 13 proteins being recognized.

In order to determine whether antibody specific for EBV structural proteins can react with Cyno-EBV, 3 human sera positive for EBV VCA were included in the

Figure 9. Cross-reactivity of human and cynomolgus monkey serum antibodies with EBV and Cyno-EBV structural proteins.

Western Blot analysis of the structural proteins of Cyno-EBV and EBV. Purified viral preparations were resolved by SDS-PAGE 8% and transferred to Immobilon membranes. The viral proteins were reacted with 3 EBV VCA positive human sera and 5 Cyno-EBV positive cynomolgus monkey sera as indicated on the figure. Strips of Cyno-EBV and EBV proteins were juxtaposed as indicated on top of figure. Molecular weight markers are shown to the left and the arrow indicates the migration front. Major recognized polypeptides are shown to the right with their estimated apparent molecular weight in kilodaltons.

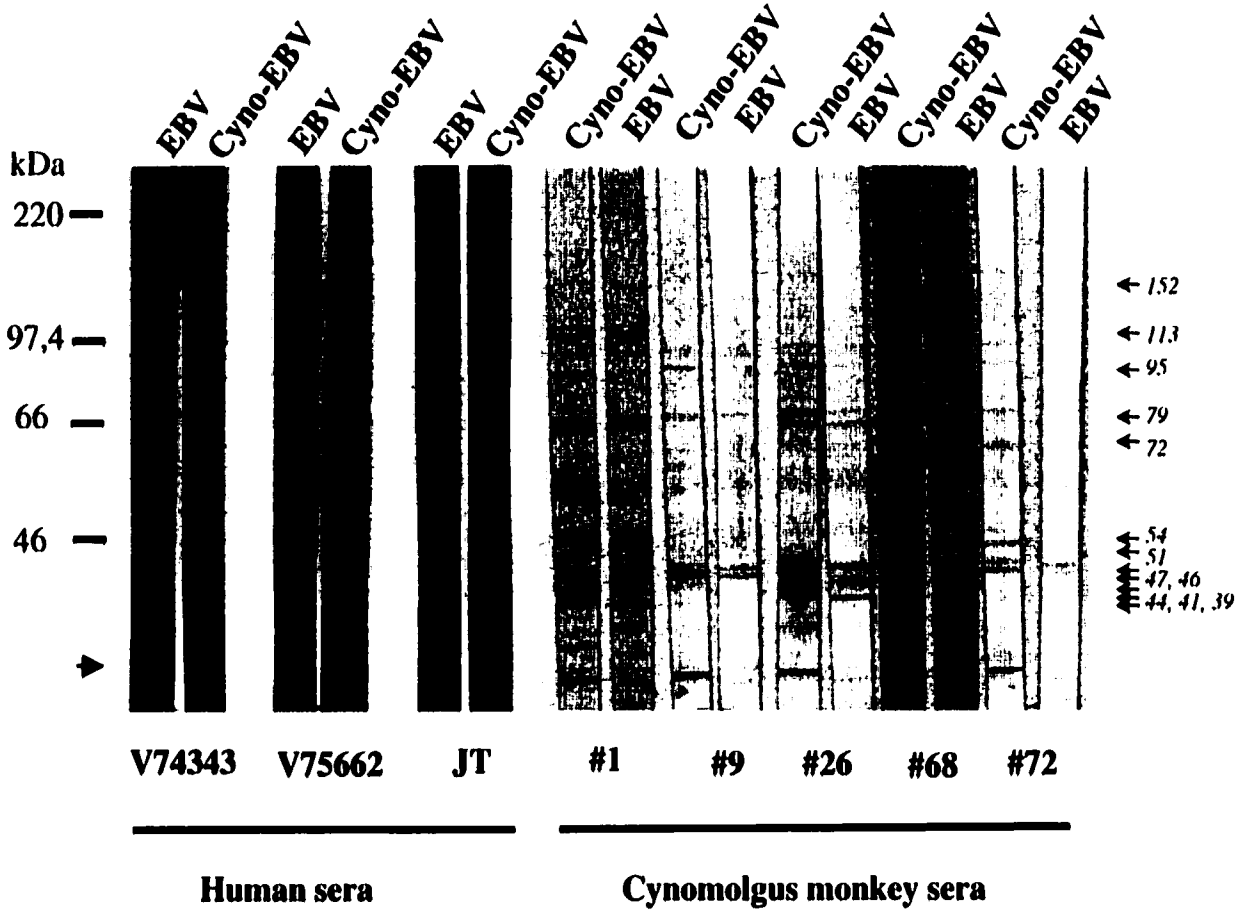
EBV
Cyno-EBV
kDa
220
97,4
66
46
152
113
95
79
72
54
51
47, 46
44, 41, 39
V74343
V75662
JT
#1
#9
#26
#68
#72
Human sera
Cynomolgus monkey sera

analysis. All 3 sera recognized similar polypeptides when assayed against purified EBV, although signals varied in intensity. Serum V74343 showed the strongest reactivity while serum V75662 reacted weakly to the same polypeptides. Serum V74343 detected a major polypeptide of approximately 47 kDa, which may correspond to the known EBV 40 kDa capsid protein (Serio et al. 1997), and a polypeptide migrating at 95 kDa which may correspond to the envelope glycoprotein gp85 or another undescribed capsid protein. Other polypeptides were also observed at 39, 44, 51, 54, 72, 79, 113 and 150 kDa. The latter, although only weakly reactive, likely corresponds to the EBV major capsid protein p150 while the bands migrating at 72 or 79 kDa may be the products of the BILF2 ORF, encoding an envelope protein of 55 to 80 kDa (Mackett et al. 1990). The same band pattern was observed with serum JT however, this serum reacted most strongly with the 72 kDa polypeptide. All 3 human sera detected polypeptides in purified Cyno-EBV migrating identically to those described for EBV, and identically to bands detected with the monkey sera. The two major polypeptides of 47 kDa and 95 kDa recognized by serum V74343 in EBV were also strongly reactive in Cyno-EBV as well as the major polypeptide of 72 kDa recognized by serum JT. Overall, human and monkey sera showed an apparent stronger reactivity to Cyno-EBV polypeptides than to EBV. Although equivalent amounts of viral preparations were loaded on each gel, differences in cellular contaminants and/or protein transfer efficiency may account for the uneven amount of viral preparations on the membrane.

(ii) Viral lytic cycle antigens detected by IFA

The pool of Cyno-EBV reactive monkey sera (see Figure 7) was tested for cross-reactivity to EBV and H. papio shedding cell lines by indirect immunofluorescence

assay. The Cyno-EBV positive plasma reacted with both the EBV and H. papio shedding cells, with a fluorescence pattern mainly localized at the nuclear periphery with detectable signal throughout the nucleus (Figure 10). These reactivity patterns, as well as the low frequency of reactive cells (data not shown), may reflect cross-reactivity of the lytic antigens as these viruses assemble and bud from the nuclear membrane (see Figure 2). No fluorescence signal was detected in absence of sera, or in presence of a pool of 3 Cyno-EBV negative sera (data not shown). Uninfected human or baboon cell lines were unavailable for inclusion as controls.

(iii) Envelope protein gp350 and early antigen

To look at antigenic cross reactivity between EBV and Cyno-EBV in more detail monoclonal antibodies (MAbs) specific to EBV proteins were tested for binding to Cyno-EBV shedding cells by IFA (Figure 11). One of these MAbs was directed to the EBV envelope glycoprotein gp350, a target for neutralizing antibodies and a major antigen of interest in the development of an EBV vaccine. The other MAb, R3, was specific to the diffuse early antigen (EA-D), a 50 kDa non-structural component of the virion associated with the early events of the virus productive cycle. In the EBV positive B95-8 cell line, most anti-gp350 reactivity surrounded the nucleus and filled the cell cytoplasm. Granular and diffuse fluorescence was detected throughout the nucleus. In contrast, the R3 MAb was localized in discrete patches throughout the nucleus and was not detected in the cell cytoplasm. Both monoclonal antibodies cross-reacted to Cyno-EBV antigens. The anti-gp350 reactivity was found mainly, but not exclusively, at the nuclear periphery. Localized and diffuse fluorescence was also observed in the nucleus and the cytoplasm. The R3 MAb was found exclusively throughout the cell nucleus in a

Figure 10. Cross-reactivity of cynomolgus monkey serum antibodies with H. papio and EBV

Five cynomolgus monkey sera were pooled and tested for reactivity with H. papio cell line S594, and EBV cell line B95-8 in an indirect immunofluorescence assay. Cells were fixed in cold acetone for 5 min. and reacted with pooled sera (1/20) diluted in 10% (v/v) goat serum at 37° C for 1 hour. The primary antibodies were detected with rabbit anti-monkey IgG-FITC (1/160). Cells were examined on a Zeiss epifluorescence microscope using a FITC filter. The cells were photographed at a magnification of 100X (with a 10X eyepiece) using a Kodak 400 ASA film.

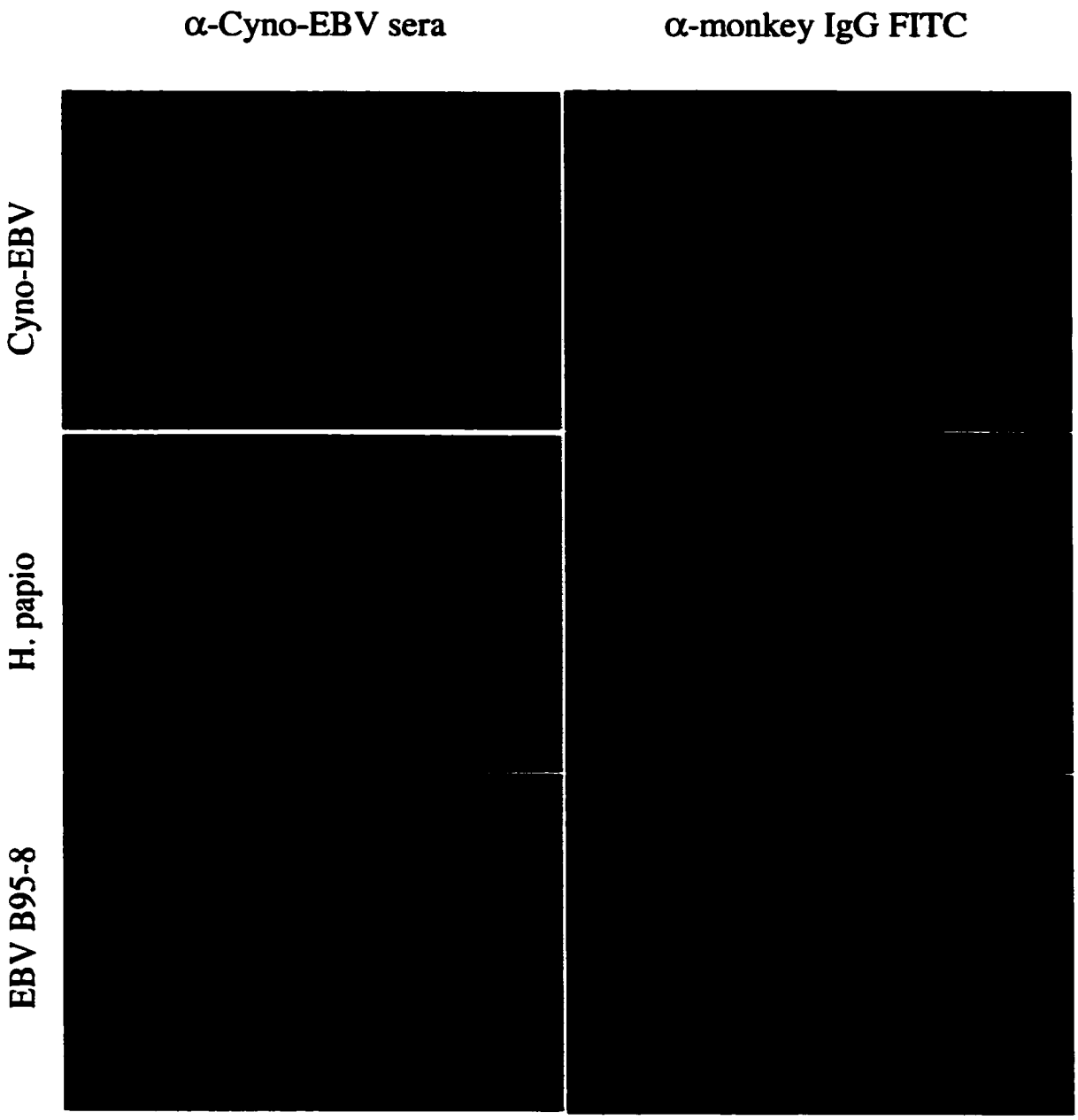
α-Cyno-EBV sera
α-monkey IgG FITC
Cyno-EBV
H. papio
EBV B95-8

Figure 11. Cross-reactivity of EBV gp350 MAb and EA R3 MAb with Cyno-EBV

EBV gp350 MAb and EA-D MAb R3 were tested for reactivity to EBV positive cell line B95-8 (left column) and Cyno-EBV cell line (right column) by indirect immunofluorescence assays. Cells were fixed in cold acetone for 5 min. and reacted with MAbs (gp350 : undiluted culture supernatant, R3 : ascitic fluid 1/250) at 37° C for 1 hour. The primary antibodies were detected with goat anti-mouse IgG-FITC (1/100). Cells were examined on a Zeiss epifluorescence microscope using a FITC filter. Photographs were taken on a Kodak 400 ASA film for color slides at a magnification of 100X (with a 10X eyepiece).

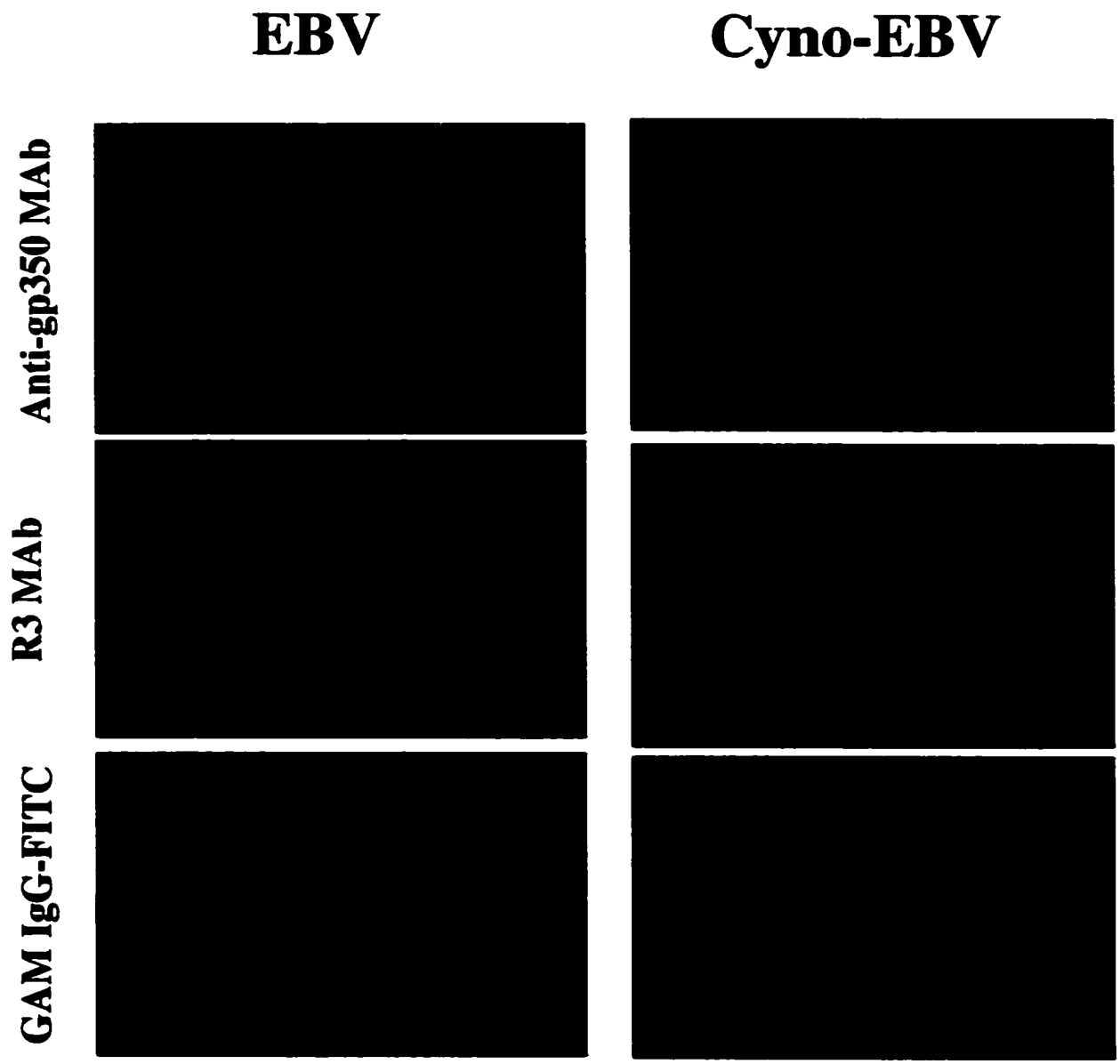
EBV
Cyno-EBV
Anti-gp350 MAb
R3 MAb
GAM IgG-FITC

pattern similar to that observed in the EBV positive cells. However, discrete fluorescent patches, as seen in B95-8 cells, could not be visualized on these photographs.

(iv) Latent Membrane Protein 1 (LMP1)

Two MAb preparations to EBV LMP1 (S12 and CS1-4) were tested for cross-reactivity to Cyno-EBV by Western blot and flow cytometry. The CS1-4 preparation is a mix of 4 MAbs directed to at least 3 different epitopes (Rowe et al. 1987). The S12 MAb, developed by Mann et al. (1985), recognizes an epitope that appears to be distinct from those detected by the CS1-4 preparation (Jiwa et al. 1995). Both MAb preparations were tested by flow cytometry and Western blot analysis using cell lysates of Cyno-EBV LMP1 DNA transfected 293 cells (see below). Both assays demonstrated that EBV anti-LMP1 MAbs failed to recognize Cyno-EBV antigen (Figure 19 and 20) under conditions that showed positive binding to EBV LMP1. As all these MAb preparations are directed to epitopes located within the carboxy tail of EBV LMP1 (Mann et al. 1985; Rowe et al. 1987), and as both conformation and linear epitopes of Cyno-EBV LMP1 failed to be recognized, it is likely that these two proteins share quite divergent carboxy tails.

3. Functional analyses

The ability to transform B lymphocytes *in vivo* and *in vitro* constitutes one of the unique features of the EBV-like group of viruses. EBV transforms lymphocytes from humans, apes, New and some Old World monkey species. H. papio, on the other hand, can transform B lymphocytes from a larger number of monkey species (Rabin et al. 1978). Taking advantage of this feature, it should be possible to directly compare the

transforming ability of the Cyno-EBV isolate with that of its baboon counterpart in cultures of cynomolgus monkey B lymphocytes.

Among EBV proteins known to play a role in transformation, LMP1 has attracted most attention. Studies of the LMP1 homologue from various species offers a unique approach to determine conserved functional domains essential to its activity. Here, the LMP1 homologue of Cyno-EBV was cloned, sequenced and compared to EBV LMP1 in functional assays.

A. Transforming activity of Cyno-EBV

Routinely, H. papio is the virus used for the production of immortalized monkey B cell lines for cellular immunology studies. Preliminary experiments comparing the ability of Cyno-EBV to H. papio to generate monkey B cell lines suggested that Cyno-EBV had a much better success rate than H. papio in immortalizing cynomolgus monkey B lymphocytes. Qualitative observation had shown that the frequency of transformed cynomolgus monkey PBMC cultures obtained with Cyno-EBV was always higher than with its counterpart, H. papio. To confirm and quantify this observation, the transforming titers of both Cyno-EBV and H. papio were determined. PBMC from 8 cynomolgus monkeys were infected with 500 to 18,000-fold dilutions of both viruses and the transformed cultures were enumerated as described in Materials and Methods. PBMC from 7 of the 8 monkeys were transformed by Cyno-EBV, whereas H. papio induced transformation of cells from only 2 of the 8 monkeys. Figure 12 shows that Cyno-EBV supernatant transformed approximately 50% of the cultures when diluted 4000 times. Such an estimate could not be calculated for H. papio since 50% transformation was not reached even at a dilution of 1/500.

Figure 12. Growth transforming titers of Cyno-EBV and H. papio with cynomolgus B cells

PBMC cultures were infected with various dilutions of Cyno-EBV or H. papio stocks and monitored for growth transformation. Cell clumping, medium acidification and cell proliferation were criteria used in combination to determine growth transformation. The fraction of growth transformed cells from two separate experiments (exp. 1 empty bars, exp. 2 hatched bars) were monitored at 4 to 6 weeks from time of infection. These fractions are expressed for each virus dilution tested and the mean of transformed cultures at each dilution was used to calculate the 50% transforming titer (insert).

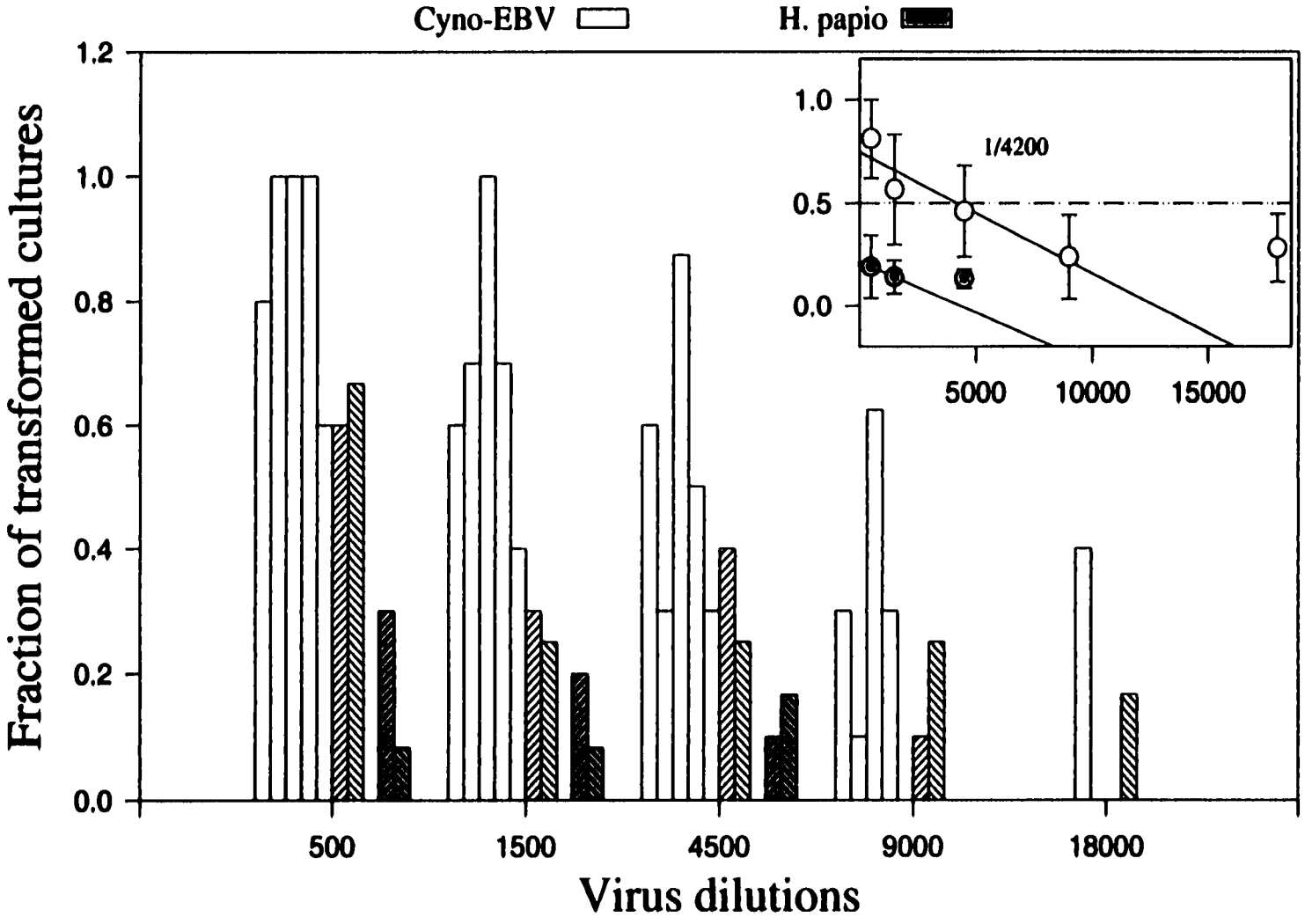
Cyno-EBV
H. papio
Fraction of transformed cultures
1.2
1.0
0.8
0.6
0.4
0.2
0.0
500
1500
4500
9000
18000
Virus dilutions
1/4200
1.0
0.5
0.0
5000
10000
15000

In order to determine whether increased transforming activity of Cyno-EBV stocks was due to differences in the virus or simply due to increased amounts of virus in the stocks it was necessary to quantify the viral content of both virus stocks. Because *in vitro* EBV infection of cell monolayers resulting in productive infection and cytopathic effects is not possible, no plaque assay system exists for monitoring EBV titers in a given stock (Rickinson and Kieff 1996). To compare the viral content of Cyno-EBV and H. papio stocks, three approaches were chosen. First, the number of viral particles in both stocks was estimated by electron microscopic enumeration of a negatively stained viral preparation. Viral particle counts were deduced from counting a standard solution of polystyrene beads added to the viral preparations. The supernatant from H. papio shedding cells had to be concentrated 5-fold to get sufficient viral particles for counting, whereas Cyno-EBV containing supernatant was used unconcentrated. Counts revealed that the Cyno-EBV stock contained on average 10.5 times more viral particles than the unconcentrated H. papio stock (Table 7). Note that the concentration of 10^{10} viral particles/mL observed for Cyno-EBV is unusually high for a herpes virus concentration.

The second approach was to compare the amount of DNA extracted from a given amount of purified Cyno-EBV and H. papio virus. Genomic DNA was isolated from shedding cell line supernatant used in the transformation assays. Their relative DNA concentration was determined by visual comparison of the DNA band intensities as revealed by ethidium bromide staining after migration in agarose. The two viral preparations were then adjusted in order to generate bands of similar intensity. This was achieved when the Cyno-EBV and H. papio DNA preparation were used at a ratio of 12:1

TABLE 7. Quantification of viral particles in Cyno-EBV and H. papio shedding cell line supernatants

	viral particles / mL	
	Cyno-EBV	H. papio
exp. #1	4.67×10^{10}	0.72×10^{9}
exp. #2	2.02×10^{10}	5.50×10^{9}
exp. #3	n.d.	3.36×10^{9}
mean	**3.35×10^{10}**	**3.19×10^{9}**
S.D.	**1.87**	**2.39**
ratio Cyno-EBV/H. papio	**10.5**	

(data not shown), confirming the results from the counting experiment. The third approach was to quantify the number of cells shedding virus in the two cell lines. In order to assess the proportion of shedding cells in the Cyno-EBV shedding cell line; productively infected cells were detected by flow cytometry using a pool of Cyno-EBV positive cynomolgus sera. Sera from cynomolgus monkeys negative for virus by IFA was used as a negative control. The cells were permeabilized using Ortho PermaFix and stained intracellularly before analysis. This approach allows the detection of viral antigens present in the cell cytoplasm. Typically, the Cyno-EBV shedding cell line carried approximately 13% (4% - 29%) positive cells (Figure 13). As lytic gene antigens are related among EBV and EBV-like viruses, and as demonstrated above by IFA, the same pool of sera should also detect H. papio proteins associated with virus producing cells. As assessed using cynomolgus specific antibodies, the proportion of shedding cells in the H. papio cell line constituted less than 3% of the total cells with values ranging from 2 to 13%. EBV and EBV-like virus shedding cell lines differ in their capacity to support productive infection and many of them carry from 1-3% of virus producing cells.

B. Cloning of EBV and Cyno-EBV LMP1 coding region in pCR-Script™Amp SK(+)

To date, the EBV LMP1 homologue of rhesus and baboon EBV-like viruses have been cloned and sequenced (Franken et al. 1996). Because of the high incidence of lymphomas and the numerous reports on their association with cynomolgus EBV-like virus, it would be valuable to characterize the LMP1 homologue of this virus.

First attempts to clone the gene for LMP1 by PCR from Cyno-EBV used primers designed from the published sequence of EBV LMP1, as the sequences of any

Figure 13. Intracellular staining of Cyno-EBV and H. papio by Flow cytometry

Cyno-EBV and H.papio shedding cell lines were tested for virus producing cells by flow cytometry. The cells were fixed and permeabilized using the Ortho-Permeafix™ solution and stained for viral antigen using a pool of 5 cynomolgus sera (1/40) positive to Cyno-EBV producing cells by IFA. A pool of Cyno-EBV sera negative to Cyno-EBV shedding cells by IFA was used as a control. The bound antibodies were revealed using goat anti-monkey IgG-FITC (diluted 1/400). The cells were analysed immediately after staining on an EPICS XL (Beckman Coulter) flow cytometer equipped with a 488nm argon laser.

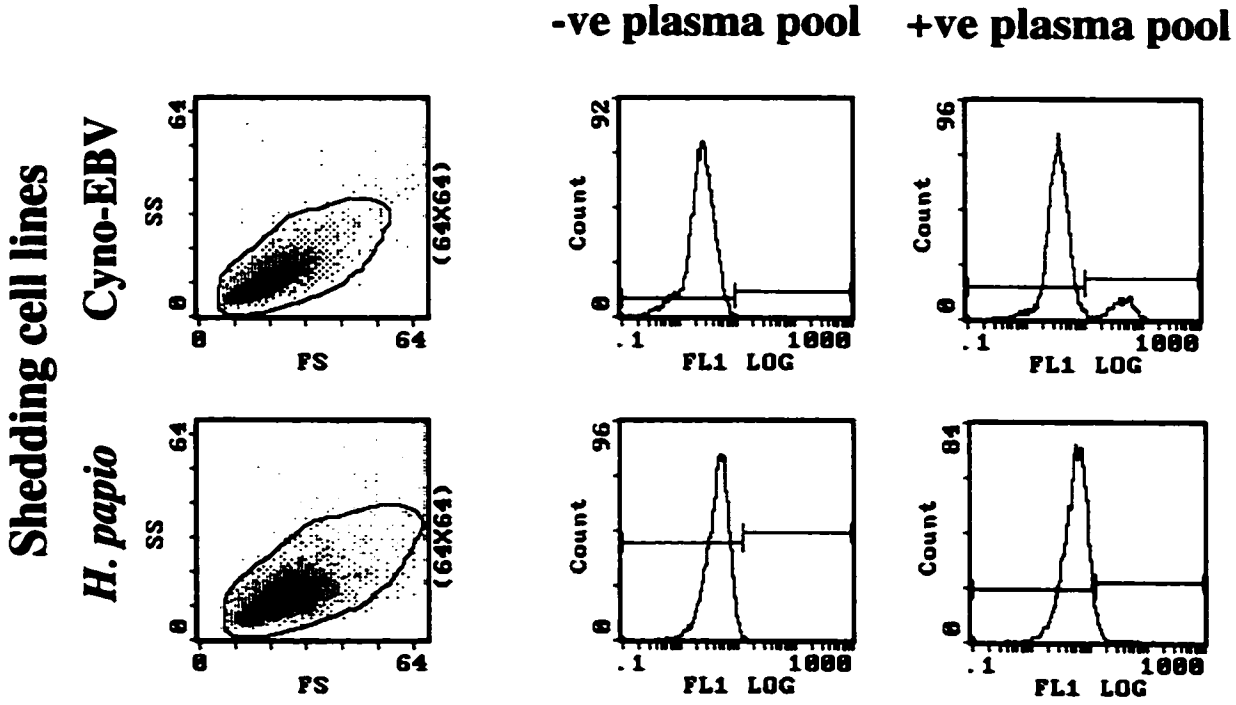
-ve plasma pool
+ve plasma pool
Shedding cell lines
Cyno-EBV
H. papio
SS
FS
64
0
(64X64)
Count
92
96
84
.1
1000
FL1 LOG

related monkey virus LMP1 homologues were not yet available. As a control, EBV LMP1 was amplified from EBV B95-8 genomic DNA. These attempts failed to amplify the LMP1 homologue of Cyno-EBV. Subsequently, the coding sequence of the Rhesus-EBV LMP1 was reported (Franken et al. 1996) and new primers were designed based on 5' and 3' LMP1 homology regions between the rhesus monkey virus, H. papio and EBV (Table 4). These new primers (LMP1F2/R2) amplified a fragment from Cyno-EBV genomic DNA of approximately 1900 bp (1833-1983 bp) as calculated by electrophoresis (shown in Figure 14). The LMP1 coding region of EBV (1566 bp) was amplified from viral genomic DNA using the original primer pair LMP1-F/R (Table 4) designed from published sequence of EBV LMP1 (Baer et al. 1984) (Figure 15A). Both Cyno-EBV and EBV LMP1 amplicons were blunt-end cloned into the plasmid pCR-Script™ SK(+) (Stratagene, CA).

The Cyno-EBV LMP1 clone #28 (4809 bp) was isolated after size screening of plasmid DNA from 167 colonies (3 cloning experiments). This clone was sequenced and found to contain LMP1 sequence based on homology to published sequences of LMP1 from EBV, Rhesus-EBV and H. papio. For comparison, a clone containing the EBV LMP1 sequence (EBV LMP1 clone #29, 4527 bp) was isolated, and its identity was confirmed by restriction digestion with BamHI and XhoI (Figure 15B). The pCR-Script™ SK(+) plasmid contains a single BamHI site located in proximity to the SrfI cloning site ($G_{723}G_{724}$) and no XhoI site (Figure 15C). On the other hand, the EBV LMP1 insert is expected to contain a single XhoI site ($C_{1474}T_{1475}$) and no BamHI site (Figure 15C). BamHI digestion of EBV LMP1 clone #29 generated a fragment of ~4480 bp in concordance with the predicted linearized construct size of 4527 bp. BamHI/XhoI

Figure 14. Agarose gel analysis of PCR amplified Cyno-EBV LMP1 (partial sequence)

Cyno-EBV LMP1 was amplified from viral genomic DNA by PCR using the primer pair LMP1F2/R2 (Table 4). The amplified fragment corresponded to a partial fragment of Cyno-EBV LMP1 coding region and migrated at approximately 1900 bp on a 0.8% agarose gel. The size of the amplified fragment concurred with the size of the corresponding Cyno-EBV LMP1 fragment (1848 bp) determined subsequently from sequence analysis (see below).

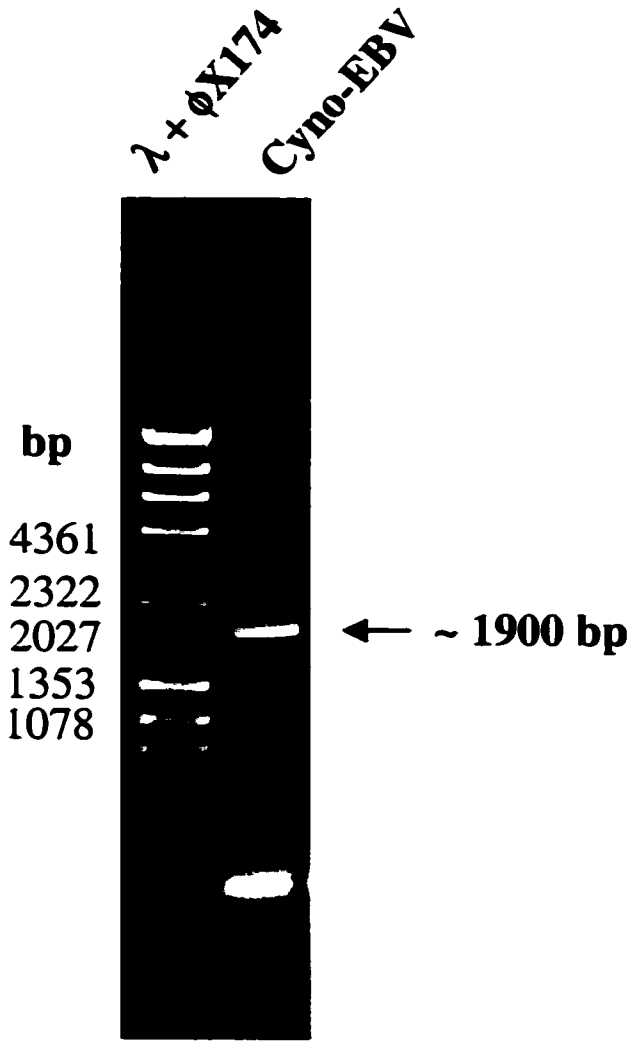
λ + φX174
Cyno-EBV
bp
4361
2322
2027
1353
1078
~ 1900 bp

Figure 15. Agarose gel analysis of PCR amplified EBV LMP1 and restriction analysis of EBV LMP1 clone#29

A. EBV LMP1 was amplified from viral genomic DNA by PCR using the primer pair LMP-1F/R (see Table 4). The amplified fragment had a size of approximately 1540 bp on a 0.8% agarose gel and coincided with the predicted 1566 bp fragment size of EBV B95-8 LMP1 (Baer et al. 1984).

B. The EBV LMP1 amplified fragment was cloned into the vector pCR-Script SK(+) by blunt end cloning and identity of the clone #29 was assessed by restriction analysis. The BamHI enzyme was chosen to linearize the construct. BamHI has a single recognition site in the vector ($G_{723}G_{724}$) and no predicted site in the EBV LMP1 insert. The BamHI digest generated a single fragment that migrated at ~ 4480 bp, a fair match for the expected size of the linearized construct (4527 bp). The enzyme XhoI recognizes a single site in the predicted EBV LMP1 amplicon at $C_{1474}T_{1475}$ and no site in pCR-Script SK(+). XhoI restriction of EBV LMP1 clone #29 generated two fragments that migrated at ~3075 and ~1610 bp corresponding to the size predicted from the EBV LMP1 sequence (3047 and 1480 bp).

C. Predicted nucleotide sequence of the 1566 bp EBV LMP1 (Baer et al. (1984)) amplified fragment cloned at the SrfI site of pCR-Script SK(+). Position of BamHI and XhoI restriction sites are shown in pink and the size of the predicted restriction fragments are indicated above the sequence.

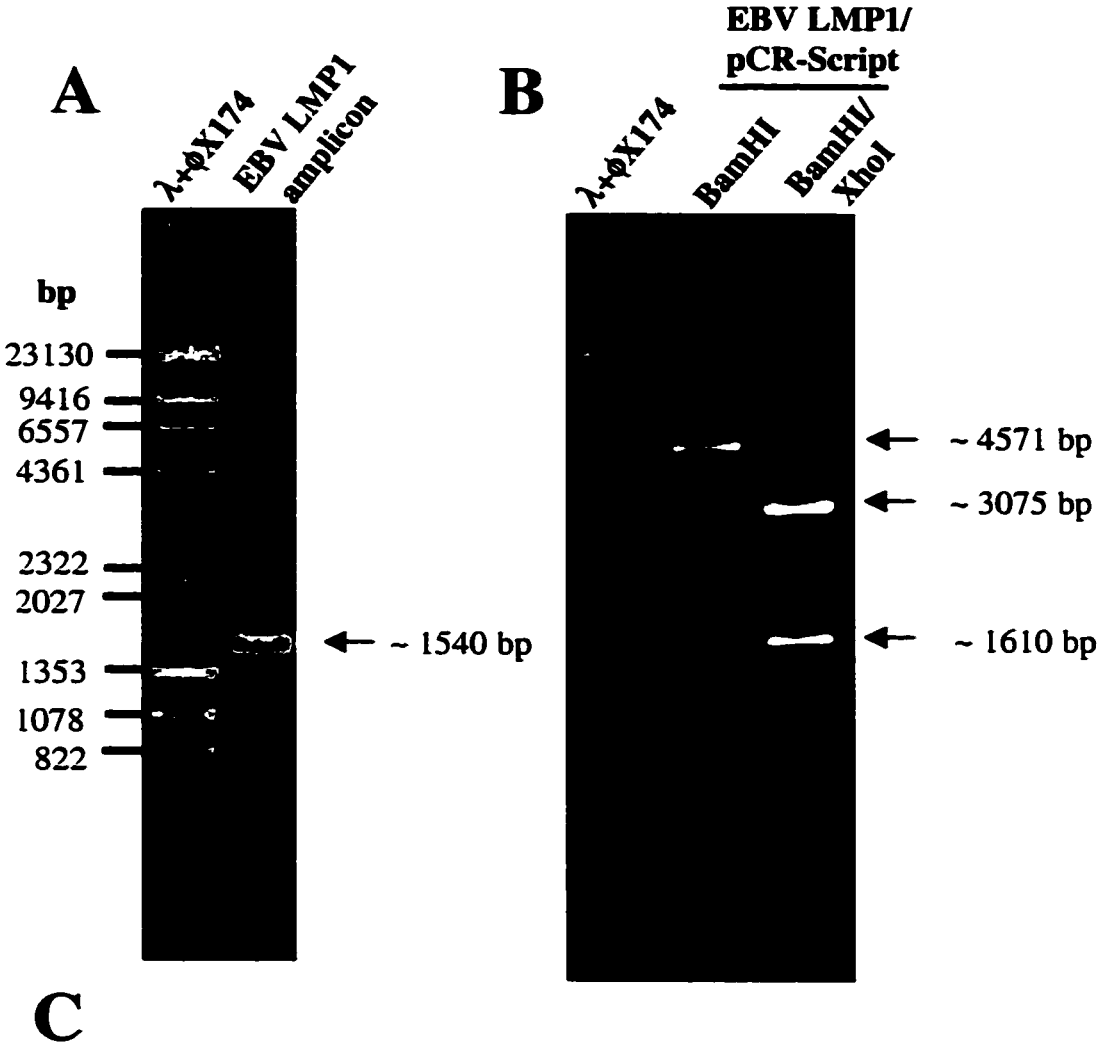
A
λ+ϕX174
EBV LMP1 amplicon
bp
23130
9416
6557
4361
2322
2027
1353
1078
822
~ 1540 bp
B
EBV LMP1/ pCR-Script
λ+ϕX174
BamHI
BamHI/ XhoI
~ 4571 bp
~ 3075 bp
~ 1610 bp

C

restriction generated only the two expected fragments with a size of approximately 3075 and 1610 bp on a 0.8% agarose gel. These corresponded to the 3047 and 1480 bp fragments predicted from the EBV LMP1 sequence (Figure 15C).

C. Cloning of the ends of Cyno-EBV LMP1 coding region

The Cyno-EBV clone #28 represented an internal region of the coding sequence of LMP1. Based on comparison to the Rhesus-EBV LMP1 sequence, 85 and 5 nucleotides were missing from the 5' and 3' ends respectively. The missing sequences were retrieved from the viral genome by shotgun cloning. The Cyno-EBV viral DNA was first digested with several enzymes and screened with a ^{32}P-labeled probe derived from the Cyno-EBV partial LMP1 clone #28. As shown in Figure 16, the Apa I digest generated two clonable fragments of approximately 3000 and 3700 bp thought to contain the ends of the LMP1 coding region. The whole ApaI digest was cloned into pGEM-7Zf(+) and the colonies

were screened by hybridization using the same LMP1 specific probe. Colonies were picked and two clones, one for each fragment, were selected based on expected sizes. These clones, Cyno-EBV LMP1 #6 and #8, contained respectively a 3000 and 3700 bp inserts. Both were subsequently sequenced and their identity confirmed.

To generate a complete clone of Cyno-EBV LMP1 under the control of an eukaryotic promoter, a new PCR fragment was produced and cloned into the expression vector pcDNA3. New primers (LMP5'/3', Table 4) encompassing the entire coding region of LMP1 of Cyno-EBV were used to amplify the gene from genomic DNA (Figure 17). As a control, EBV LMP1 was also cloned (primers EBVLMP5'/3', Table

Figure 16. Determination of clonable size LMP1 fragments from Cyno-EBV viral DNA digests.

A. Southern blot analysis of Cyno-EBV viral DNA digested with various restriction enzymes and probed with ^{32}P-labeled partial LMP1 from clone #28. Two clonable fragments of approx. 3000 and 3700 bp were generated from the ApaI digestion (indicated by the arrows) and likely contain the ends of the LMP1 coding region.

B. Agarose gel analysis of Cyno-EBV viral DNA ApaI digest used for cloning into pGEM-7f(+).

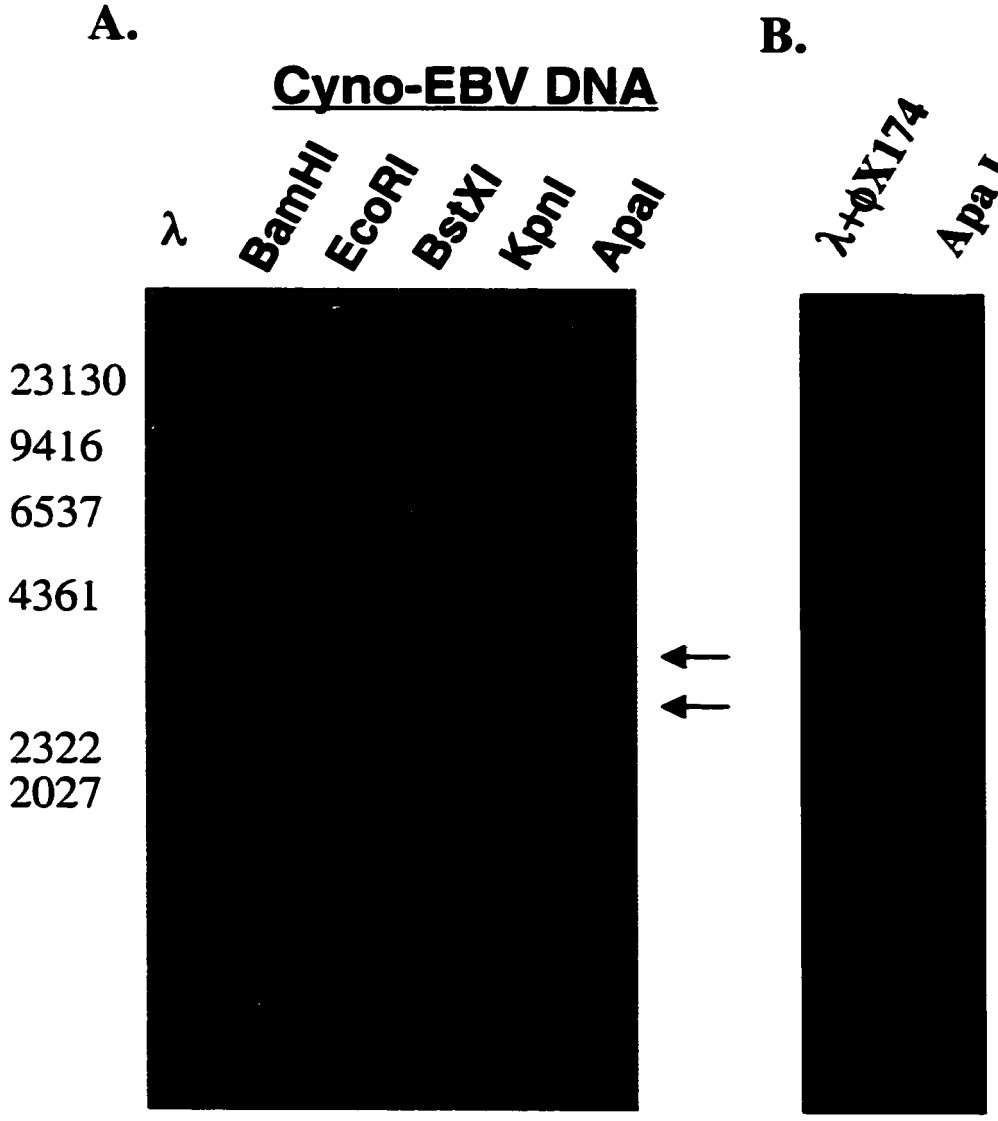
A.
B.
Cyno-EBV DNA
λ
BamHI
EcoRI
BstXI
KpnI
ApaI
λ+φX174
Apa I
23130
9416
6537
4361
2322
2027

Figure 17. PCR amplification of the full length Cyno-EBV LMP1 coding region.

Cyno-EBV genomic DNA was amplified by PCR using the primer pair LMP5'/3' (Table 4). These primers flanked the entire coding region of Cyno-EBV LMP1 gene and amplified a fragment migrating at ~ 2015 bp on a 0.8% agarose gel (shown by the arrow). Subsequent sequence analysis of Cyno-EBV LMP1 confirmed that the coding region corresponded to 1987 bp.

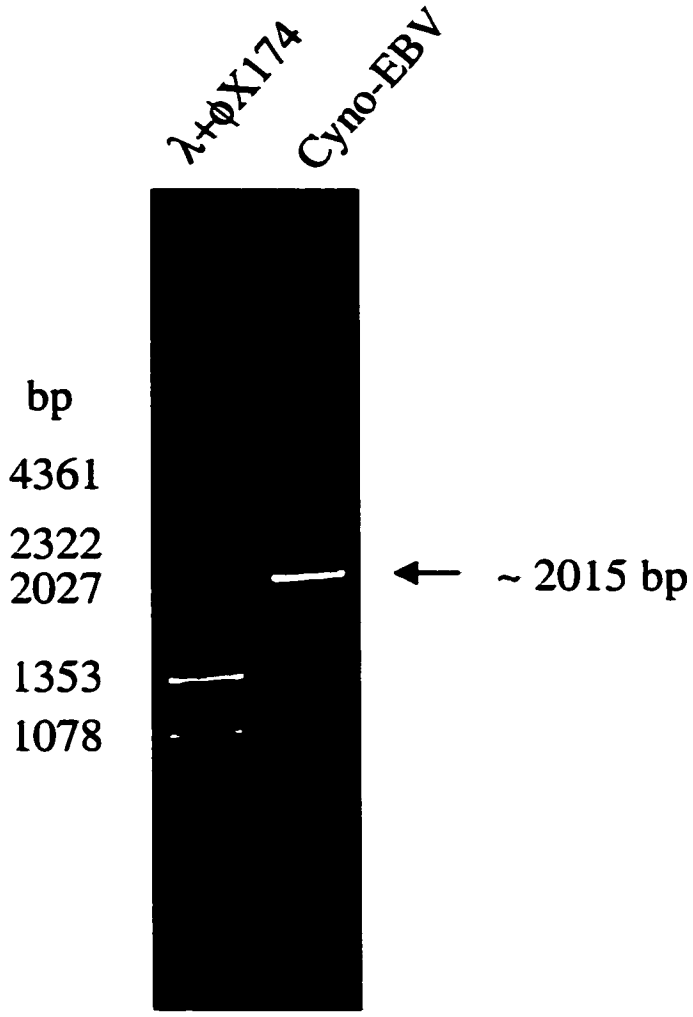
λ+φX174
Cyno-EBV
bp
4361
2322
2027
1353
1078
~ 2015 bp

4). Both sets of primers were designed with KpnI and NotI digestion sites to allow directional insertion into the cloning site of pcDNA3.

D. Nucleotide sequence of Cyno-EBV LMP1 region

Figure 18 shows the nucleotide sequence of 2972 residues from Cyno-EBV LMP1 gene region. The sequence was derived from 3 Cyno-EBV clones, #28, #6 and #8 (Appendix I). From the predicted start site to the termination codon, (shown in blue on Figure 18) the Cyno-EBV LMP1 coding region contained 1933 nt. Except for 80 nt at the 5' end and 5 nt at the 3' end, the entire coding sequence was verified from two clones. Seven in-frame tandem repeats of 27 nt were found from nt 811 to nt 999 from start site. Two additional 60 nt in-frame repeats were found 3' of the 7 repeats (shown in red on Figure 18).

E. Localization of Cyno-EBV LMP1 introns by RT-PCR

Similar to EBV LMP1, the Cyno-EBV LMP1 homologue also appeared to contain two short introns. To confirm these, cDNA was prepared and amplified from 293 cells transfected with Cyno-EBV LMP1 in pcDNA3. Total cellular RNA was reverse transcribed using the primer LMP3' (Table 4). The cDNA was amplified by PCR using the primer pair LMP3'/5' (Table 4) and sequenced. Two introns were found by comparing sequences derived from RNA and DNA LMP1 (data not shown). The first intron (87 nt) was located at nt 263-349 and contained the consensus splice sites $^{5'}$GTGAGT and a $^{3'}$C(N_{11})CAG. The second intron of 82 nt spanned the residues 437-518 and comprised the splice sites $^{5'}$GTAAGC and $^{3'}$C(N_{11})CAG (Figure 18).

Figure 18. Nucleotide sequence of Cyno-EBV LMP1 region.

The nucleotide sequence from Cyno-EBV LMP1 gene region derived from clone #28, #6 and #8. The 2972 nt region sequence contained the predicted start and termination codons (shown in bleu). Two short introns are predicted at positions 263-349 and 437-518 from the start site (shown in green) and splice site consensus sequences are shown in boxes. The predicted coding sequence contains 1764 residues (588 a.a.). The seven 27 nt-tandem repeats and the two 60 nt-repeats are shown in red.

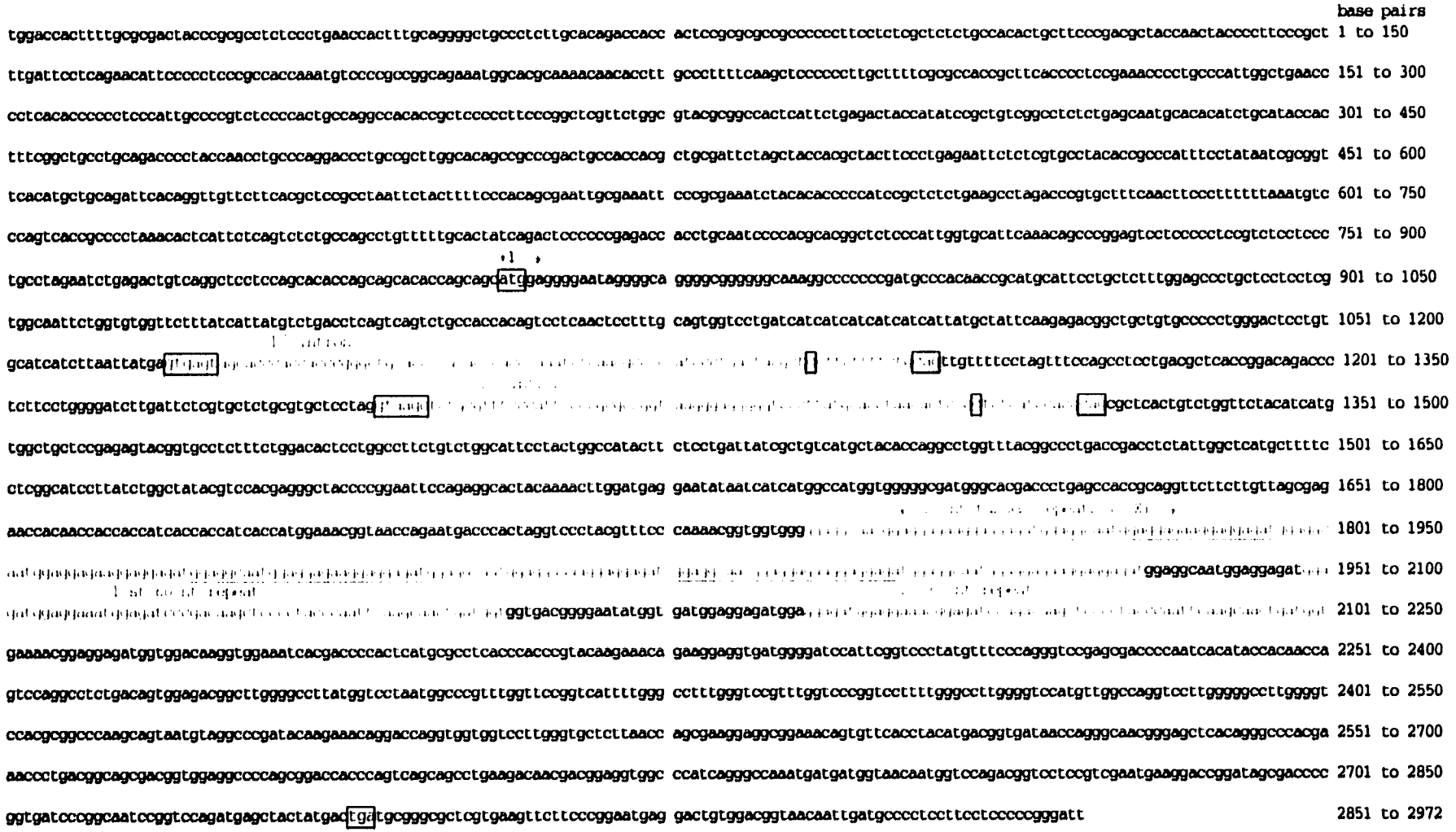
base pairs
1 to 150
151 to 300
301 to 450
451 to 600
601 to 750
751 to 900
901 to 1050
1051 to 1200
1201 to 1350
1351 to 1500
1501 to 1650
1651 to 1800
1801 to 1950
1951 to 2100
2101 to 2250
2251 to 2400
2401 to 2550
2551 to 2700
2701 to 2850
2851 to 2972

F. Predicted amino acid sequence

The predicted amino acid sequence contained 588 a.a. encoded by 3 exons : #1 from nt 1 to 262; # 2, nt 350 to 436 and # 3, nt 519 to 1933 (Figure 18). The size of the protein is the same as the Rhesus-EBV LMP1 (587 a.a.) but it is considerably larger than the EBV and H. papio LMP1s (386 and 389 a.a. respectively). The predicted protein sequence is composed of a short 19 a.a. cytoplasmic amino terminus, 6 transmembrane domains of 22-23 residues each, separated by short stretches of 3-19 a.a. predicted using the software TMHMM2.0 (Sonnhammer et al. 1998) (http://expasy.cbr.nrc.ca/), and a long 404 a.a. cytoplasmic carboxy tail (Figure 19). The difference in size observed between EBV and Cyno-EBV LMP1s resided in the carboxy tail of the two proteins. Cyno-EBV LMP1 contains a carboxy tail twice the size of EBV LMP1. A cluster of 8 histidine residues was found (a.a. 229-236) proximal to the last transmembrane domain in the carboxy tail. The Rhesus-EBV LMP1 also expresses a similar HIS cluster (HIS-10) whereas EBV LMP1 contains a HIS-3 located in a region rich in HIS (H_{187}XXXHXXXHHH) (Appendix III). The seven 27 nt-repeats encode a tandem of the nonapeptide GGNGGEGGD covering residues 256 to 318. The two additional 60 nt. in-frame repeats, encode two 20 a.a. repeats found proximal to the tandem nonapeptides at residues 326-345 and 357-376. The predicted protein contains 6 core motifs PXQXT/S (at residues 338, 369, 396, 425, 485, 581) described as potential binding sites for TRAFs. Interestingly, two of these motifs were part of the two 20 a.a. repeats (Figure 19). Several potential phosphorylation sites were predicted (9 serines, 4 tyrosines) with the program Netphos 2.0 and are shown by black dots on Figure 19 (http://expasy.cbr.nrc.ca/). One potential N-glycosylation site was predicted at N_{518}

Figure 19. Predicted amino acid sequence of Cyno-EBV LMP1.

The predicted Cyno-EBV LMP1 amino acid sequence is shown with the various predicted domains, phosphorylation (marked by black dots) and glycosylation sites (bold). The following domains are shown:

	position	length (a.a.)	symbol
N-terminus	1-19	19	
transmembrane 1	20-41	22	blue
loop (outside)	42-47	6	
transmembrane 2	48-70	23	blue
loop (inside)	71-73	3	
transmembrane 3	74-96	23	blue
loop (outside)	97-102	6	
transmembrane 4	103-125	23	blue
loop (inside)	126-134	9	
transmembrane 5	135-157	23	blue
loop (outside)	158-161	4	
transmembrane 6	162-184	23	blue
C-terminus	185-588	404	
HIS-8 cluster	229-236	8	underlined
9a.a.-tandem repeats (7x)	256-318	63	red
20 a.a.-repeats (2x)	326-345	20	pink
	357-376	20	
$[GPXXPX_6]_3GPXXP$	439-476	38	green with
$[GPXXPX_6]_1GPXXP$	523-538	16	GPXXP
	550-565	16	underlined
P X Q X T/S (6x)	338-342	5	in boxes
	369-373	5	
	396-400	5	
	425-429	5	
	485-489	5	
	581-585	5	

The nucleotide sequence was translated with the Translate Tool, the transmembrane regions and potential phosphorylation sites were predicted with the softwares TMHMM2.0 and Net Phos 2.0 (http://expasy.cbr.nrc.ca/).

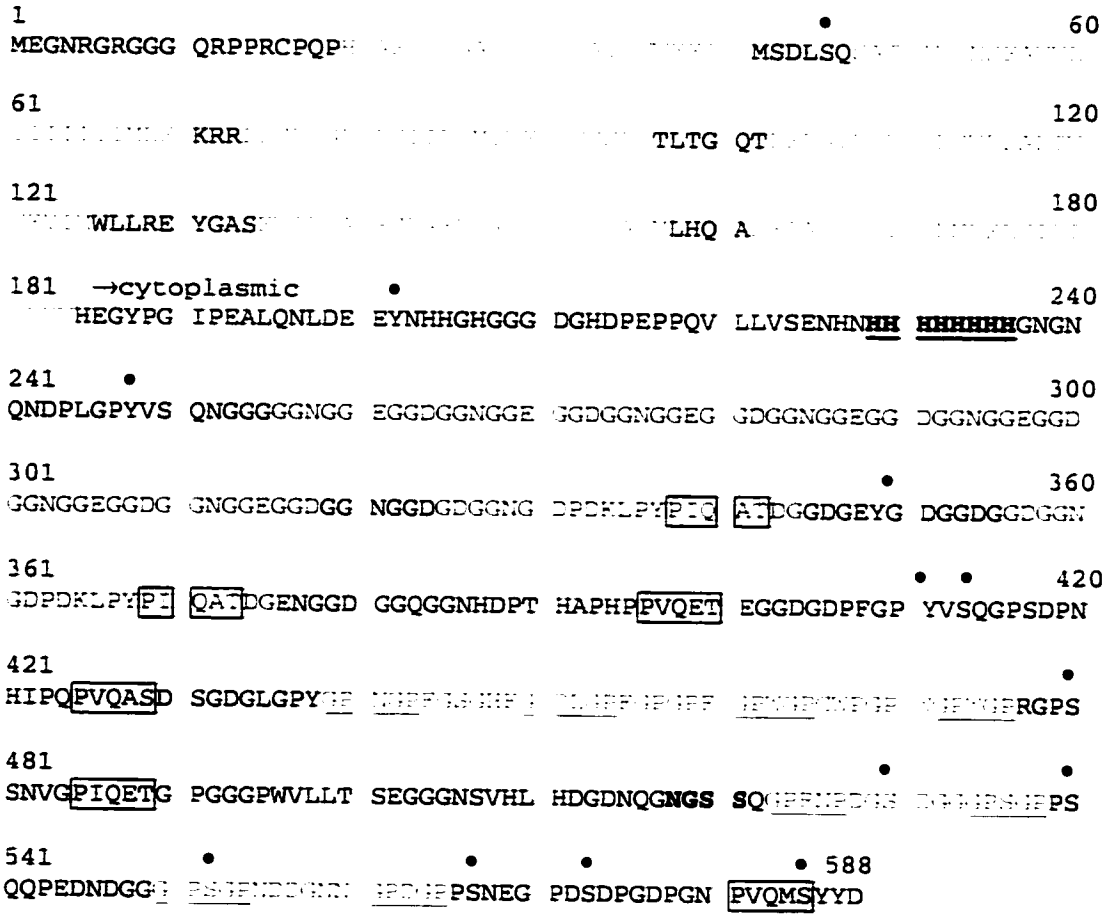
1
MEGNRGRGGG QRPPRCPQP
MSDLSQ
60
61
KRR
TLTG QT
120
121
WLLRE YGAS
LHQ A
180
181 →cytoplasmic
HEGYPG IPEALQNLDE EYNHHGHGGG DGHDPEPPQV LLVSENHNHH HHHHHHGNGN
240
241
QNDPLGPYVS QNGGGGGNGG EGGDGGNGGE GGDGGNGGEG GDGGNGGEGG DGGNGGEGGD
300
301
GGNGGEGGDG GNGGEGGDGG NGGDGDGGNG DPDKLPYPIQ AIDGGDGEYG DGGDGGDGGN
360
361
GDPDKLPYPI QAIDGENGGD GGQGGNHDPT HAPHPPVQET EGGDGDPFGP YVSQGPSDPN
420
421
HIPQPVQASD SGDGLGPY
RGPS
481
SNVGPIQETG PGGGPWVLLT SEGGGNSVHL HDGDNQGNGS SQ
PS
541
QQPEDNDGG
PSNEG PDSDPGDPGN PVQMSYYD
588

(PPSearch, http://workbench.sdsc.edu) however, no glycosylation has been reported for other LMP1s and this would be an uncommon modification as this site is cytoplasmic. Fatty acylation remains another potential modification to the protein. No myristoylation sites were present, however palmitoylation might be involved. The theoritical molecular weight of Cyno-EBV LMP1 was estimated at 60.0 kDa (Protparam, http://expasy.cbr.nrc.ca/). A Kyte and Doolittle (1982) hydropathy plot of the predicted a.a. sequence of Cyno-EBV LMP1 is shown in Appendix II (ProtScale, http://expasy.cbr.nrc.ca/). The six transmembrane domains are clearly delineated and constitute the most hydrophobic regions of the protein. Interestingly, the most hydrophilic region appears to correspond to the HIS cluster (a.a. 229-236). Histidine clusters in other known proteins have been implicated in metal binding and protein-protein interactions (Kondo et al. 1995).

The overall amino acid composition of Cyno-EBV LMP1 was compared to different strains EBV LMP1s (CAO, B95-8, RAJI, Thaiwan) according to Myers and Miller (1989). The conservation varied from 30.3 to 31.5 % identity. The region of poorest homology was the C-terminal 404 amino acids, with only 21.5-22.8% a.a. identity. The transmembrane region showed the best conservation with 51.5 to 54.3% identity. Similarly, H. papio LMP1 shared only 34.7% identical residues with Cyno-EBV LMP1 with 29.7% and 64.8% shared residues in the carboxy and transmembrane regions respectively. In contrast, the Rhesus-EBV LMP1 demonstrated an overall identity of 71.6% with its cynomolgus counterpart. The two proteins were 85-86% identical at their N-terminal and transmembrane regions and 65.6% at their C-terminal.

G. Expression of Cyno-EBV and EBV LMP1 in 293 cells

The poor homology between the LMP1 of Cyno EBV and the LMP1 of EBV suggested that these proteins might have functional differences. Studies were undertaken to compare the ability of the Cyno-EBV and EBV LMP1 proteins to induce NFκB in human 293 cells, and to transform rodent fibroblasts. However, prior to initiating these experiments, it was necessary to assess expression of the genes in transfected cells. Constructs of Cyno-EBV and EBV LMP1/pcDNA3 were transfected into 293 cells (5 μg of LMP1/pcDNA3) and attempts were made to assess LMP1 expression by flow cytometry and Western blot at 16 and 40 hours post-transfection. Transfection efficiencies were monitored by co-transfecting the LMP1/pcDNA3 constructs with a galactosidase expression vector. Comparable levels of galactosidase enzymatic activity in the Cyno-EBV LMP1 and EBV LMP1 transfected cells indicated that both DNA preparations had been transfected with equal efficiency. Previous experiments had demonstrated that the 2 MAb preparations specific for EBV LMP1 did not cross-react with Cyno-EBV shedding cells when assessed either by flow cytometry or Western blot analysis (data not shown). However, to rule out the possibility of lack of reactivity of these MAbs to Cyno-EBV LMP1 due to low antigen concentration, the S12 MAb and the CS1-4 MAbs were tested for their ability to detect Cyno-EBV LMP1 in transfected 293 cells. Neither MAb bound to Cyno-EBV LMP1 when analysed by flow cytometry or Western blot under conditions where EBV LMP1 was detected (Figure 20 and 21). The epitopes recognized by both MAb preparations are known to be in the cytoplasmic tail of LMP1 (Mann et al. 1985; Rowe et al. 1987) a region now known to have only 22% a.a. identity with Cyno-EBV LMP1 (Appendix III). Reports on the presence of LMP1 serum

Figure 20. Flow cytometry detection of Cyno-EBV and EBV LMP1 in transfected 293 cells.

Human 293 cells were transfected with Cyno-EBV LMP1/pcDNA3 or EBV LMP1/pcDNA3 and assayed for LMP1 expression 16 hours post transfection. Cells were permeabilized and reacted with EBV LMP1 MAb S12 or anti-HIS6 MAb. Bound antibodies were revealed with goat anti-mouse IgG-FITC and cells were analyses on an EPICS XL flow cytometer.

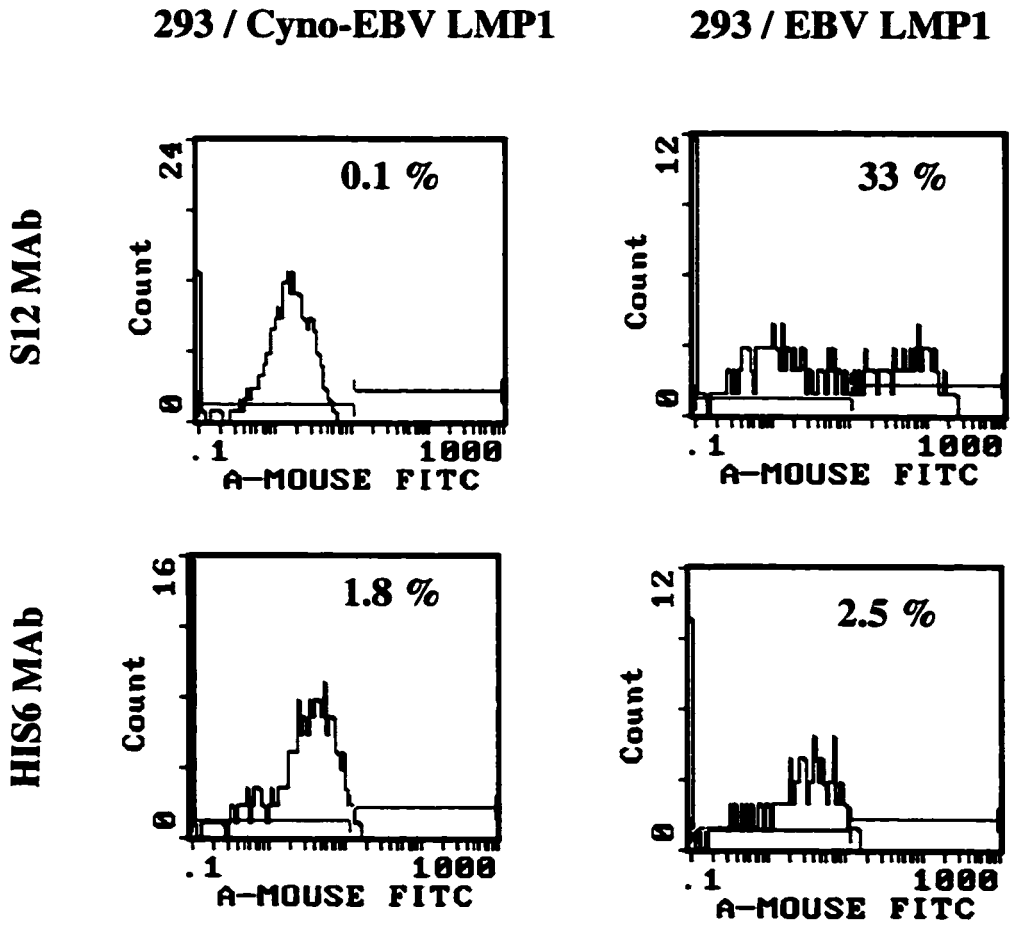
293 / Cyno-EBV LMP1
293 / EBV LMP1
S12 MAb
HIS6 MAb
0.1 %
33 %
1.8 %
2.5 %
Count
24
16
12
0
.1
1000
A-MOUSE FITC

Figure 21. Expression of Cyno-EBV and EBV LMP1 in transfected 293 cells.

Human 293 cells were transfected with Cyno-EBV LMP1/pcDNA3 or EBV LMP1/pcDNA3 and assayed for LMP1 expression 40 hours post-transfection by Western blot analysis. Cell lysates were probed with an anti-HIS6 MAb or the EBV LMP1 MAb S12 as indicated on the figure. Reactivity of the anti-HIS6 MAb for nickel purified preparations of Cyno-EBV LMP1 and lysate of Cyno-EBV is also shown. Molecular weight standards are indicated on the left and the arrow indicates the migration front.

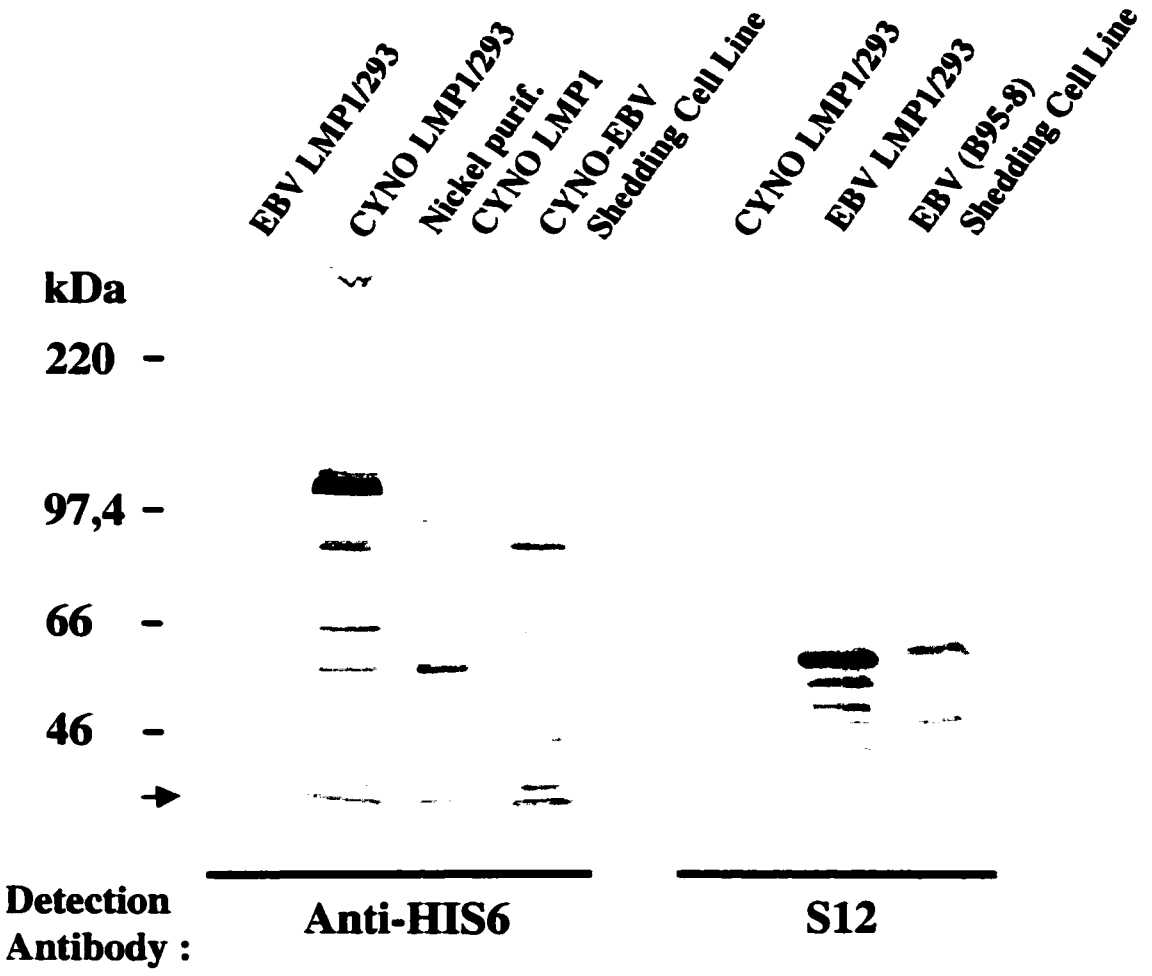
EBV LMP1/293
CYNO LMP1/293
Nickel purif.
CYNO LMP1
CYNO-EBV
Shedding Cell Line
CYNO LMP1/293
EBV LMP1/293
EBV (B95-8)
Shedding Cell Line
kDa
220
97,4
66
46
Detection
Antibody :
Anti-HIS6
S12

antibodies in EBV seropositive carriers (Sulitzeanu et al. 1988; Xu et al. 2000) suggested the possibility that such antibodies might be present in cynomolgus sera. Attempts to detect Cyno-EBV LMP1 using 4 cynomolgus sera and a pool of 5 sera positive to Cyno-EBV poducing cells by IFA were unsuccessful (data not shown).

The presence of a HIS cluster in Cyno-EBV LMP1 allowed for the possibility of detection of the protein using a commercially available MAb to a HIS-6 cluster. Attempts to detect the Cyno-EBV LMP1 by flow cytometry using intracellular staining with this anti-HIS6 MAb were unsuccessful (Figure 20). This lack of reactivity may have resulted from the epitope being inaccessible in LMP1 native state. HIS clusters have been implicated in protein-protein interactions (Kondo et al. 1995). Given that the LMP1 is known to aggregate in the cell membrane, it is conceivable that the HIS cluster is involved in LMP1 aggregation or in the interaction with other cell proteins. The high hydrophilic index predicted for this region in Cyno-EBV LMP1 (Appendix II) is compatible with a role for the HIS cluster in protein interaction. When the anti-HIS6 MAb was tested for reactivity to Cyno-EBV LMP1 transfected cell lysate by Western blot analysis, a major ~110 kDa protein was observed (Figure 21). This protein was not detected when the same cell line was transfected with EBV LMP1/pcDNA3. The size of the protein detected on SDS-PAGE contrasted with the 60 kDa MW predicted from the amino acid composition of Cyno-EBV LMP1. Post-translational modifications of the protein are likely to contribute to this discrepancy, however, MWs obtained from SDS-PAGE analysis of intrinsic membrane proteins can also be unreliable (Gennis 1989). Weaker reactivity was also observed for 10-12 other polypeptides of lower molecular weight. Many of these lower MW polypeptides co-migrated with polypeptides found in

lysates of the Cyno-EBV shedding cell line. None of these polypeptides were detected when the anti-HIS MAb was reacted to 293 cells transfected with EBV LMP1.

The presence of the HIS cluster in LMP1 also suggested the possibility of purification of the protein through the known interaction of HIS with nickel. Attempts were made to purify the LMP1 using a nickel column. A preparation of nickel binding proteins purified from 293 cells transfected with Cyno-EBV LMP1, then probed by Western blot with the anti-HIS6 MAb, revealed many of the low MW polypeptides detected in 293 cells transfected with Cyno-EBV LMP1 and the shedding cell line, but not the major band (Figure 21).

Figure 20 shows that 293 cells transfected with EBV LMP1/pcDNA3 were positive for LMP1 expression, as detected with the S12 MAb by flow cytometry. Cultures harvest 16 hours post-transfection contained 33 % LMP1 expressing cells. This number increased to 50-60 % when cells were harvested 40 hrs post-transfection (data not shown). EBV LMP1 in 293 cells was also visualized by Western blot. The S12 MAb recognized a 55-60 kDa protein in lysates of EBV LMP1/293 cells that co-migrated with a protein detected by the S12 MAb in lysates of EBV shedding cells (Figure 21).

H. Induction of NFκB activity by Cyno-EBV LMP1

The Cyno-EBV LMP1 contains TRAF binding motifs and a carboxy terminus sharing good a.a. conservation with the CTAR2 region of EBV LMP1 (Appendix III). As these regions have been implicated in the induction of NFκB activity in other LMP1s (Franken et al. 1996) Cyno-EBV LMP1 was than tested for its ability to induce NFκB. The induction of NFκB activity by Cyno-EBV and EBV LMP1 in 293 cells was monitored by CAT activity after co-transfection of the constructs LMP1 / pcDNA3 with

NFκB-pBLCAT2, a vector containing 3 NFκB responsive elements upstream of a thymidine kinase promoter driving the chloramphenicol acetyl transferase (CAT) gene. The NFκB specificity of CAT expression in this system was demonstrated using a NFκB negative pBLCAT2 vector, produced by excision of a 60 bp fragment containing the NFκB responsive elements (data not shown). Because it was not possible to normalize CAT activity to amounts of the two LMP1 proteins, all measures of CAT activity were adjusted according to the efficiency of transfection assessed by β-galactosidase activity after co-transfection of the β-galactosidase expression vector.

In the absence of any LMP1 DNA, 293 cells expressed levels of NFκB activity 5 times the background levels. This was demonstrated by the CAT activity induced in 293 cells co-transfected with the vector pcDNA3 alone and the NFκB-pBLCAT2 reporter construct. The levels of NFκB activity in these cells resulted in a 5 fold increase in CAT activity compared to cells that were transfected with pcDNA3 and a CAT reporter construct unresponsive to NFκB (Table 8). This NFκB negative-CAT reporter construct was identical to the original NFκB-pBLCAT2 construct except that the NFκB responsive elements located upstream of the CAT gene had been removed. However, co-transfection of Cyno-EBV LMP1/pcDNA3 and NFκB-pBLCAT2 in 293 cells resulted in a 3,6-fold increase in CAT activity compared to levels seen in cells transfected with pcDNA3 alone. EBV LMP1/pcDNA3 induced a 4,6-fold increase in CAT activity (Table 8). These results are the mean of 4 separate experiments. The CAT activity detected in LMP1 transfected cells appeared to be the result of NFκB activity. The cells co-transfected with the LMP1/pcDNA3 and the NFκB negative-CAT vectors expressed 10

TABLE 8. Induction of NFκB driven CAT activity by Cyno-EBV and EBV LMP1

PROTEIN TESTED	REPORTER CONSTRUCT	MEAN ± SD (n=4)
VECTOR	**NF-κB-CAT**	**1**
EBV LMP-1	**NF-κB-CAT**	**4.6 ± 0.9**
CYNO-EBV LMP-1	**NF-κB-CAT**	**3.6 ± 1.4**
VECTOR	**---------CAT**	**0.2 ± 0.05**
EBV LMP-1	**---------CAT**	**0.4 ± 0.1**
CYNO-EBV LMP-1	**---------CAT**	**0.3 ± 0.1**

times less CAT activity than the same cells co-transfected with the NFκB responsive-CAT construct (Table 8).

I. Toxicity of LMP1 in 293 cells

In the course of these experiments, it was noticed that cells transfected with EBV LMP1 tend to loose adherence in higher proportion than the Cyno-EBV LMP1 cells. Although LMP1 is generally believed to prevent cell death, a report by Hammerschmidt et al. (1989) showed that high levels of EBV LMP1 expression was toxic for human B lymphoid and rodent fibroblast cells, a property that might be associated with a LMP1 domain essential for inducing anchorage independent cell growth. The next experiments were conducted to quantify the toxicity of Cyno-EBV LMP1 in 293 cells relative to what was described for EBV LMP1. Two approaches were taken to demonstrate the toxicity. First, the loss of cell adherence was monitored over time by counting adherent and non-adherent cell populations in transfected cells. Secondly, changes in light scattering properties and viability by propidium iodide staining were performed by flow cytometry.

Loss of cell adherence over time in transfected 293 cells was determined in duplicate cultures at 16 and 48 hours post-transfection (Figure 22). The number of adherent cells after transfection with empty pcDNA3 continued to increase out to 48 hours (Figure 22, insert). Under conditions where transfection efficiencies for all plasmids were the same, the number of adherent cells transfected with Cyno-EBV LMP1 remained static over 48 hours whereas the number of adherent cells following EBV LMP1 transfection declined by 48%. Co-incident with this, the proportion of non-adherent cells increased in EBV LMP1 transfected cultures. For cells transfected with

Figure 22. Cellular growth and loss of cell adherence of human 293 cells transfected with Cyno-EBV LMP1/pcDNA3.

Cell densities of duplicate cultures of 293 cells transfected with Cyno-EBV LMP1/pcDNA3 (triangles), EBV LMP1/pcDNA3 (squares) or pcDNA3 alone (circles) were evaluated by microscopic cell counting in both adherent and non-adherent cell populations. Cell counts done at 16 and 48 hrs post-tranfection showed that the number of adherent cells after EBV LMP1 transfection declined with time whereas cells transfected with Cyno-EBV LMP1 or the vector alone had stable or increased density of adherent cells (insert). This trend in cellular growth was also reflected by the presence of a higher proportion of non-adherent cells in EBV LMP1 transfected cells when compared to cells transfected with Cyno-EBV LMP1 or the vector alone. Values represent the mean of duplicate samples.

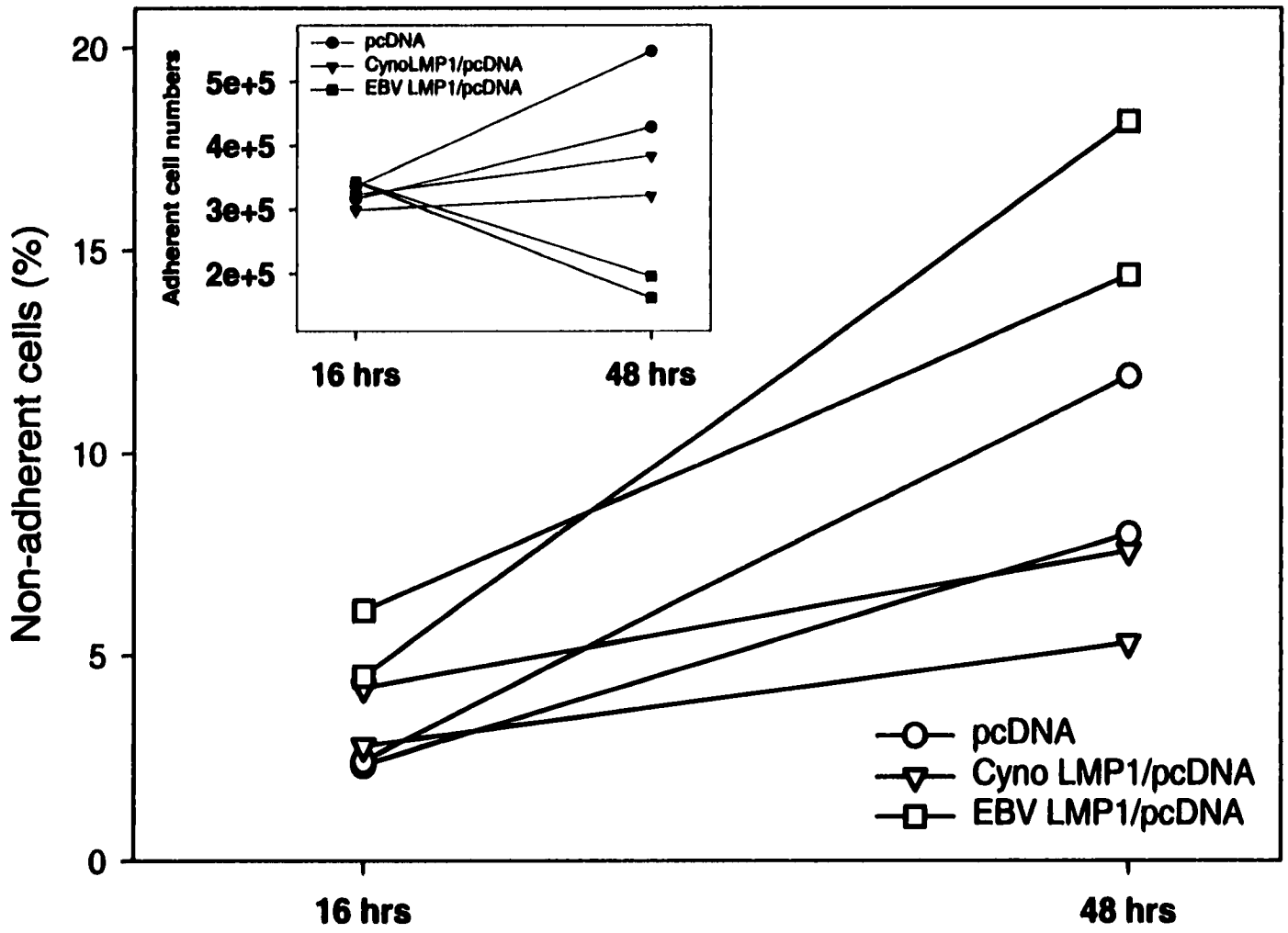
Non-adherent cells (%)
20
15
10
5
0
16 hrs
48 hrs
pcDNA
Cyno LMP1/pcDNA
EBV LMP1/pcDNA
Adherent cell numbers
5e+5
4e+5
3e+5
2e+5
16 hrs
48 hrs
pcDNA
CynoLMP1/pcDNA
EBV LMP1/pcDNA

the vector alone or Cyno-EBV LMP1, the proportion of non-adherent cells never exceeded 10%.

Light scatter properties were assessed using forward (FS) and 90° angle light (SS) scatter. In dying cells, granularity and shrinkage result in increased SS and lower FS values (Sgonc and Gruber 1998). At a single time point, 16 hours post-transfection, adherent and non-adherent cells were analysed for light scatter properties and viability by PI staining (Figure 23). For each transfection, the proportion of cells with scatter properties identical to healthy non-transfected cells (region A, Figure 23) and high SS/low FS properties (region B, Figure 23) were determined in both adherent and non-adherent populations.

For all transfection conditions, the majority of adherent cells showed normal SS/FS properties (93-95%), while over 95% of non-adherent cells were found in region B. As expected, the PI staining confirmed that the non-adherent granular populations contained the highest proportions of non-viable cells (indicated in red). Moreover, these results showed that cell death was higher in cells transfected with EBV LMP1. The percentage of non-viable cells in the EBV LMP1-transfected non-adherent cells was close to 63% compared to 35% in populations transfected with Cyno-EBV LMP1 and 28% in cells transfected with empty vector.

J. Establishment of EBV and Cyno-EBV LMP1 stable transfectants

The establishment of LMP1 expressing cell lines was undertaken in order to better define the long-term effects of LMP1 expression. Stable expression of EBV LMP1 in rodent fibroblast cells was instrumental in the demonstration of the growth transformation and oncogenic properties of LMP1 (Wang et al. 1985). Here, attempts

Figure 23. Viability and light scatter properties of LMP1 transfected 293 cells.

Human 293 cells were transfected with 5 μg of Cyno-EBV LMP1/pcDNA3. EBV LMP1/pcDNA3 or pcDNA3 alone by the calcium phosphate precipitation. Adherent and and non-adherent cells were analysed for viability by propidium iodide (PI) staining and light scatter properties 16 hours post-transfection. The proportion of cells with normal (region A) or high side scatter (SS)/low forward scatter (FS) properties (region B) are shown in blue. Most adherent cells (93-95%) showed normal scatter properties whereas, 95-98% of non-adherent cells showed high SS/low FS properties. The proportion of PI positive cells are shown in red. The analysis was done on a XL flow cytometer (Beckman Coulter) equipped with a 488 nm argon laser.

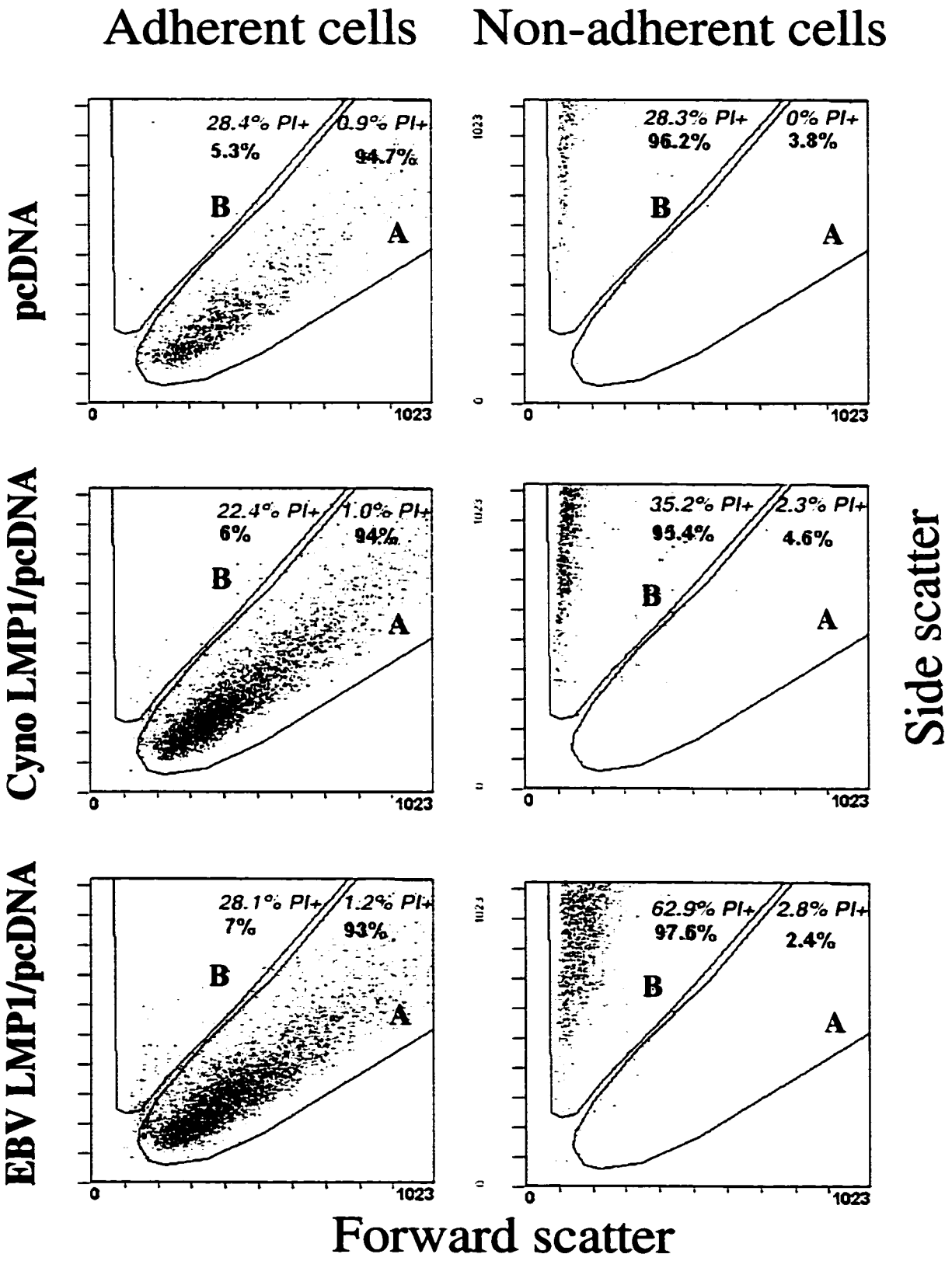
Adherent cells
Non-adherent cells
pcDNA
Cyno LMP1/pcDNA
EBV LMP1/pcDNA
28.4% PI+
5.3%
0.9% PI+
94.7%
28.3% PI+
96.2%
0% PI+
3.8%
22.4% PI+
6%
1.0% PI+
94%
35.2% PI+
95.4%
2.3% PI+
4.6%
28.1% PI+
7%
1.2% PI+
93%
62.9% PI+
97.6%
2.8% PI+
2.4%
B
A
0
1023
Side scatter
Forward scatter

were made to generate stable Cyno-EBV LMP1 expressing cell lines to assess the transformation and oncogenic potential of this protein compared to that of EBV LMP1. NIH 3T3 and Rat-1 cells were transfected with either Cyno-EBV LMP/pcDNA3 or EBV LMP1/pcDNA3 by the calcium chloride method and selected in the presence of G418 antibiotic. Several resistant colonies of NIH 3T3 were isolated and propagated in the presence of G418 for at least 6 weeks. Nine and 5 surviving cell lines transfected with Cyno-EBV LMP1 and EBV LMP1 respectively were screened for expression of LMP1 by flow cytometry and Western blot. None of these cells expressed LMP1 from either virus. Four attempts to generate stable transfectants of Cyno-EBV LMP1 in Rat-1 cells also failed, as all cells died a few days after exposure to G418. In contrast, Rat-1 cells transfected with the vector alone or with EBV LMP1/pcDNA3 survived and expanded in the presence of G418. One cell line expressing EBV LMP1 (clone #19) was isolated from the screening of 30 G418 resistant cell lines. LMP1 expression was demonstrated by flow cytometry analysis of permeabilized cells using both S12 and CS1-4 MAbs (Figure 24). The positive cells constituted 74% of the total cell population and were 10 times brighter than the control LMP1 negative G418 resistant cell lines stained under the same conditions. The EBV LMP1-expressing cells showed no apparent morphologic differences from G418 resistant cells not expressing LMP1. Since no Cyno-EBV LMP1 transfectants were obtained, the transformation and oncogenic properties of the EBV LMP1 clone were not further investigated.

Figure 24. EBV LMP1 expression in Rat-1 stable transfectants

Stable expression of EBV LMP1 in the rodent fibroblast Rat-1 cells. Cells were transfected with EBV LMP1/pcDNA3 by calcium phosphate precipitation and selected in the presence of G418 antibiotic. Intracellular LMP1 staining was done after the cells were permeabilized with the Ortho PermeaFix™ solution. LMP1 was detected using the S12 (hybridoma supernatant dil. ½) and CS1-4 (0.1 μg) MAbs and goat anti-mouse IgG-FITC (1/400). The cells were fixed in 2% paraformaldehyde and analysed on an EPICS XL equipped with a 488 nm argon laser. Analysis of 3 G418 resistant cell lines is shown here.

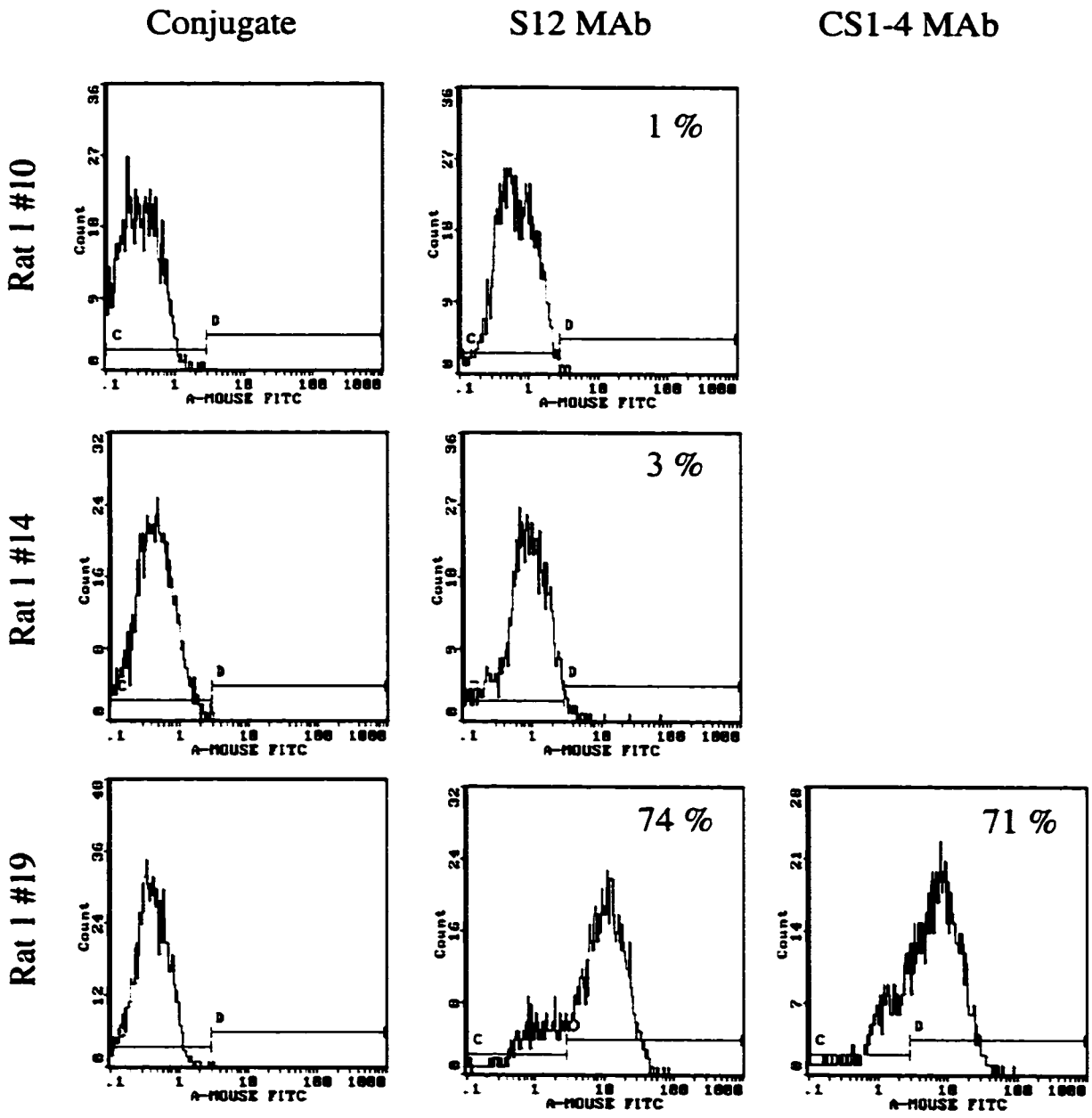
Conjugate
S12 MAb
CS1-4 MAb
Rat 1 #10
Rat 1 #14
Rat 1 #19
1 %
3 %
74 %
71 %
Count
A-MOUSE FITC
C
D

DISCUSSION

The present study of Cyno-EBV was focussed on two aspects of the virus; first, the structural characterization of the virus and its relatedness to EBV and the baboon EBV-like virus H. papio, and secondly, the characterization of its LMP1 gene and some of its functions related to its ability to transform cells.

Like EBV, Cyno-EBV is ubiquitous in the host species, cynomolgus monkey, where the virus was present in 100% of adult animals tested. The proportion of Cyno-EBV seropositive animals in the 5.5 to 9 month old group (60-65%) is within the seroconversion rate reported by Fujimoto et al. (1991). According to these authors, the seronegative animals in this age group are likely to represent individuals who have lost their maternal antibodies but have not yet developed their own.

Fujimoto et al. (1990) have reported that up to 30% of cells in several TsB shedding cell lines harbor viral particles. One of these cell lines, TsB-B6, used in the present study, was assayed for levels of virus producing cells by flow cytometry using a pool of anti-Cyno-EBV sera. Levels of virus producing cells varied from 4 to 29% in agreement with the electron microscopic observations of Fujimoto et al. (1990). Percentages of virus producing cells detected in the H. papio cell line S594 ranged from 2 to 13% with an average of 3% using cynomolgus anti-Cyno-EBV sera. Consistently, Rabin et al. (1977) also reported 3% of virus positive S594 cells as measured using human anti-EBV VCA sera. The high levels of productive infection in the Cyno-EBV shedding cells observed here (Figure 13) support the higher transforming viral titers measured in the Cyno-EBV stock (Figure 12). Whether this ability to grow to high titer

is due to the fact that cynomolgus B cells can support higher level of lytic infection or whether this is a property of Cyno-EBV per se, is not known. However, considering the high rate of lymphomas in immunosuppressed cynomolgus monkeys it is tempting to speculate that a high level of Cyno-EBV productive infection may lead to larger numbers of latently infected cells, which may be a contributing factor to tumor development in these monkeys.

Given the evolutionary distance separating non-human primates from humans, one would expect gamma herpesviruses from Old World Monkeys to be showing more similarity to each other than to the human virus. Surprisingly, the electrophoretic profiles of Cyno-EBV and EBV structural proteins were almost indistinguishable whereas H. papio had a unique profile with only a few proteins co-migrating with those from Cyno-EBV (Figure 6). Most of the major polypeptides detected in the two viruses corresponded to major EBV polypeptides described by Dolyniuk et al. (1976). However, differences in the relative amounts of some polypeptides were noted. Three polypeptides of 28, 152 and 160 kDa, were observed in the EBV preparations of Dolyniuk et al. but did not constitute major constituents in the present viral preparations. The estimated apparent molecular weights of the corresponding polypeptides in the present preparations were estimated to be 30, 145 and 152 kDa. Dolyniuk did report that the relative amounts of the 152 and 160 kDa bands, but not the 28 kDa, varied among viral preparations. This could explain in part the relatively low proportion of these polypeptides observed here. In contrast, these three polypeptides were major constituents of H. papio preparation.

These results of close relatedness between Cyno-EBV and human EBV were confirmed by cross-reactivity studies of monkey and human sera to structural proteins in

Western blots. Antigenic homology between Cyno-EBV, H. papio and EBV as revealed by the cross-reactivity of cynomolgus monkey sera to structural proteins (Figure 8 and 9) confirmed the similarity between Cyno-EBV and EBV antigens and the distinct antigenic profile of H. papio. The polypeptides in EBV recognized by the cynomolgus monkey sera migrated into 4 regions (30, 45-50, 65-80 and 90-120 kDa) and co-localized with the recognized Cyno-EBV antigens. These results were confirmed when EBV positive human sera were tested for reactivity to Cyno-EBV antigens (Figure 9). Cyno-EBV positive sera cross-reacted also with H. papio antigens but, with the exception of the 30 kDa antigen, all other H. papio polypeptides had distinct apparent molecular weight from the other two viruses.

Assays with polyclonal sera revealed the close overall homology between the structural proteins of the human and Cynomolgus viruses, however they did not allow the identification of specific proteins. For this purpose, monoclonal antibodies specific to EBV antigens were tested for cross-reactivity with Cyno-EBV. The observed cross-reativity of anti-gp350 MAb with Cyno-EBV has important implications since gp350 is the major target for vaccine development. In addition, since the gp350 MAb is neutralizing in EBV infection, these observations suggest that the viruses may share neutralizing epitopes. Neutralization assays of Cyno-EBV infection using EBV gp350 MAb would demonstrate such a point. The use of cynomolgus monkeys for testing such a vaccine would have tremendous potential.

In addition to these studies that focused on the relatedness of the structural proteins, the cross-reactivity of a non-structural protein found in the early antigen complex of EBV (EA-D) was also addressed. Homology of the EBV EA-D with a

protein of Cyno-EBV was shown by the cross-reactivity of the EA-D specific R3 MAb with Cyno-EBV in an immunofluorescence assay. This early protein has a diffuse pattern and has been reported to be found in the cell cytoplasm and the nucleus (Henle et al. 1971). Here, proteins from both viruses appeared to localize in the nucleus or at the nuclear periphery (Figure 11).

In contrast with the structural proteins, the latency proteins of the various EBV-like viruses have been shown to be less conserved (Falk et al. 1976; Ohno et al. 1977; Rabin et al. 1980). The results here confirm that LMP1 from Cyno-EBV in particular shares poor homology with the EBV LMP1. The lack of cross-reactivity of all 4 epitopes recognized by the anti-EBV LMP1 MAb preparations S12 and CS1-4 was observed even when the Cyno-EBV LMP1 was presumably present in increased concentration (transfection studies). These MAbs detected the majority of LMP1 encoded by various EBV isolates (Rowe et al. 1987) although antigenic diversity has also been reported among human LMP1s. The S12 MAb does not react with the LMP1 of the EBV strain C15 while the protein is recognized by the CS1-4 MAbs (Miller et al. 1994) despite 97% overall a.a. identity to the B95-8 LMP1 (Miller et al. 1994). In this context, the lack of reactivity of these MAbs with Cyno-EBV LMP1 was indicative of the subsequent divergence observed between the two LMP1 a.a. sequences (see below).

With regard to transforming function of Cyno-EBV, experiments quantifying ability to transform cynomolgus monkey B cells indicated that both Cyno-EBV and H. papio possessed this function. When comparing amount of virus stock required for 50% transforming ability, Cyno-EBV was considerably more efficient (8X). However subsequent experiments indicated that this was due to increased amounts of Cyno-EBV in

stocks rather than to any an inherent property of the virus. Enumeration of negatively stained viral particles against a known concentration of microspheres showed 10 times more viral particles in the Cyno-EBV preparation. This ratio was further confirmed by the estimation of total DNA extracted from viral pellets of both stocks. Although, both of these approaches are semi-quantitative, they supported the conclusion that the apparent superior transforming activity of Cyno-EBV could be explained by a higher viral titer of Cyno-EBV preparation. The possibility of reactivation of endogenous Cyno-EBV in the transformation assays of cynomolgus lymphocytes cannot be excluded since the animals used in these assays were all seropositive. However, spontaneous transformation did not appear to happen frequently since no transformation was observed when PBMC were cultured in the absence of exogenous Cyno-EBV.

The Cyno-EBV LMP1 predicted protein shared only 32% overall a.a. identity with EBV B95-8 LMP1 and an even poorer conservation at the carboxy domain with only 22% a.a. identity. Cyno-EBV LMP1 demonstrated no better homology to EBV LMP1 derived from BL and NPC tumors (Chen et al. 1992; Hatfull et al. 1988). The best homology between the cynomolgus and human viruses was found in the transmembrane domains with conservation of 51-54% a.a. identity. Interestingly, H. papio and Cyno-EBV LMP1 sequences were as distinct from each other as they were from EBV LMP1. H. papio LMP1 shared 35% overall a.a. identity with Cyno-EBV and 32% with EBV LMP1, and only 30 and 27% identity with their respective C-terminal domains. Not surprisingly, the LMP1 protein of Cyno-EBV was most closely related to the homologous protein from the rhesus monkey with 72% overall and 66% C-terminal a.a. identity (Franken et al. 1996). Interestingly, the multialignment analysis showed that the 10 a.a.

deleted region (B95-8 res. 345-354) that occurs in EBV strains CAO and C15 and that has been associated with higher tumorigenicity in rodents appeared to be deleted as well in Cyno-EBV and Rhesus-EBV LMP1s.

Several structural domains have been identified in LMP1. The presence of amino acid repeats within the carboxy tail of LMP1 is a common feature of all human LMP1 proteins examined to date. These repeats are usually 11 a.a in length, with the sequence PQDPDNTDDNG and are positioned in a tandem array of 4 to 7 copies depending on the isolate. The repeats in Cyno-EBV LMP1 contained 9 a.a., reiterated 7 times, and are also aligned in a tandem array (Figure 19). These repeats (GGNGGEGGD) share no homology to the repeats of EBV LMP1 and were not found in *H. papio* or Rhesus-EBV LMP1. In EBV, the number of repeats is usually conserved within a given strain and has been used to type LMP1 proteins. Interestingly, the 11 a.a.-motif $GPXXPX_6$ expressed as part of the repeats in EBV LMP1 (see underlined residues in the sequence above) is conserved in Cyno-EBV and the Rhesus-EBV LMP1s (Appendix VI) although in both monkeys, the motifs were not found within repeats. Cyno-EBV harbored a series of 3 $GPXXPX_6$ sequence downstream from its own repeat regions as well as 2 more reiterations $GPXXPX_6GPXXP$ closer to the carboxy terminus. A series of 3 $GPXXPX_6$ sequence and two additional reiterations $GPXXPX_6GPXXP$ were also observed in Rhesus-EBV LMP1. As expected, human LMP1s expressed the $[GPXXPX_6]_n$ sequence with a variable length of n=4 to n=7 depending on the number of repeats characteristic of individual virus strain (Appendix VI). At present, no function has been described for this motif and its expression in the Rhesus-EBV LMP1 had not been reported. Interestingly, Gires et al. (1999) recently report the association of the Janus kinase 3 (JAK3) to the

proline rich 11 a.a.-repeat region of EBV LMP1. This interaction lead to phosphorylation of JAK3, an essential step for the activation of the STAT transcription factors. The authors claimed to have found a third functional region in the LMP1 carboxy tail involving the JAK/STAT pathway. In light of the motif found within the 11 a.a. repeats of EBV LMP1 and its conservation in both Cyno-EBV and Rhesus-EBV LMP1s, it is tempting to speculate that this motif might be involved in this new LMP1-kinase interaction.

Another interesting finding about the repeats has been reported by Millet et al. (1994). These authors showed that the number of repeats is not always fixed in a given strain and can increases during viral replication. The presence of multiple numbers of repeats was demonstrated in LMP1 derived from oral hairy leukoplakia (HLP) isolates, a tissue supporting permissive infection. PCR amplification of a fragment spanning the repeats of the HLP derived LMP1 DNA revealed the presence of a mix of LMP1 genes with various numbers of repeats. The authors confirmed the presence of a single viral strain, as opposed to a co-infection, by sequencing regions flanking the repeats from individual clones and showed that they were identical except for the numbers of repeats. Amplification of the same DNA fragment in LMP1 derived from latently infected tissues consistently yielded a single number of repeats. These observations lead the authors to suggest that the LMP1 repeats recombined during viral replication leading to the observed LMP1 heterogeneity. The repeats could then constitute a region prone to recombination events.

The presence of several TRAF binding motifs "PXQXT/S" in H. papio and Rhesus-EBV LMP1 contrasts with the EBV LMP1 which harbors only one binding

motif. Like its monkey counterparts, Cyno-EBV LMP1 has several TRAF motifs. In EBV LMP1, the TRAF motif is located proximal to the last transmembrane domain within the CTAR1 region (a.a. 187-231) and upstream from the region harboring the 11 a.a.-repeats. From the multialignment of the monkey and human LMP1s (Appendix III) the PXQXT motif of the monkey LMP1s would define a CTAR1 region distal from the transmembrane domains in these proteins. Interestingly, some of the extra TRAF binding motifs in both H. papio and Rhesus-EBV LMP1 are contained within regions of longer DNA repeats, a feature that was also found in Cyno-EBV LMP1 (Figure 19). Four of the 8 TRAF binding motifs of H. papio LMP1 are part of a 24-a.a. tandem repeat, while two of 6 TRAF binding motifs of Rhesus-EBV LMP1 are found in two 24-a.a. repeats. Similarly, Cyno-EBV LMP1 contained two perfect 20 a.a. repeats harboring two of its 6 TRAF binding motifs. The location of these functional domains within repeat regions in LMP1 of all 3 monkey viruses clearly suggests that this is a common feature of monkey LMP1 and perhaps necessary to their function. The observations by Miller et al. (1994) on the amplification of the numbers of LMP1 repeats during EBV replication and the fact that TRAF binding regions of monkey LMP1s are localized within repeats, support the possibility that these EBV-like viruses might use a recombination mechanism to amplify the numbers of functional motifs important in altering cell survival. A recent report by Mehl et al. (1998) showed that the TRAF motif amplification might not be a restricted feature of monkey virus LMP1s. These authors reported the isolation of a Hodgkin's lymphoma EBV isolate containing two TRAF binding motifs. This isolate had an in-frame insertion within the 11 a.a.-repeat region that coded for 44 a.a. containing an additional TRAF binding motif.

Franken et al. (1996) observed that the core motif PXQXT was not sufficient for functional binding to TRAF3. They tested the binding of TRAF3 to the 12-14 a.a. peptides corresponding to each core motif and their surrounding residues (Appendix V) and defined that a larger motif composed of $P/I,L_{-3}$ $P/H,R_{-2}$ (PXQXT/S) $E,D/G_{+5}$ was expressed in TRAF3 binding motifs. From the alignment of the Cyno-EBV TRAF motifs to those described by Franken et al. (1996) (Appendix V), 4 of the 6 TRAF motifs found in Cyno-EBV LMP1 would be expected to have TRAF3 binding properties (a.a. 338, 369, 396 and 425) including the 2 motifs found in the 20 a.a.-repeat region.

Since interactions with TRAFs lead to the activation of the NFκB pathway, one would expect that additional TRAF binding motifs in the monkey LMP1s would increase the NFκB activity of LMP1. In the present study, Cyno-EBV and EBV LMP1 induced similar levels of NFκB activity in human 293 cells. Very comparable levels were also reported by Franken et al. (1996) with human, rhesus and baboon LMP1s using the same CAT-reporter construct. The reporter construct used in these studies yielded a low signal to noise ratio and this might have contributed to the failure to detect subtle increases in NFκB activity. It is possible that even if many of these predicted TRAF motifs interacted with TRAFs, the effect on NFκB activity might have remain undetected, since for EBV LMP1, the TRAF binding domain CTAR1 is not the sole activator of NFκB activity (Sandberg et al. 1997). Moreover, the contribution of the CTAR1 domain to NFκB activation is likely underestimated in 293 cells since these cells do not express TRAF1 (Devergne et al. 1996). Although the results with Cyno-EBV do not demonstrate an additive effect of the multiple TRAF motifs on NFκB activity, it would be unwise at this point to reject the contribution of additional TRAF motifs to LMP1 function considering

that NFκB activity is not the sole mechanism involved in the transforming potential of LMP1. The transformation of Balb/3T3 cells by LMP1 does not appear to involve NFκB activation (Baichwal and Sugden 1988) and mutants of LMP1 lacking the CTAR1 region are not transforming but are still capable of NFκB activation (Izumi et al. 1997; Mitchell and Sugden 1995). Hence, the finding that the amplification of TRAF motifs may be a conserved mechanism among human and non-human primate viruses suggest that the additional TRAF binding motifs may confer advantages to LMP1 perhaps by altering other cellular signaling pathways that contribute to the transforming properties of LMP1.

Beside TRAF binding motifs, Cyno-EBV LMP1 possesses a HIS-8 cluster located proximal to the last transmembrane domain. This cluster is well conserved in the rhesus and human LMP1s, although only as a HIS-3 cluster in the latter. The HIS-3 cluster of human LMP1s is located in a HIS-rich region (HXXXHXXXHHH) and as for the monkey LMP1s, it corresponds to the protein lowest hydrophobicity region (not shown). Multiple alignment of Cyno-EBV LMP1 with the rhesus and human LMP1s (Appendix III) suggest that this may constitute a conserved feature of the CTAR1 region. No function as been described for this cluster in human or rhesus LMP1s. Such clusters in other proteins have been implicated in metal binding and protein oligomerization (Kondo et al. 1995). It is tempting to speculate that these HIS residues may contribute to LMP1 self-aggregation or interaction with other cellular proteins. LMP1 aggregation in the cell membrane plays a crucial role in the protein's function and this oligomerization relies on the interaction between transmembrane domains of adjacent LMP1 molecules (Gires et al. 1997). So far, the characterization of the CTAR1 region has focused only on its known TRAF binding properties. The LMP1 mutant lacking the core motif of CTAR1

region (a.a. 185-211) also include the HIS-rich region (a.a. 187-197) so it is not clear if these residues contribute to CTAR1 functional properties. A role for these HIS clusters in LMP1 protein structure/function awaits to be demonstrated.

The presence of a HIS-8 cluster in Cyno-EBV LMP1 was fortuitous as this a rather uncommon event in protein sequences. Hence, HIS clusters are often used as an immunologic tag in protein expression studies. Here, the natural HIS-8 tag of Cyno-EBV LMP1 was used to identify the protein with an anti-HIS MAb in lysates of Cyno-EBV LMP1 transfected 293 cells. Several polypeptides detected by the anti-HIS MAb ranged from ~35-110 kDa with a major polypeptide migrating at a M_r of ~110 kDa. The predicted molecular weight value for Cyno-EBV LMP1 was estimated to be 59.8 kDa. By analogy, the predicted molecular weight of EBV LMP1 is estimated at 42.0 kDa but the protein shows a M_r of approximately 63 kDa on SDS-PAGE, a difference of 50% from the predicted M.W. It is assumed that post-translational protein modifications account in part for this discrepancy. Phosphorylation is likely to be involved as this modification is found in EBV LMP1. Several phosphorylation sites have also been predicted in Cyno-EBV LMP1. Fatty acylation is another post-translational modification that could be envisaged since many transmembrane receptors are palmitoylated at cysteine residues adjacent to or within the transmembrane domains (Resh 1999). A recent report from Higuchi et al. (2001) showed that palmitoylation occurred at Cys78 (B95-8) of EBV LMP1 near the cytoplasmic end of the third transmembrane domain. This Cys residue correspond to Cys76 in Cyno-EBV LMP1 and is part of a 6 a.a.-region (LLCPLG) shared by all human and monkey LMP1s (Appendix IV). Conjugation of polyubiquitin chains to the protein may also contribute to the higher molecular weight

observed. EBV LMP1 has recently been shown to be a substrate of the ubiquitin pathway (Aviel et al. 2000). Ubiquitination appeared to involve the free-amino group at the N-terminal as truncation of the first 12 residues prevent the protein degradation. No ubiquitination recognition motif has yet been defined but it is believed to reside in the protein N-terminal Cyno-EBV LMP1 N-terminal domain shares 10 identical residues with EBV LMP1 N-terminal domain (Appendix III). Multialignment of Cyno-EBV LMP1 N-terminal with various strains of EBV LMP1, Rhesus-EBV LMP1 and MyoD, a human transcriptional activator targeted by ubiquitin at the N-terminal (Breitschopf et al. 1998), did not reveal any conserved motifs except for the presence of a glutamic acid at position 2, a proline residue at position 16 (P_{14} in Cyno-EBV and Rhesus-EBV LMP1) and proline doublets in all LMP1 except for the Rhesus-EBV LMP1 (Appendix VII). Whether Cyno-EBV LMP1 is also a target for the ubiquitin degradation pathway remains to be established.

The interaction of the HIS cluster with nickel was also exploited in the present study however; such an interaction had not been reported for any other LMP1s. Nickel purified Cyno-EBV LMP1 preparations yielded multiple bands all of weak intensities ranging from 60 to 90 kDa and no major polypeptide. It is assumed that mature Cyno-EBV LMP1 would be much larger than 60 kDa and that the pattern of bands observed is likely to represent degradation products, especially as similar bands were also present in Cyno-EBV shedding cells and in transfected 293 cells. Baichwal and Sugden have reported similar degradation products in expression studies of EBV LMP1 (1987).

The toxicity of Cyno-EBV LMP1 appeared to vary in different cellular context. In 293 cells, a human epithelial cell line, the transient expression of Cyno-EBV LMP1

impaired cell proliferation and showed little toxicity compare to EBV LMP1 expression as demonstrated by the levels of dead cells (Figure 23). Percentage of dead cells was similar in cells transfected with Cyno-EBV LMP1 and control cells whereas dead cell level was twice as high in EBV LMP1-expressing cultures. Reduced toxicity has also been reported for other monkey LMP1s in another human cell line (Franken et al. 1996) however, no mechanism has been elucidated. Difficulties in stable and transient expression of human LMP1 has often been associated with LMP1 cell toxicity (Hammerschmidt et al. 1989). According to these authors, the N-term. domain would be involved in LMP1 toxicity. Cytostatic activity of LMP1 has also been reported in human epithelial and murine fibroblastic cell lines by Kaykas and Sugden (2000). This effect would be mediated by the EBV LMP1 N-term. and its transmembrane domains. In this regard, although the predicted N-term. domain of Cyno-EBV LMP1 shares limited conservation with EBV LMP1s, its transmembrane region demonstrated a good conservation (Appendix III). One postulate about the inhibition of cell proliferation by EBV LMP1 is that the protein transmembrane domains associate with cellular membrane proteins to induce cytostasis (Kaykas and Sugden 2000). The presence of a palmitoylation site at C_{78} in EBV LMP1 third transmembrane domain and its conservation in the monkey LMP1s (Appendix IV) further support an important role of the transmembrane region in targetting the protein to membrane microdomains, lipid rafts, known to facilitate protein-protein interaction and receptor signaling (Resh 1999).

Inhibition of cell proliferation by LMP1 might be advantageous to EBV life cycle *in vivo*. LMP1 modulation of proliferation of EBV infected cells may contribute to stabilize viral DNA content by promoting proliferation of clones expressing only limited

amount of LMP1 and inhibiting those with high LMP1 levels resulting from high DNA content. This control of proliferation may be contributing to escape from external apoptotic signals as well as from immune surveillance.

In contrast to EBV LMP1, Cyno-EBV LMP1 appeared to be extremely toxic to Rat-1 cells, as the cells were all killed shortly after transfection. Although toxicity of EBV LMP1 has been reported for rodent fibrobasts (Hammerschmidt et al. 1989) here, no marked toxicity was observed when EBV LMP1 was transfected in Rat-1 cells and stable expression of LMP1 was established. Integration of the large 7.4 kb Cyno-EBV LMP1 construct in the cellular genome might also be implicated in the failure to generate a stable transfectant although integration of the EBV LMP1 construct of 7.0 kb did not impair cell survival. The choice of a smaller expression vector would clarify this point. There has been no report of any stable monkey LMP1 transfection in Rat-1 cells. Hence, whether the marked toxicity of Cyno-EBV LMP1 for fibroblast cells Rat-1 is unique to this virus or a common feature of other monkey LMP1s remains to be demonstrated.

CONCLUSION

Cyno-EBV was ubiquitous in the 40 captive adult cynomolgus monkeys tested. Infection appeared to occur horizontally and early in life as 60-65% of 5 to 9 month old monkeys carried Cyno-EBV antibodies. Structural proteins of Cyno-EBV are closely related to EBV proteins. The electrophoretic profile of Cyno-EBV structural proteins was almost indistinguishable from EBV proteins whereas the more closely related virus H. papio harbored a unique protein profile. Using monkey anti-Cyno-EBV and human anti-EBV sera, antigenic homologies between Cyno-EBV and EBV structural proteins were seen for all the major constituents of the virions. Cross-reactivity of cynomolgus antibodies for H. papio structural proteins was also observed and further confirmed the distinct apparent molecular weights of the H. papio proteins. Cyno-EBV appears to possess a gp350 homologue antigenically related to EBV gp350. Interestingly, the gp350 MAb tested here recognized a neutralizing epitope. The conservation of a neutralizing epitope between these two viruses further supports the close relatedness between Cyno-EBV and EBV and suggests the potential utility of Cyno-EBV in testing of anti-gp350 based vaccines.

The Cyno-EBV LMP1 gene sequence predicted a 588 a.a. protein with a short 19 a.a. N-terminus, 6 transmembrane domains and a long carboxy tail of 404 a.a. Both N and C-terminal domains are predicted to face the cell cytoplasm. Cyno-EBV LMP1 shared poor conservation (30-34 % overall a.a. identity) with all other known LMP1s except for the rhesus monkey virus LMP1 with which it shared 72% a.a. identity. However, the cynomolgus monkey protein contained series of repeats in its carboxy tail

(7 reiterations of 9 a.a.-repeats and two 20 a.a.-repeats), a feature shared with all human LMP1s. These repeats have been implicated in recombination events in EBV LMP1. Curiously, despite the lack of conservation between human and Cyno-EBV LMP1 repeats, the motif $GPXXPX_6$ found within the 11 a.a.-repeats of EBV LMP1 was conserved in both Cyno-EBV and Rhesus-EBV LMP1 carboxy tails. This proline-rich motif might be involved in the recently described association of tyrosine kinase JAK3 to the 11 a.a.-repeats of EBV LMP1.

A rather uncommon metal binding cluster of HIS-8 was found in proximity to the last transmembrane domain of Cyno-EBV LMP1. A shorter cluster HIS-3 was also noticed in EBV LMP1 however no function has yet been associated with it. In the present study, the HIS-8 cluster of Cyno-EBV LMP1 was exploited as a protein tag in LMP1 expression studies. Western blot analysis of Cyno-EBV LMP1 transfected 293 cells were probed with an anti-HIS-6 MAb and revealed a major polypeptide of approximately 110 kDa as well as several smaller polypeptides of weaker intensities.

Known LMP1 functional domains were conserved in the Cyno-EBV LMP1 carboxy tail. Six TRAF motifs were found along the carboxy tail with 4 of them expected to have TRAF binding properties. Interestingly, 2 of these TRAF binding motifs were located in the 20 a.a.-repeats. This phenomenon is interesting as amplification of these repeats would therefore increases the numbers of TRAF binding motifs, such a hypothesis has recently been proposed for human LMP1. The LMP1 of Cyno-EBV was tested for its ability to induce NFκB in the human cell line 293 and despite the presence of extra TRAF binding motifs, upregulated NFκB to levels equal to

those induced by EBV LMP1. These results failed to demonstrate an additive effect of the multiple TRAF motifs on NFκB activity in 293 cells.

Several attempts to establish stable Cyno-EBV LMP1 expressing cell lines in the rodent cell line Rat-1 were unsuccessful as cellular death ensued each time shortly after transfection. In contrast, when EBV LMP1 was transfected under the same conditions, stable expression was successfully established.

The marked toxicity of Cyno-EBV LMP1 to Rat-1 cells prevented further comparison of its transforming activity to EBV LMP1 and the other functional assay demonstrated no difference between Cyno-EBV and EBV LMP1s in their capacity to induce NFκB in 293 cells. However, since NFκB activity is very much dependent on the cellular context and does not constitute the sole mechanism involved in the transforming potential of LMP1, the role of the additional TRAF motifs in Cyno-EBV LMP1 function awaited to be demonstrated from further functional studies.

REFERENCES

Ablashi, D.V., P. Gerber, and J. Easton. 1979. Oncogenic herpesviruses of nonhuman primates. Comp Immunol Microbiol Infect Dis 2:229-241.

Agrba, V.Z., L.A. Yakovleva, B.A. Lapin, I.A. Sangulija, V.V. Timanovskaya, D.S. Markarjan, G.N. Chuvirov, and E.A. Salmanova. 1975. The establishment of continuous lymphoblastoid suspension cell cultures from hematopoietic organs of baboon (Papio hamadryas) with malignant lymphoma. Exp. Pathol. (Jena) 10:318-332.

Arch, R.H., R.W. Gedrich, and C.B. Thompson. 1998. Tumor necrosis factor receptor-associated factors (TRAFs)--a family of adapter proteins that regulates life and death. Genes Dev 12:2821-2830.

Aviel, S., G. Winberg, M. Massucci, and A. Ciechanover. 2000. Degradation of the epstein-barr virus latent membrane protein 1 (LMP1) by the ubiquitin-proteasome pathway. Targeting via ubiquitination of the N-terminal residue. J Biol Chem JID - 2985121R 275:23491-23499.

Babcock, G.J., L.L. Decker, M. Volk, and D.A. Thorley-Lawson. 1998. EBV persistence in memory B cells in vivo. Immunity 9:395-404.

Baer, R., A.T. Bankier, M.D. Biggin, P.L. Deininger, P.J. Farrell, T.J. Gibson, G. Hatfull, G.S. Hudson, S.C. Satchwell, C. Seguin, P.S. Tuffnell, and B.G. Barrell. 1984. DNA sequence and expression of the B95-8 Epstein-Barr virus genome. Nature 310:207-211.

Baeuerle, P.A. and V.R. Baichwal. 1997. NF-kappa B as a frequent target for immunosuppressive and anti- inflammatory molecules. Advances in Immunology 65:111-137.

Baichwal, V.R. and B. Sugden. 1987. Posttranslational processing of an Epstein-Barr virus-encoded membrane protein expressed in cells transformed by Epstein-Barr virus. J Virol 61:866-875.

Baichwal, V.R. and B. Sugden. 1988. Transformation of Balb 3T3 cells by the BNLF-1 gene of Epstein-Barr virus. Oncogene 2:461-467.

Baker, S.J. and E.P. Reddy. 1998. Modulation of life and death by the TNF receptor superfamily. Oncogene 17:3261-3270.

Birkenbach, M., D. Liebowitz, F. Wang, J. Sample, and E. Kieff. 1989. Epstein-Barr virus latent infection membrane protein increases vimentin expression in human B-cell lines. J Virol 63:4079-4084.

Blacklow, N.R., B.K. Watson, G. Miller, and B.M. Jacobson. 1971. Mononucleosis with heterophil antibodies and EB virus infection. Acquisition by an elderly patient in hospital. Am J Med 51:549-552.

Bocker, J.F., K.H. Tiedemann, G.W. Bornkamm, and H. zur Hausen. 1980. Characterization of an EBV-like virus from African green monkey lymphoblasts. Virology 101:291-295.

Boldin, M.P., E.E. Varfolomeev, Z. Pancer, I.L. Mett, J.H. Camonis, and D. Wallach. 1995. A novel protein that interacts with the death domain of Fas/APO1 contains a sequence motif related to the death domain. J Biol Chem 270:7795-7798.

Breitschopf, K., E. Bengal, T. Ziv, A. Admon, and A. Ciechanover. 1998. A novel site for ubiquitination: the N-terminal residue, and not internal lysines of MyoD, is essential for conjugation and degradation of the protein. EMBO J JID - 8208664 17:5964-5973.

Brodeur, S.R., G. Cheng, D. Baltimore, and D.A. Thorley-Lawson. 1997. Localization of the major NF-kappaB-activating site and the sole TRAF3 binding site of LMP-1 defines two distinct signaling motifs. J Biol Chem 272:19777-19784.

Chen, H.L., K. Hayashi, T.R. Koirala, H. Ino, K. Fujimoto, Y. Yoshikawa, C.R. Choudhury, and T. Akagi. 1997. Malignant lymphoma induction in rabbits by oral inoculation of crude virus fraction prepared from Ts-B6 cells (cynomolgus B-lymphoblastoid cells harboring Epstein-Barr virus-related simian herpesvirus). Acta Medica Okayama 51:141-147.

Chen, M.L., C.N. Tsai, C.L. Liang, C.H. Shu, C.R. Huang, D. Sulitzeanu, S.T. Liu, and Y.S. Chang. 1992. Cloning and characterization of the latent membrane protein (LMP) of a specific Epstein-Barr virus variant derived from the nasopharyngeal carcinoma in the Taiwanese population. Oncogene 7:2131-2140.

Chen, M.R., S.J. Chang, H. Huang, and J.Y. Chen. 2000. A protein kinase activity associated with Epstein-Barr virus BGLF4 phosphorylates the viral early antigen EA-D in vitro. J Virol 74:3093-3104.

Chiang, A.K., K.Y. Wong, A.C. Liang, and G. Srivastava. 1999. Comparative analysis of Epstein-Barr virus gene polymorphisms in nasal T/NK-cell lymphomas and normal nasal tissues: implications on virus strain selection in malignancy. Int J Cancer 80:356-364.

Chinnaiyan, A.M., K. O'Rourke, M. Tewari, and V.M. Dixit. 1995. FADD, a novel death domain-containing protein, interacts with the death domain of Fas and initiates apoptosis. Cell 81:505-512.

Cox, C., B.A. Naylor, M. Mackett, J.R. Arrand, B.E. Griffin, and N. Wedderburn. 1998. Immunization of common marmosets with Epstein-Barr virus (EBV) envelope glycoprotein gp340: effect on viral shedding following EBV challenge. J. Med. Virol. 55:255-261.

D'Souza, B., M. Rowe, and D. Walls. 2000. The bfl-1 gene is transcriptionally upregulated by the Epstein-Barr virus LMP1, and its expression promotes the survival of a Burkitt's lymphoma cell line. J Virol 74:6652-6658.

Dawson, C.W., J. Dawson, R. Jones, K. Ward, and L.S. Young. 1998. Functional differences between BHRF1, the Epstein-Barr virus-encoded Bcl-2 homologue, and Bcl-2 in human epithelial cells. J Virol 72:9016-9024.

Deinhardt, F., L. Falk, L.G. Wolfe, A. Schudel, M. Nonoyama, P. Lai, B. Lapin, and L. Yakovleva. 1978. Susceptibility of marmosets to Epstein-Barr virus-like baboon herpesviruses. Primates Med 10:163-170.

Deinhardt, F., L.A. Falk, and L.G. Wolfe. 1974. Transformation of nonhuman primate lymphocytes by Epstein-Barr virus. Cancer Research 34:1241-1244.

Devergne, O., E. Hatzivassiliou, K.M. Izumi, K.M. Kaye, M.F. Kleijnen, E. Kieff, and G. Mosialos. 1996. Association of TRAF1, TRAF2, and TRAF3 with an Epstein-Barr virus LMP1 domain important for B-lymphocyte transformation: role in NF-kappaB activation. Mol. Cell Biol. 16:7098-7108.

Devergne, O., E.C. McFarland, G. Mosialos, K.M. Izumi, C.F. Ware, and E. Kieff. 1998. Role of the TRAF binding site and NF-kappaB activation in Epstein-Barr virus latent membrane protein 1-induced cell gene expression. J Virol 72:7900-7908.

Dhanasekaran, N. 1998. Cell signaling: an overview. Oncogene 17:1329-1330.

Dillner, J., H. Rabin, N. Letvin, W. Henle, G. Henle, and G. Klein. 1987. Nuclear DNA-binding proteins determined by the Epstein-Barr virus-related simian lymphotropic herpesviruses H. gorilla, H. pan, H. pongo and *H. papio*. J Gen Virol 87:1587-1596.

Djatchenko, A.G., V.V. Kakubava, B.A. Lapin, V.Z. Agrba, L.A. Yakovleva, and E.I. Samilchuk. 1976. Continuous lymphoblastoid suspension cultures from cells of haematopoietic organs of baboons with malignant lymphoma--biological characterization and biological properties of the herpes virus associated with culture cells. Exp. Pathol. (Jena) 12:163-168.

Dolyniuk, M., R. Pritchett, and E. Kieff. 1976. Proteins of Epstein-Barr virus. I. Analysis of the polypeptides of purified enveloped Epstein-Barr virus. J Virol 17:935-949.

Dragovich, T., C.M. Rudin, and C.B. Thompson. 1998. Signal transduction pathways that regulate cell survival and cell death. Oncogene 17:3207-3213.

Eliopoulos, A.G., S.M. Blake, J.E. Floettmann, M. Rowe, Young, and LS. 1999. Epstein-Barr virus-encoded latent membrane protein 1 activates the JNK pathway through its extreme C terminus via a mechanism involving TRADD and TRAF2. J Virol 73:1023-1035.

Eliopoulos, A.G., C.W. Dawson, G. Mosialos, J.E. Floettmann, M. Rowe, R.J. Armitage, J. Dawson, J.M. Zapata, D.J. Kerr, M.J. Wakelam, J.C. Reed, E. Kieff, and L.S. Young. 1996. CD40-induced growth inhibition in epithelial cells is mimicked by Epstein-Barr Virus-encoded LMP1: involvement of TRAF3 as a common mediator. Oncogene 13:2243-2254.

Eliopoulos, A.G., N.J. Gallagher, S.M. Blake, C.W. Dawson, and L.S. Young. 1999. Activation of the p38 mitogen-activated protein kinase pathway by Epstein-Barr virus-encoded latent membrane protein 1 coregulates interleukin-6 and interleukin-8 production. J Biol Chem 274:16085-16096.

Eliopoulos, A.G., M. Stack, C.W. Dawson, K.M. Kaye, L. Hodgkin, S. Sihota, M. Rowe, and L.S. Young. 1997. Epstein-Barr virus-encoded LMP1 and CD40 mediate IL-6 production in epithelial cells via an NF-kappaB pathway involving TNF receptor-associated factors. Oncogene 14:2899-2916.

Emini, E.A., J. Luka, M.E. Armstrong, F.S. Banker, P.J. Provost, and G.R. Pearson. 1986. Establishment and characterization of a chronic infectious mononucleosislike syndrome in common marmosets. J. Med. Virol. 18:369-379.

Emini, E.A., W.A. Schleif, M. Silberklang, D. Lehman, and R.W. Ellis. 1989. Vero cell-expressed Epstein-Barr virus (EBV) gp350/220 protects marmosets from EBV challenge. J. Med. Virol. 27:120-123.

Epstein, M.A., B.C. Achong, and Y.M. Barr. 1964. Virus particles in cultured lymphoblasts from Burkitt's lymphoma. Lancet i:702-703.

Epstein, M.A., A.J. Morgan, S. Finerty, B.J. Randle, and J.K. Kirkwood. 1985. Protection of cottontop tamarins against Epstein-Barr virus-induced malignant lymphoma by a prototype subunit vaccine. Nature 318:287-289.

Erickson, K.D. and J.M. Martin. 1997. Early detection of the lytic LMP-1 protein in EBV-infected B-cells suggests its presence in the virion. Virology 234:1-13.

Ernberg, I., G. Klein, B.C. Giovanella, J. Stehlin, K.J. McCormick, M. Andersson-Anvret, P. Aman, and D. Killander. 1983. Relationship between the amounts of EBV-DNA and EBNA per cell, clonability and tumorigenicity in two ebv-negative lymphoma lines and their EBV-converted sublines. Int J Cancer 83:163-169.

Fahraeus, R., L. Rymo, J.S. Rhim, and G. Klein. 1990. Morphological transformation of human keratinocytes expressing the LMP gene of Epstein-Barr virus. Nature 345:447-449.

Falk, L., F. Deinhardt, M. Nonoyama, L.G. Wolfe, and C. Bergholz. 1976. Properties of a baboon lymphotropic herpesvirus related to Epstein-Barr virus. Int J Cancer 18:798-807.

Falk, L., L. Wolfe, F. Deinhardt, J. Paciga, L. Dombos, G. Klein, W. Henle, and G. Henle. 1974. Epstein-Barr virus: transformation of non-human primate lymphocytes in vitro. Int J Cancer 13:363-376.

Falk, L.A., G. Henle, W. Henle, F. Deinhardt, and A. Schudel. 1977. Transformation of lymphocytes by Herpesvirus papio. Int J Cancer 20:219-226.

Farrell, P.J., M. Hollyoake, G. Niedobitek, A. Agathanggelou, A. Morgan, and N. Wedderburn. 1997. Direct demonstration of persistent Epstein-Barr virus gene expression

in peripheral blood of infected common marmosets and analysis of virus- infected tissues in vivo. J Gen Virol 78 (Pt 6):1417-1424.

Feichtinger, H., S.L. Li, E. Kaaya, P. Putkonen, K. Grunewald, K. Weyrer, D. Bottiger, I. Ernberg, A. Linde, G. Biberfeld, and P. Biberfeld. 1992. A monkey model for Epstein Barr virus-associated lymphomagenesis in human acquired immunodeficiency syndrome. J. Exp. Med. 176:281-286.

Feichtinger, H., P. Putkonen, C. Parravicini, S.L. Li, E.E. Kaaya, D. Bottiger, G. Biberfeld, and P. Biberfeld. 1990. Malignant lymphomas in cynomolgus monkeys infected with simian immunodeficiency virus. Am. J. Pathol. 137:1311-1315.

Finerty, S., J. Tarlton, M. Mackett, M. Conway, J.R. Arrand, P.E. Watkins, and A.J. Morgan. 1992. Protective immunization against Epstein-Barr virus-induced disease in cottontop tamarins using the virus envelope glycoprotein gp340 produced from a bovine papillomavirus expression vector. J Gen Virol 73 (Pt 2):449-453.

Fischer, E., C. Delibrias, and M.D. Kazatchkine. 1991. Expression of CR2 (the C3dg/EBV receptor, CD21) on normal human peripheral blood T lymphocytes. J Immunol 146:865-869.

Floettmann, J.E., A.G. Eliopoulos, M. Jones, L.S. Young, and M. Rowe. 1998. Epstein-Barr virus latent membrane protein-1 (LMP1) signalling is distinct from CD40 and involves physical cooperation of its two C-terminus functional regions. Oncogene 17:2383-2392.

Franken, M., B. Annis, A.N. Ali, and F. Wang. 1995. 5' Coding and regulatory region sequence divergence with conserved function of the Epstein-Barr virus LMP2A homolog in herpesvirus papio. J Virol 69:8011-8019.

Franken, M., O. Devergne, M. Rosenzweig, B. Annis, E. Kieff, and F. Wang. 1996. Comparative analysis identifies conserved tumor necrosis factor receptor-associated factor 3 binding sites in the human and simian Epstein-Barr virus oncogene LMP1. J Virol 70:7819-7826.

Fregeau, C.J., R.A. Aubin, J.C. Elliott, S.S. Gill, and R.M. Fourney. 1995. Characterization of human lymphoid cell lines GM9947 and GM9948 as intra- and interlaboratory reference standards for DNA typing. Genomics 28:184-197.

Fries, K.L., W.E. Miller, and N. Raab-Traub. 1996. Epstein-Barr virus latent membrane protein 1 blocks p53-mediated apoptosis through the induction of the A20 gene. J Virol 70:8653-8659.

Fries, K.L., T.B. Sculley, J. Webster-Cyriaque, P. Rajadurai, R.H. Sadler, and N. Raab-Traub. 1997. Identification of a novel protein encoded by the BamHI A region of the Epstein-Barr virus. J Virol 71:2765-2771.

Fuentes-Panana, E.M., S. Swaminathan, and P.D. Ling. 1999. Transcriptional activation signals found in the Epstein-Barr virus (EBV) latency C promoter are conserved in the latency C promoter sequences from baboon and Rhesus monkey EBV-like lymphocryptoviruses (cercopithicine herpesviruses 12 and 15). J Virol 73:826-833.

Fujimoto, K. and S. Honjo. 1991. Presence of antibody to Cyno-EBV in domestically bred cynomolgus monkeys (Macaca fascicularis). J Med Primat 20:42-45.

Fujimoto, K., K. Terato, J. Miyamoto, H. Ishiko, M. Fujisaki, F. Cho, and S. Honjo. 1990. Establishment of a B-lymphoblastoid cell line infected with Epstein-Barr-related virus from a cynomolgus monkey (Macaca fascicularis). J Med Primat 19:21-30.

Gaffey, M.J. and L.M. Weiss. 1992. Association of Epstein-Barr virus with human neoplasia. Pathol Annu 27 Pt 1:55-74.

Gennis, R.B. 1989. Characterization and Structural Principles of Membrane Proteins. p. 85-137. In C.R. Cantor (ed.) Biomembranes, Molecular Structure and Function. Springer-Verlag, New York.

Gerber, P., S.S. Kalter, G. Schidlovsky, W.D.J. Peterson, and M.D. Daniel. 1977. Biologic and antigenic characteristics of Epstein-Barr virus-related Herpesviruses of chimpanzees and baboons. Int J Cancer 20:448-459.

Gires, O., F. Kohlhuber, E. Kilger, M. Baumann, A. Kieser, C. Kaiser, R. Zeidler, B. Scheffer, M. Ueffing, and W. Hammerschmidt. 1999. Latent membrane protein 1 of Epstein-Barr virus interacts with JAK3 and activates STAT proteins. EMBO Journal 18:3064-3073.

Gires, O., U. Zimber-Strobl, R. Gonnella, M. Ueffing, G. Marschall, R. Zeidler, D. Pich, and W. Hammerschmidt. 1997. Latent membrane protein 1 of Epstein-Barr virus mimics a constitutively active receptor molecule. EMBO Journal 16:6131-6140.

Greifenegger, N., M. Jager, L.A. Kunz-Schughart, H. Wolf, and F. Schwarzmann. 1998. Epstein-Barr virus small RNA (EBER) genes: differential regulation during lytic viral replication. J Virol 72:9323-9328.

Griffiths, G. and P. Rottier. 1992. Cell biology of viruses that assemble along the biosynthetic pathway. Semin. Cell Biol. 3:367-381.

Grogan, E., H. Jenson, J. Countryman, L. Heston, L. Gradoville, and G. Miller. 1987. Transfection of a rearranged viral DNA fragment, WZhet, stably converts latent Epstein-Barr viral infection to productive infection in lymphoid cells. Proc Natl Acad Sci U S A 84:1332-1336.

Hammerschmidt, W., B. Sugden, and V.R. Baichwal. 1989. The transforming domain alone of the latent membrane protein of Epstein- Barr virus is toxic to cells when expressed at high levels. J Virol 63:2469-2475.

Hatfull, G., A.T. Bankier, B.G. Barrell, and P.J. Farrell. 1988. Sequence analysis of Raji Epstein-Barr virus DNA. Virology 164:334-340.

Hatzoglou, A., J. Roussel, M.F. Bourgeade, E. Rogier, C. Madry, J. Inoue, O. Devergne, and A. Tsapis. 2000. TNF receptor family member BCMA (B cell maturation) associates with TNF receptor-associated factor (TRAF) 1, TRAF2, and TRAF3 and activates NF-kappa B, elk-1, c-Jun N-terminal kinase, and p38 mitogen-activated protein kinase. J Immunol 165:1322-1330.

Hayashi, K., T.R. Koirala, H. Ino, H.L. Chen, N. Ohara, N. Teramoto, T. Yoshino, K. Takahashi, M. Yamada, and S. Nii. 1995. Malignant lymphoma induction in rabbits by intravenous inoculation of Epstein-Barr-virus-related herpesvirus from HTLV-II-transformed cynomolgus leukocyte cell line (Si-IIA). Int J Cancer 63:872-880.

Hayashi, K., N. Ohara, T.R. Koirala, H. Ino, H.L. Chen, N. Teramoto, E. Kondo, T. Yoshino, K. Takahashi, and M. Yamada. 1994. HTLV-II non-integrated malignant lymphoma induction in Japanese white rabbits following intravenous inoculation of HTLV-II-infected simian leukocyte cell line (Si-IIA). Jpn. J. Cancer Res. 85:808-818.

Heberling, R.L., C.P. Bieber, and S.S. Kalter. 1981. Establishment of a lymphoblastoid cell line from a lymphomatous cynomolgus monkey. p. 385-386. In D.S. Yohn and J.R. Blakoslee (eds.) Advances in Comparative Leukemia Research. Elsevier North Holland, Inc.

Heller, M., P. Gerber, and E. Kieff. 1981. Herpesvirus papio DNA is similar in organization to Epstein-Barr virus DNA. J Virol 37:698-709.

Heller, M. and E. Kieff. 1981. Colinearity between the DNAs of Epstein-Barr virus and herpesvirus papio. J Virol 37:821-826.

Henderson, S., M. Rowe, C. Gregory, D. Croom-Carter, F. Wang, R. Longnecker, E. Kieff, and A. Rickinson. 1991. Induction of bcl-2 expression by Epstein-Barr virus latent membrane protein 1 protects infected B cells from programmed cell death. Cell 65:1107-1115.

Henle, G., W. Henle, and G. Klein. 1971. Demonstration of two distinct components in the early antigen complex of Epstein-Barr virus-infected cells. Int J Cancer 8:272-282.

Herrero, J.A., P. Mathew, and C.V. Paya. 1995. LMP-1 activates NF-kappa B by targeting the inhibitory molecule I kappa B alpha. J Virol 69:2168-2174.

Higgins, D.G., A.J. Bleasby, and R. Fuchs. 1992. CLUSTAL V: improved software for multiple sequence alignment. Comput Appl Biosci 8:189-191.

Higuchi, M., K.M. Izumi, and E. Kieff. 2001. Epstein-Barr virus latent-infection membrane proteins are palmitoylated and raft-associated: protein 1 binds to the cytoskeleton through TNF receptor cytoplasmic factors. Proc Natl Acad Sci U S A JID - 7505876 98:4675-4680.

Holth, L.T., D.N. Chadee, V.A. Spencer, S.K. Samuel, J.R. Safneck, and J.R. Davie. 1998. Chromatin, nuclear matrix and the cytoskeleton: role of cell structure in neoplastic transformation (review). Int J Oncol 13:827-837.

Hsu, H., J. Huang, H.B. Shu, V. Baichwal, and D.V. Goeddel. 1996. TNF-dependent recruitment of the protein kinase RIP to the TNF receptor-1 signaling complex. Immunity 4:387-396.

Hsu, H., J. Xiong, and D.V. Goeddel. 1995. The TNF receptor 1-associated protein TRADD signals cell death and NF-kappa B activation. Cell 81:495-504.

Hu, L.F., E.R. Zabarovsky, F. Chen, S.L. Cao, I. Ernberg, G. Klein, and G. Winberg. 1991. Isolation and sequencing of the Epstein-Barr virus BNLF-1 gene (LMP1) from a Chinese nasopharyngeal carcinoma. J Gen Virol 72 (Pt 10):2399-2409.

Hudson, G.S., P.J. Farrell, and B.G. Barrell. 1985. Two related but differentially expressed potential membrane proteins encoded by the EcoRI Dhet region of Epstein-Barr virus B95-8. J Virol 53:528-535.

Huen, D.S., S.A. Henderson, D. Croom-Carter, and M. Rowe. 1995. The Epstein-Barr virus latent membrane protein-1 (LMP1) mediates activation of NF-kappa B and cell surface phenotype via two effector regions in its carboxy-terminal cytoplasmic domain. Oncogene 10:549-560.

Hummel, M. and E. Kieff. 1982. Epstein-Barr virus RNA. VIII. Viral RNA in permissively infected B95-8 cells. J Virol 43:262-272.

Hummel, M. and E. Kieff. 1982. Mapping of polypeptides encoded by the Epstein-Barr virus genome in productive infection. Proc Natl Acad Sci U S A 79:5698-5702.

Ichijo, H. 1999. From receptors to stress-activated MAP kinases. Oncogene 18:6087-6093.

Imai, S., J. Nishikawa, and K. Takada. 1998. Cell-to-cell contact as an efficient mode of Epstein-Barr virus infection of diverse human epithelial cells. J Virol 72:4371-4378.

Ino, H., K. Hayashi, H. Yanai, N. Teramoto, T.R. Koirala, Chen, HL, T. Oka, T. Yoshino, K. Takahashi, and T. Akagi. 1997. Analysis of the genome of an Epstein-Barr-virus (EBV)-related herpesvirus in a cynomolgus monkey cell line (Si-IIA). Acta Medica Okayama 51:207-212.

Ishida, T. and P. Varavudhi. 1992. Wild long-tailed macaques (Macaca fascicularis) in Thailand are highly infected with gamma herpes virus but not with simian T-lymphotropic retrovirus of type 1. Fol. Primatol. 59:163-168.

Ishida, T. and K. Yamamoto. 1987. Survey of nonhuman primates for antibodies reactive with Epstein- Barr virus (EBV) antigens and susceptibility of their lymphocytes for immortalization with EBV. J Med Primat 16:359-371.

Izumi, K.M., K.M. Kaye, and E.D. Kieff. 1997. The Epstein-Barr virus LMP1 amino acid sequence that engages tumor necrosis factor receptor associated factors is critical for primary B lymphocyte growth transformation. Proc Natl Acad Sci U S A 94:1447-1452.

Izumi, K.M. and E.D. Kieff. 1997. The Epstein-Barr virus oncogene product latent membrane protein 1 engages the tumor necrosis factor receptor-associated death domain protein to mediate B lymphocyte growth transformation and activate NF-kappaB. Proc Natl Acad Sci U S A 94:12592-12597.

Izumi, K.M., E.C. McFarland, E.A. Riley, D. Rizzo, Y. Chen, and E. Kieff. 1999. The residues between the two transformation effector sites of epstein- barr virus latent membrane protein 1 are not critical for B-lymphocyte growth transformation. J Virol 73:9908-9916.

Izumi, K.M., E.C. McFarland, A.T. Ting, E.A. Riley, B. Seed, and E.D. Kieff. 1999. The Epstein-Barr virus oncoprotein latent membrane protein 1 engages the tumor necrosis factor receptor-associated proteins TRADD and receptor-interacting protein (RIP) but does not induce apoptosis or require RIP for NF-kappaB activation. Mol. Cell Biol. 19:5759-5767.

Jiwa, N.M., J.J. Oudejans, D.F. Dukers, W. Vos, A. Horstman, P. Van der Valk, J.M. Middledorp, J.M. Walboomers, and C.J. Meijer. 1995. Immunohistochemical demonstration of different latent membrane protein-1 epitopes of Epstein-Barr virus in lymphoproliferative diseases. Journal of Clinical Pathology 48:438-442.

Karin, M. 1999. How NF-kappaB is activated: the role of the IkappaB kinase (IKK) complex. Oncogene 18:6867-6874.

Kasamatsu, H. and A. Nakanishi. 1998. How do animal DNA viruses get to the nucleus? Annu Rev Microbiol 52:627-686.

Kawanishi, M. 2000. The Epstein-Barr virus latent membrane protein 1 (LMP1) enhances TNF alpha-induced apoptosis of intestine 407 epithelial cells: the role of LMP1 C-terminal activation regions 1 and 2. Virology 270:258-266.

Kaye, K.M., O. Devergne, J.N. Harada, K.M. Izumi, R. Yalamanchili, E. Kieff, and G. Mosialos. 1996. Tumor necrosis factor receptor associated factor 2 is a mediator of NF-kappa B activation by latent infection membrane protein 1, the Epstein- Barr virus transforming protein. Proc Natl Acad Sci USA 93:11085-11090.

Kaye, K.M., K.M. Izumi, H. Li, E. Johannsen, D. Davidson, R. Longnecker, and E. Kieff. 1999. An epstein-barr virus that expresses only the first 231 LMP1 amino acids efficiently initiates primary B-lymphocyte growth transformation. J Virol 73:10525-10530.

Kaykas, A. and B. Sugden. 2000. The amino-terminus and membrane-spanning domains of LMP-1 inhibit cell proliferation. Oncogene 19:1400-1410.

Kieff, E. 1996. Epstein-Barr Virus and its Replication. p. 1109-1146. In B.N. Fields, D.M. Knipe, and P.M. Howley (eds.) Fundamental Virology. Lippincott-Raven, Philadelphia.

Kieser, A., E. Kilger, O. Gires, M. Ueffing, W. Kolch, and W. Hammerschmidt. 1997. Epstein-Barr virus latent membrane protein-1 triggers AP-1 activity via the c-Jun N-terminal kinase cascade. EMBO Journal 16:6478-6485.

Kikuta, H., Y. Taguchi, K. Tomizawa, K. Kojima, N. Kawamura, A. Ishizaka, Y. Sakiyama, S. Matsumoto, S. Imai, T. Kinoshita, and et al. 1988. Epstein-Barr virus genome-positive T lymphocytes in a boy with chronic active EBV infection associated with Kawasaki-like disease. Nature 333:455-457.

Kingma, D.W., W.B. Weiss, E.S. Jaffe, S. Kumar, K. Frekko, and M. Raffeld. 1996. Epstein-Barr virus latent membrane protein-1 oncogene deletions: correlations with malignancy in Epstein-Barr virus--associated lymphoproliferative disorders and malignant lymphomas. Blood 88:242-251.

Klein, G. 1994. Epstein-Barr virus strategy in normal and neoplastic B cells. Cell 77:791-793.

Koirala, T.R., K. Hayashi, H.L. Chen, H. Ino, N. Kariya, Yanai, C.R. Choudhury, and T. Akagi. 1997. Malignant lymphoma induction of rabbits with oral spray of Epstein-Barr virus-related herpesvirus from Si-IIA cells (HTLV-II-transformed Cynomolgus cell line): a possible animal model for Epstein-Barr virus infection and subsequent virus-related tumors in humans. Pathol. Intern. 47:442-448.

Kokosha, L.V., V.Z. Agrba, B.A. Lapin, L.A. Yakovleva, N.N. Arshba, T.P. Markova, and V.V. Pimanovskaja. 1977. Continuous lymphoblastoid suspension cultures from cells of haematopoietic organs of baboons with malignant lymphoma. Report III: Immunological studies. Exp. Pathol. (Jena) 13:247-254.

Kondo, K., T. Ozaki, Y. Nakamura, and S. Sakiyama. 1995. DAN gene product has an affinity for Ni2+. Biochem Biophys Res Commun 216:209-215.

Krappmann, D., F. Emmerich, U. Kordes, E. Scharschmidt, B. Dorken, and C. Scheidereit. 1999. Molecular mechanisms of constitutive NF-kappaB/Rel activation in Hodgkin/Reed-Sternberg cells. Oncogene 18:943-953.

Kulwichit, W., R.H. Edwards, E.M. Davenport, J.F. Baskar, V. Godfrey, and N. Raab-Traub. 1998. Expression of the Epstein-Barr virus latent membrane protein 1 induces B cell lymphoma in transgenic mice. Proc Natl Acad Sci USA 95:11963-11968.

Kuppers, R. and K. Rajewsky. 1998. The origin of Hodgkin and Reed/Sternberg cells in Hodgkin's disease. Annu Rev Immunol 16:471-493.

Kurilla, M.G., T. Heineman, L.C. Davenport, E. Kieff, and L.M. Hutt-Fletcher. 1995. A novel Epstein-Barr virus glycoprotein gp150 expressed from the BDLF3 open reading frame. Virology 209:108-121.

Kyte, J. and R.F. Doolittle. 1982. A simple method for displaying the hydropathic character of a protein. J Mol Biol 157:105-132.

Laabi, Y. and A. Strasser. 2000. Immunology. Lymphocyte survival--ignorance is BLys. Science 289:883-884.

Laemmli, U.K. 1970. Cleavage of structural proteins during the assembly of the head of bacteriophage T4. Nature 227:680-685.

Lee, M.A., M.E. Diamond, and J.L. Yates. 1999. Genetic evidence that EBNA-1 is needed for efficient, stable latent infection by Epstein-Barr virus. J Virol 73:2974-2982.

Leppa, S. and D. Bohmann. 1999. Diverse functions of JNK signaling and c-Jun in stress response and apoptosis. Oncogene 18:6158-6162.

Levitskaya, J., A. Sharipo, A. Leonchiks, A. Ciechanover, and M.G. Masucci. 1997. Inhibition of ubiquitin/proteasome-dependent protein degradation by the Gly-Ala repeat domain of the Epstein-Barr virus nuclear antigen 1. Proc Natl Acad Sci USA 94:12616-12621.

Li, B.M., Z.W. Ji, Z.S. Liu, and Y. Zeng. 1997. Epstein-Barr virus in synergy with tumor-promoter-induced malignant transformation of immortalized human epithelial cells. J Cancer Res Clin Oncol 123:441-446.

Li, Q., M.K. Spriggs, S. Kovats, S.M. Turk, M.R. Comeau, B. Nepom, and L.M. Hutt-Fletcher. 1997. Epstein-Barr virus uses HLA class II as a cofactor for infection of B lymphocytes. J Virol 71:4657-4662.

Li, Q., S.M. Turk, and L.M. Hutt-Fletcher. 1995. The Epstein-Barr virus (EBV) BZLF2 gene product associates with the gH and gL homologs of EBV and carries an epitope critical to infection of B cells but not of epithelial cells. J Virol 69:3987-3994.

Li, S.L., P. Biberfeld, and I. Ernberg. 1994. DNA of lymphoma-associated herpesvirus (HVMF1) in SIV-infected monkeys (Macaca fascicularis) shows homologies to EBNA-1, -2 and - 5 genes. Int J Cancer 59:287-295.

Li, S.L., H. Feichtinger, E. Kaaya, P. Migliorini, P. Putkonen, G. Biberfeld, J.M. Middeldorp, P. Biberfeld, and I. Ernberg. 1993. Expression of Epstein-Barr-virus-related nuclear antigens and B- cell markers in lymphomas of SIV-immunosuppressed monkeys. Int J Cancer 55:609-615.

Liebowitz, D., R. Kopan, E. Fuchs, J. Sample, and E. Kieff. 1987. An Epstein-Barr virus transforming protein associates with vimentin in lymphocytes. Molecular and Cellular Biology 7:2299-2308.

Liebowitz, D., D. Wang, and E. Kieff. 1986. Orientation and patching of the latent infection membrane protein encoded by Epstein-Barr virus. J Virol 58:233-237.

Ling, P.D. and S.D. Hayward. 1995. Contribution of conserved amino acids in mediating the interaction between EBNA2 and CBF1/RBPJk. J Virol 69:1944-1950.

Ling, P.D., J.J. Ryon, and S.D. Hayward. 1993. EBNA-2 of herpesvirus papio diverges significantly from the type A and type B EBNA-2 proteins of Epstein-Barr virus but retains an efficient transactivation domain with a conserved hydrophobic motif. J Virol 67:2990-3003.

Liu, Z., Y. Liu, and Y. Zeng. 1998. Synergistic effect of Epstein-Barr virus and tumor promoters on induction of lymphoma and carcinoma in nude mice. J Cancer Res Clin Oncol 124:541-548.

Luckow, B. and G. Schutz. 1987. CAT constructions with multiple unique restriction sites for the functional analysis of eukaryotic promoters and regulatory elements. Nucleic Acids Res 15:5490.

Mackett, M., M.J. Conway, J.R. Arrand, R.S. Haddad, and L.M. Hutt-Fletcher. 1990. Characterization and expression of a glycoprotein encoded by the Epstein-Barr virus BamHI I fragment. J Virol 64:2545-2552.

Mackey, D. and B. Sugden. 1997. Studies on the mechanism of DNA linking by Epstein-Barr virus nuclear antigen 1. J. Biol. Chem. 272:29873-29879.

Malinin, N.L., M.P. Boldin, A.V. Kovalenko, and D. Wallach. 1997. MAP3K-related kinase involved in NF-kappaB induction by TNF, CD95 and IL-1. Nature 385:540-544.

Mann, K.P., D. Staunton, and D.A. Thorley-Lawson. 1985. Epstein-Barr virus-encoded protein found in plasma membranes of transformed cells. J Virol 55:710-720.

Mannick, J.B., J.I. Cohen, M. Birkenbach, A. Marchini, and E. Kieff. 1991. The Epstein-Barr virus nuclear protein encoded by the leader of the EBNA RNAs is important in B-lymphocyte transformation. J Virol 65:6826-6837.

Masucci, M.G. 1993. Viral immunopathology of human tumors. Curr Opin Immunol 5:693-700.

McClure, H.M. 1973. Tumors in nonhuman primates: observations during a six-year period in the Yerkes primate center colony. Am J Phys Anthropol 38:425-429.

Mehl, A.M., N. Fischer, M. Rowe, F. Hartmann, H. Daus, L. Trumper, M. Pfreundschuh, N. Muller-Lantzsch, and F.A. Grasser. 1998. Isolation and analysis of two strongly transforming isoforms of the Epstein-Barr-Virus(EBV)-encoded latent membrane protein-1 (LMP1) from a single Hodgkin's lymphoma. Int J Cancer 76:194-200.

Menezes, J., W. Leibold, and G. Klein. 1975. Biological differences between Epstein-Barr virus (EBV) strains with regard to lymphocyte transforming ability, superinfection and antigen induction. Exp Cell Res 92:478-484.

Mercurio, F. and A.M. Manning. 1999. NF-kappaB as a primary regulator of the stress response. Oncogene 18:6163-6171.

Miller, G. 1990. The switch between latency and replication of Epstein-Barr virus. J Infect Dis 161:833-844.

Miller, G., T. Shope, D. Lisco, D. Stitt, and M. Lipman. 1972. Epstein-Barr Virus. Transformation, Cytopathic Changes and Viral Antigens in Squirrel Monkey and Marmoset Leukocytes. Proc Natl Acad Sci U S A 69:383-387.

Miller, W.E., J.L. Cheshire, and N. Raab-Traub. 1998. Interaction of tumor necrosis factor receptor-associated factor signaling proteins with the latent membrane protein 1 PXQXT motif is essential for induction of epidermal growth factor receptor expression. Molecular and Cellular Biology 18:2835-2844.

Miller, W.E., H.S. Earp, and N. Raab-Traub. 1995. The Epstein-Barr virus latent membrane protein 1 induces expression of the epidermal growth factor receptor. J Virol 69:4390-4398.

Miller, W.E., R.H. Edwards, D.M. Walling, and N. Raab-Traub. 1994. Sequence variation in the Epstein-Barr virus latent membrane protein 1 [published erratum appears in J Gen Virol 1995 May;76(Pt 5):1305]. J Gen Virol 75:2729-2740.

Minarovits, J., L.F. Hu, S. Imai, Y. Harabuchi, A. Kataura, S. Minarovits-Kormuta, T. Osato, and G. Klein. 1994. Clonality, expression and methylation patterns of the Epstein-Barr virus genomes in lethal midline granulomas classified as peripheral angiocentric T cell lymphomas. J Gen Virol 75:77-84.

Mitchell, T. and B. Sugden. 1995. Stimulation of NF-kappa B-mediated transcription by mutant derivatives of the latent membrane protein of Epstein-Barr virus. J Virol 69:2968-2976.

Miyamoto, K., N. Tomita, K. Hayashi, and T. Akagi. 1990. Transformation of animal cells with human T-cell leukemia virus type II. Jpn. J. Cancer Res. 81:720-722.

Miyashita, E.M., B. Yang, G.J. Babcock, and D.A. Thorley-Lawson. 1997. Identification of the site of Epstein-Barr virus persistence in vivo as a resting B cell [published erratum appears in J Virol 1998 Nov;72(11):9419]. J Virol 71:4882-4891.

Monroe, J.H. and P.M. Brandt. 1970. Rapid semiquantitative method for screening large numbers of virus samples by negative staining electron microscopy. Appl Microbiol 20:259-262.

Moorthy, R. and D.A. Thorley-Lawson. 1992. Mutational analysis of the transforming function of the EBV encoded LMP-1. Curr Top Microbiol Immunol 182:359-365.

Moorthy, R.K. and D.A. Thorley-Lawson. 1993. All three domains of the Epstein-Barr virus-encoded latent membrane protein LMP-1 are required for transformation of rat-1 fibroblasts. J Virol 67:1638-1646.

Moorthy, R.K. and D.A. Thorley-Lawson. 1993. Biochemical, genetic, and functional analyses of the phosphorylation sites on the Epstein-Barr virus-encoded oncogenic latent membrane protein LMP-1. J Virol 67:2637-2645.

Morgan, A.J. 1995. Development of Epstein-Barr Virus Vaccines. In Andrew J.Morgan (ed.)R. G. Landes Company, Austin, Texas.

Mori, M., H. Kurozumi, K. Akagi, Y. Tanaka, S. Imai, and T. Osato. 1992. Monoclonal proliferation of T cells containing Epstein-Barr virus in fatal mononucleosis [letter]. N Engl J Med 327:58.

Mosialos, G., M. Birkenbach, R. Yalamanchili, T. VanArsdale, C. Ware, and E. Kieff. 1995. The Epstein-Barr virus transforming protein LMP1 engages signaling proteins for the tumor necrosis factor receptor family. Cell 80:389-399.

Mueller, N. 1999. Overview of the epidemiology of malignancy in immune deficiency. J Acquir Immune Defic Syndr 21 Suppl 1:S5-10.

Myers, E.W. and W. Miller. 1989. CABIOS 4:11-17.

Neil, J.C., E.R. Cameron, and E.W. Baxter. 1997. p53 and tumour viruses: catching the guardian off-guard. Trends Microbiol 5:115-120.

Neubauer, R.H., H. Rabin, B.C. Strnad, M. Nonoyama, and W.A. Nelson-Rees. 1979. Establishment of a lymphoblastoid cell line and isolation of an Epstein-Barr-related virus of gorilla origin. J Virol 79:845-848.

Nolan, L.A. and A.J. Morgan. 1995. The Epstein-Barr virus open reading frame BDLF3 codes for a 100-150 kDa glycoprotein. J Gen Virol 76 (Pt 6):1381-1392.

Oba, D.E. and L.M. Hutt-Fletcher. 1988. Induction of antibodies to the Epstein-Barr virus glycoprotein gp85 with a synthetic peptide corresponding to a sequence in the BXLF2 open reading frame. J Virol 62:1108-1114.

Ohno, S., J. Luka, L. Falk, and G. Klein. 1977. Detection of a nuclear, EBNA-type antigen in apparently EBNA- negative Herpesvirus papio (HVP)-transformed lymphoid lines by the acid-fixed nuclear binding technique. Int J Cancer 77:941-946.

Ohno, S., J. Luka, L.A. Falk, and G. Klein. 1978. Serological reactivities of human and baboon sera against EBNA and Herpesvirus papio-determined nuclear antigen (HUPNA). Eur. J. Cancer 78:955-960.

Paulson, E.J. and S.H. Speck. 1999. Differential methylation of epstein-barr virus latency promoters facilitates viral persistence in healthy seropositive individuals. J Virol 73:9959-9968.

Peng, M. and E. Lundgren. 1993. Transient expression of the Epstein-Barr virus LMP1 gene in B-cell chronic lymphocytic leukemia cells, T cells, and hematopoietic cell lines: cell-type-independent-induction of CD23, CD21, and ICAM-1. Leukemia 7:104-112.

Prachova, K., J. Roubal, V.Z. Agrba, V.V. Timanovskaya, and A.F. Voevodin. 1983. Functional complementation between Epstein-Barr virus and herpesvirus papio. Intervirology 19:52-55.

Pulford, D.J., P. Lowrey, and A.J. Morgan. 1995. Co-expression of the Epstein-Barr virus BXLF2 and BKRF2 genes with a recombinant baculovirus produces gp85 on the cell surface with antigenic similarity to the native protein. J Gen Virol 76 (Pt 12):3145-3152.

Rabin, H. 1985. In vivo Studies of Epstein-Barr Virus and Other Lymphotropic Herpesviruses of Primates. p. 147-170. In B. Roizman and C. Lopez (eds.) The Herpesviruses. Plenum Press, New York.

Rabin, H., R.H. Neubauer, R.F. Hopkins, and S. Rasheed. 1978. In vitro lymphocyte transformation by Epstein-Barr virus (EBV)-like viruses isolated from Old-World non-human primates. IARC Sci Publ 553-557.

Rabin, H., R.H. Neubauer, R.F.3. Hopkins, E.K. Dzhikidze, Z.V. Shevtsova, and B.A. Lapin. 1977. Transforming activity and antigenicity of an Epstein-Barr-like virus from lymphoblastoid cell lines of baboons with lymphoid disease. Intervirology 77;8:240-249.

Rabin, H., B.C. Strnad, R.H. Neubauer, A.M. Brown, R.F.3. Hopkins, and R.A. Mazur. 1980. Comparisons of nuclear antigens of Epstein-Barr virus (EBV) and EBV-like simian viruses. J Gen Virol 80:265-272.

Rangan, S.R., L.N. Martin, B.E. Bozelka, N. Wang, and B.J. Gormus. 1986. Epstein-Barr virus-related herpesvirus from a rhesus monkey (Macaca mulatta) with malignant lymphoma. Int J Cancer 38:425-432.

Rasheed, S., R.W. Rongey, J. Bruszweski, W.A. Nelson-Rees, H. Rabin, R.H. Neubauer, G. Esra, and M.B. Gardner. 1977. Establishment of a cell line with associated Epstein-Barr-like virus from a leukemic orangutan. Science 77:407-409.

Resh, M.D. 1999. Fatty acylation of proteins: new insights into membrane targeting of myristoylated and palmitoylated proteins. Biochim Biophys Acta 1451:1-16.

Rickinson, A.B. and E. Kieff. 1996. Epstein-Barr Virus. p. 2397-2446. In B.N. Fields, D.M. Knipe, and P.M. Howley (eds.) Fields Virology. Lippincott-Raven, Philadelphia.

Ricksten, A., B. Kallin, H. Alexander, J. Dillner, R. Fahraeus, G. Klein, R. Lerner, and L. Rymo. 1988. BamHI E region of the Epstein-Barr virus genome encodes three transformation-associated nuclear proteins. Proc Natl Acad Sci USA 88:995-999.

Ring, C.J. 1994. The B cell-immortalizing functions of Epstein-Barr virus. [Review]. J Gen Virol 75:1-13.

Rothe, M., S.C. Wong, W.J. Henzel, and D.V. Goeddel. 1994. A novel family of putative signal transducers associated with the cytoplasmic domain of the 75 kDa tumor necrosis factor receptor. Cell 78:681-692.

Rowe, M., H.S. Evans, L.S. Young, K. Hennessy, E. Kieff, and A.B. Rickinson. 1987. Monoclonal antibodies to the latent membrane protein of Epstein-Barr virus reveal heterogeneity of the protein and inducible expression in virus-transformed cells. J Gen Virol 68 (Pt 6):1575-1586.

Sambrook, J., E.F. Fritsch, and T. Maniatis. 1989. Molecular Cloning. In N. Ford, C. Nolan, and M. Ferguson (eds.)Cold Spring Harbor Laboratory Press, Cold Spring Harbor, New York.

Sanchez-Pinel, A., J. Bernad, H. Rives, L. Lapchine, J. Icart, and J. Didier. 1991. Identification of a novel EBV-induced membrane glycoprotein of 43 kDa with H667 MAb. Virology 180:31-40.

Sandberg, M., W. Hammerschmidt, and B. Sugden. 1997. Characterization of LMP-1's association with TRAF1, TRAF2, and TRAF3. J Virol 71:4649-4656.

Santon, A., C. Martin, A.I. Manzanal, M.V. Preciado, and C. Bellas. 1998. Paediatric Hodgkin's disease in Spain: association with Epstein-Barr virus strains carrying latent membrane protein-1 oncogene deletions and high frequency of dual infections. Br J Haematol 103:129-136.

Schatzl, H., M. Tschikobava, D. Rose, A. Voevodin, H. Nitschko, E. Sieger, U. Busch, K. von der Helm, and B. Lapin. 1993. The Sukhumi primate monkey model for viral lymphomogenesis: high incidence of lymphomas with presence of STLV-I and EBV-like virus. Leukemia 7 Suppl 2:S86-S92.

Scholle, F., R. Longnecker, and N. Raab-Traub. 1999. Epithelial cell adhesion to extracellular matrix proteins induces tyrosine phosphorylation of the Epstein-Barr virus latent membrane protein 2: a role for C-terminal Src kinase. J Virol 73:4767-4775.

Schultheiss, U., S. Puschner, E. Kremmer, T.W. Mak, H. Engelmann, W. Hammerschmidt, and A. Kieser. 2001. TRAF6 is a critical mediator of signal transduction by the viral oncogene latent membrane protein 1. EMBO J JID - 8208664 20:5678-5691.

Schwarzmann, F., M. Jager, N. Prang, and H. Wolf. 1998. The control of lytic replication of Epstein-Barr virus in B lymphocytes (Review). Int. J. Mol. Med. 1:137-142.

Serio, T.R., J.L. Kolman, and G. Miller. 1997. Late gene expression from the Epstein-Barr virus BcLF1 and BFRF3 promoters does not require DNA replication in cis. J Virol 71:8726-8734.

Sgonc, R. and J. Gruber. 1998. Apoptosis detection: an overview. Exp Gerontol 33:525-533.

Sixbey, J.W. and Q.Y. Yao. 1992. Immunoglobulin A-induced shift of Epstein-Barr virus tissue tropism. Science 255:1578-1580.

Sonnhammer, E.L.L., G. von Heijne, and A. Krogh. 1998. A hidden Markov model for predicting transmembrane helices in protein sequences. p. 175-182. In J. Glasgow, T. Littlejohn, F. Major, R. Lathrop, D. Sankoff, and C. Sensen (eds.) Proc. of Sixth Int. Conf. on Intelligent Systems for Molecular Biology. AAAI Press, Menlo Park, CA.

Straus, S.E., J.I. Cohen, G. Tosato, and J. Meier. 1993. NIH conference. Epstein-Barr virus infections: biology, pathogenesis, and management. Annals of Internal Medicine 118:45-58.

Sugden, B. 1992. EBV's open sesame. Trends Biochem Sci 17:239-240.

Sulitzeanu, D., R. Szigeti, A. Hatzubai, J. Dillner, M.L. Hammarskjold, G. Klein, and E. Klein. 1988. Antibodies in human sera against the Epstein-Barr virus encoded latent membrane protein (LMP). Immunology Letters 88:301-306.

Suzushima, H., N. Asou, T. Fujimoto, S. Nishimura, T. Okubo, H. Yamasaki, M. Osato, M. Matsuoka, A. Tsukamoto, and K. Takai. 1995. Lack of the expression of EBNA-2 and LMP-1 in T-cell neoplasms possessing Epstein-Barr virus. Blood 85:480-486.

Tanner, J.E. and J. Menezes. 1994. Interleukin-6 and Epstein-Barr virus induction by cyclosporine A: potential role in lymphoproliferative disease. Blood 84:3956-3964.

Tanner, J.E., M.X. Wei, C. Alfieri, A. Ahmad, P. Taylor, Ooka, and J. Menezes. 1997. Antibody and antibody-dependent cellular cytotoxicity responses against the BamHI A rightward open-reading frame-1 protein of Epstein-Barr virus (EBV) in EBV-associated disorders. Journal of Infectious Diseases 175:38-46.

Tao, Q., G. Srivastava, A.C. Chan, L.P. Chung, S.L. Loke, and F.C. Ho. 1995. Evidence for lytic infection by Epstein-Barr virus in mucosal lymphocytes instead of nasopharyngeal epithelial cells in normal individuals. J. Med. Virol. 45:71-77.

Thompson, J.D., D.G. Higgins, and T.J. Gibson. 1994. CLUSTAL W: improving the sensitivity of progressive multiple sequence alignment through sequence weighting, position-specific gap penalties and weight matrix choice. Nucleic Acids Res 22:4673-4680.

Thorley-Lawson, D.A., E.M. Miyashita, and G. Khan. 1996. Epstein-Barr virus and the B cell: that's all it takes. Trends Microbiol. 4:204-208.

Tokunaga, M., Y. Uemura, T. Tokudome, and E. Sato. 1993. Epstein-Barr virus-infected T cells in infectious mononucleosis [letter]. Acta Pathol Jpn 43:146-147.

Torii, T., K. Konishi, J. Sample, and K. Takada. 1998. The truncated form of the Epstein-Barr virus LMP-1 is dispensable or complimentable by the full-length form in virus infection and replication. Virology 251:273-278.

Tosato, G., K. Jones, M.K. Breinig, H.P. McWilliams, and J.L. McKnight. 1993. Interleukin-6 production in posttransplant lymphoproliferative disease. Journal of Clinical Investigation 91:2806-2814.

Towbin, H., T. Staehelin, and J. Gordon. 1979. Electrophoretic transfer of proteins from polyacrylamide gels to nitrocellulose sheets: procedure and some applications. Proc Natl Acad Sci U S A 76:4350-4354.

Uchida, J., T. Yasui, Y. Takaoka-Shichijo, M. Muraoka, W. Kulwichit, N. Raab-Traub, and H. Kikutani. 1999. Mimicry of CD40 signals by Epstein-Barr virus LMP1 in B lymphocyte responses. Science 286:300-303.

Veronesi, A., V. Coppola, M.L. Veronese, C. Menin, L. Bruni, E. D'Andrea, M. Mion, A. Amadori, and L. Chieco-Bianchi. 1994. Lymphoproliferative disease in human peripheral-blood- mononuclear-cell- injected scid mice. II. Role of host and donor factors in tumor generation. Int J Cancer 59:676-683.

Voevodin, A.F., B.A. Lapin, L.A. Yakovleva, T.I. Ponomaryeva, T.E. Oganyan, and E.N. Razmadze. 1985. Antibodies reacting with human T-lymphotropic retrovirus (HTLV-I) or related antigens in lymphomatous and healthy hamadryas baboons. Int J Cancer 36:579-584.

Vogelstein, B. and D. Gillespie. 1979. Preparative and analytical purification of DNA from agarose. Proc Natl Acad Sci U S A 76:615-619.

Wang, C.Y., M.W. Mayo, R.G. Korneluk, D.V. Goeddel, and A.S.J. Baldwin. 1998. NF-kappaB antiapoptosis: induction of TRAF1 and TRAF2 and c-IAP1 and c-IAP2 to suppress caspase-8 activation. Science 281:1680-1683.

Wang, D., D. Liebowitz, and E. Kieff. 1985. An EBV membrane protein expressed in immortalized lymphocytes transforms established rodent cells. Cell 43:831-840.

Wang, D., D. Liebowitz, and E. Kieff. 1988b. The truncated form of the Epstein-Barr virus latent-infection membrane protein expressed in virus replication does not transform rodent fibroblasts. J Virol 62:2337-2346.

Wang, D., D. Liebowitz, F. Wang, C. Gregory, A. Rickinson, R. Larson, T. Springer, and E. Kieff. 1988a. Epstein-Barr virus latent infection membrane protein alters the human B-lymphocyte phenotype: deletion of the amino terminus abolishes activity. J Virol 62:4173-4184.

Wang, F., C. Gregory, C. Sample, M. Rowe, D. Liebowitz, R. Murray, A. Rickinson, and E. Kieff. 1990b. Epstein-Barr virus latent membrane protein (LMP1) and nuclear proteins 2 and 3C are effectors of phenotypic changes in B lymphocytes: EBNA-2 and LMP1 cooperatively induce CD23. J Virol 64:2309-2318.

Wang, F., C.D. Gregory, M. Rowe, A.B. Rickinson, D. Wang, M. Birkenbach, H. Kikutani, T. Kishimoto, and E. Kieff. 1987a. Epstein-Barr virus nuclear antigen 2 specifically induces expression of the B-cell activation antigen CD23. Proc Natl Acad Sci U S A 84:3452-3456.

Wang, S., M. Rowe, and E. Lundgren. 1996. Expression of the Epstein Barr virus transforming protein LMP1 causes a rapid and transient stimulation of the Bcl-2 homologue Mcl-1 levels in B-cell lines. Cancer Res 56:4610-4613.

Wang, X. and L.M. Hutt-Fletcher. 1998. Epstein-Barr virus lacking glycoprotein gp42 can bind to B cells but is not able to infect. J Virol 72:158-163.

Ware, C.F., S. Santee, and A. Glass. 1998. Tumor Necrosis Factor-Related Ligands and Receptors. p. 549-592. The Cytokine Handbook. Academic Press Ltd

Watry, D., J.A. Hedrick, S. Siervo, G. Rhodes, J.J. Lamberti, J.D. Lambris, and C.D. Tsoukas. 1991. Infection of human thymocytes by Epstein-Barr virus. J Exp Med 173:971-980.

Weber, K. and M. Osborn. 1969. The reliability of molecular weight determinations by dodecyl sulfate-polyacrylamide gel electrophoresis. J Biol Chem 244:4406-4412.

Wedderburn, N., J.M. Edwards, C. Desgranges, C. Fontaine, B. Cohen, and G. de The. 1984. Infectious mononucleosis-like response in common marmosets infected with Epstein-Barr virus. J. Infect. Dis. 150:878-882.

Werner, J., G. Henle, C.A. Pinto, R.F. Haff, and W. Henle. 1972. Establishment of Continuous Lymphoblast Cultures from Leukocytes of Gibbons (Hylobates lar). Int J Cancer 10:557-567.

Whitney, R.A. 1995. Taxonomy. p. 33-47. In B.T. Bennett, C.R. Abee, and R. Henrickson (eds.) Nonhuman Primates in Biomedical Research. Academic Press, San Diego.

Wilson, J.B., W. Weinberg, R. Johnson, S. Yuspa, and A.J. Levine. 1990. Expression of the BNLF-1 oncogene of Epstein-Barr virus in the skin of transgenic mice induces hyperplasia and aberrant expression of keratin 6. Cell 61:1315-1327.

Wu, M.X., Z. Ao, K.V. Prasad, R. Wu, and S.F. Schlossman. 1998. IEX-1L, an apoptosis inhibitor involved in NF-kappaB-mediated cell survival. Science 281:998-1001.

Xu, J., A. Ahmad, M. D'Addario, L. Knafo, J.F. Jones, U. Prasad, R. Dolcetti, E. Vaccher, and J. Menezes. 2000. Analysis and significance of anti-latent membrane protein-1 antibodies in the sera of patients with EBV-associated diseases. J Immunol 164:2815-2822.

Yeh, W.C., A. Shahinian, D. Speiser, J. Kraunus, F. Billia, A. Wakeham, J.L. de la Pompa, D. Ferrick, B. Hum, N. Iscove, P. Ohashi, M. Rothe, D.V. Goeddel, and T.W. Mak. 1997. Early lethality, functional NF-kappaB activation, and increased sensitivity to TNF-induced cell death in TRAF2-deficient mice. Immunity 7:715-725.

Zandi, E., Y. Chen, and M. Karin. 1998. Direct phosphorylation of IkappaB by IKKalpha and IKKbeta: discrimination between free and NF-kappaB-bound substrate. Science 281:1360-1363.

Zimber-Strobl, U., B. Kempkes, G. Marschall, R. Zeidler, Van, C. Kooten, J. Banchereau, G.W. Bornkamm, and W. Hammerschmidt. 1996. Epstein-Barr virus latent membrane protein (LMP1) is not sufficient to maintain proliferation of B cells but both it and activated CD40 can prolong their survival. EMBO Journal 15:7070-7078.

APPENDIX I. Localization of sequencing primers for Cyno-EBV LMP1.

Cyno-EBV LMP1 gene sequence depicting the clones #6, 8 and 28 and their respective sequencing primers (see Table 5). The length of each clone is indicated above the sequence within the brackets |— clone # → and ← clone# —|. Sequencing primers are boxed and orientation is shown by an arrow. The sart and termination codons are underlined and shown in blue. Introns are shown in green and the 7 tandem repeats in red.

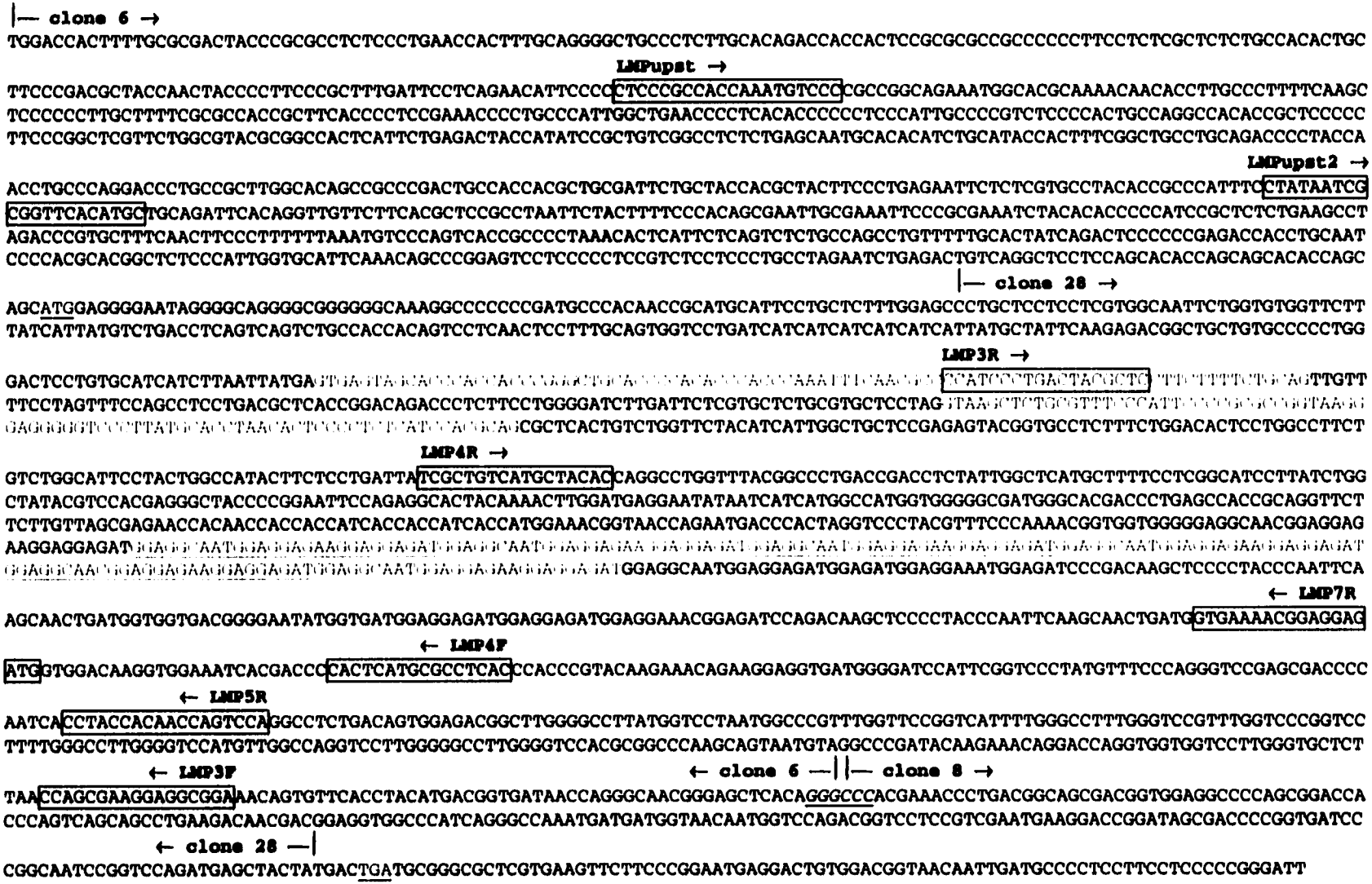
|— clone 6 →
LMPupst →
LMPupst2 →
|— clone 28 →
LMP3R →
LMP4R →
← LMP7R
← LMP4F
← LMP5R
← LMP3F
← clone 6 —|
|— clone 8 →
← clone 28 —|

APPENDIX II. Kyte and Doolittle hydropathy plot of the predicted Cyno-EBV LMP1.

A Kyte and Doolittle (1982) hydropathy plot of the predicted a.a. sequence of Cyno-EBV LMP1 is shown (ProtScale, http://expasy.cbr.nrc.ca/). The six transmembrane domains are clearly delineated and constitute the most hydrophobic regions of the protein. Interestingly, the most hydrophilic region appears to correspond to the HIS cluster (a.a. 229-236). Location of the 9 a.a.-repeat region and the 6 TRAF motifs are indicated by the arrows.

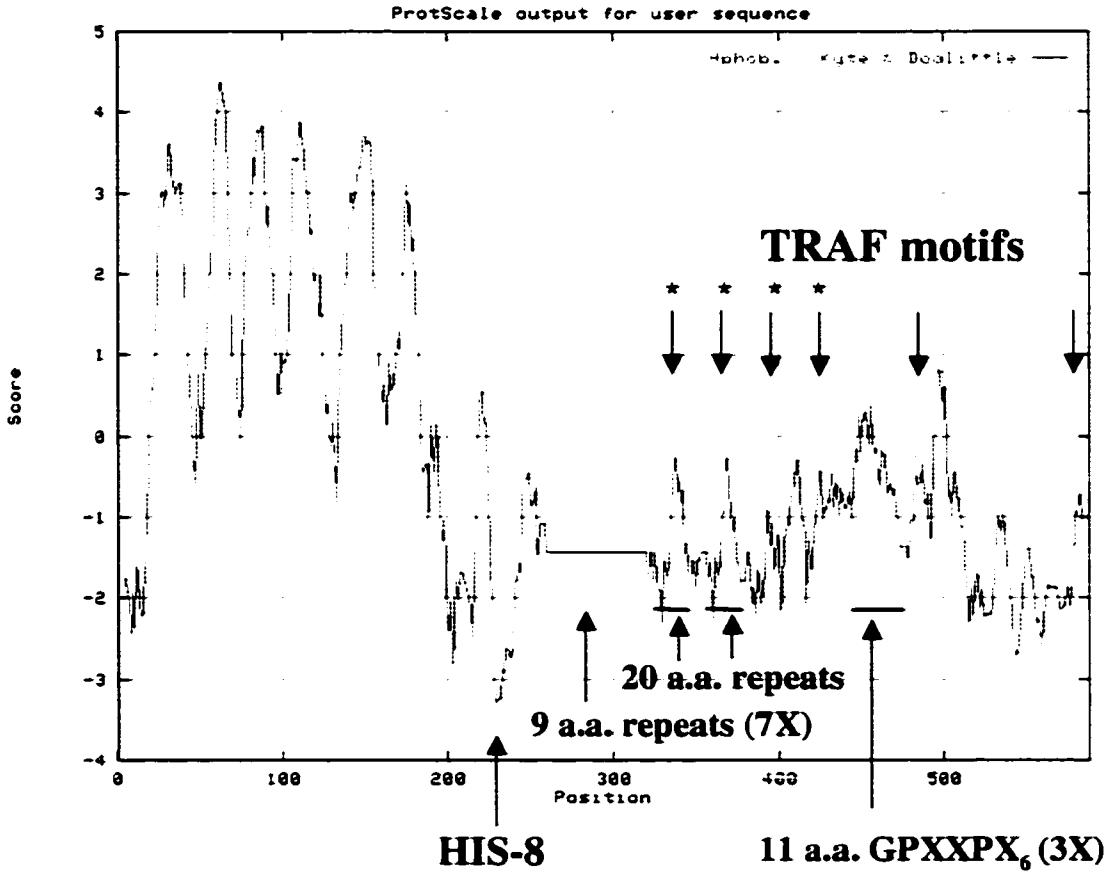
ProtScale output for user sequence
Score
Position
TRAF motifs
20 a.a. repeats
9 a.a. repeats (7X)
HIS-8
11 a.a. GPXXPX6 (3X)

APPENDIX III. Predicted amino acid sequence of Cyno-EBV LMP1 and multialignment with human and Rhesus-EBV LMP1s.

The predicted Cyno-EBV LMP1 amino acid sequence was aligned with LMP1 sequences from human EBV LMP1s (B95-8, CAO, C15) and the Rhesus-EBV LMP1s using the ClustalW program at http://workbench.sdsc.edu (Higgins et al. 1992; Thompson et al. 1994). The weigth matrix used was the gonnet series with a gap open penalty of 10 and a gap extension penalty of 0.2. Completely conserved residues are shown in magenta, identical residues, in yellow, similar residues, in grey and different residues in white. Conserved residues were observed in 5 regions : the transmembrane domains, the HIS cluster, the PXQXT, the GPXXP motifs, and the distal C-terminus region (CTAR2) .

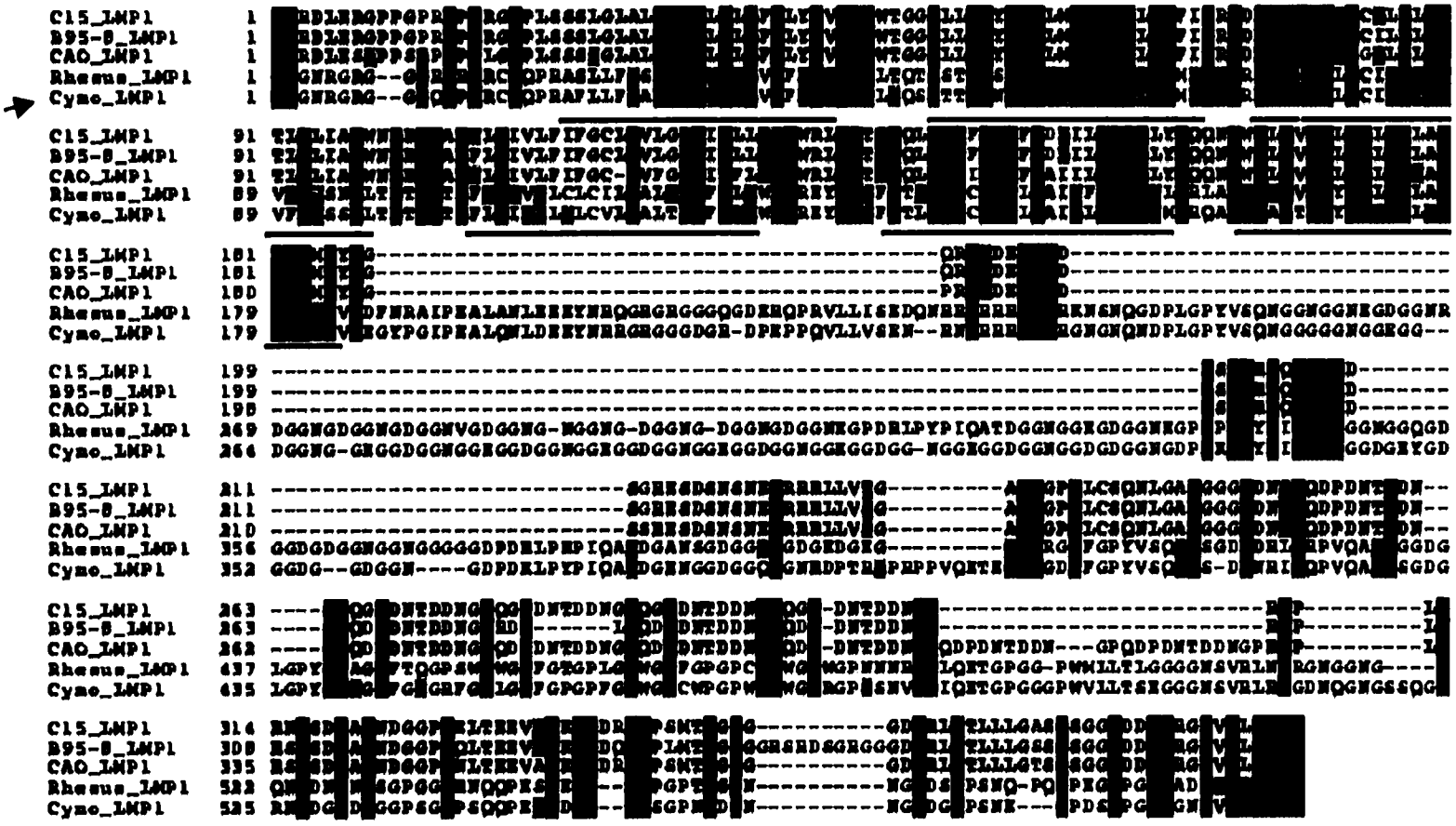
C15_LMP1
B95-8_LMP1
CAO_LMP1
Rhesus_LMP1
Cyno_LMP1

APPENDIX IV. Predicted amino acid sequence of Cyno-EBV LMP1 and multialignment with human EBV and other EBV-like monkey viruses.

The predicted Cyno-EBV LMP1 amino acid sequence was aligned with LMP1 sequences from human EBV LMP1s (B95-8, CAO, C15) and other EBV-like monkey virus LMP1s (H. papio, partial sequence and Rhesus-EBV) using the ClustalW program at http://workbench.sdsc.edu (Higgins et al. 1992; Thompson et al. 1994). The weigth matrix used was the gonnet series with a gap open penalty of 10 and a gap extension penalty of 0.2. Completely conserved residues are shown in magenta, identical residues, in yellow, similar residues, in grey and different residues in white. When all five proteins were aligned only 2 regions of conserved residues were observed; the transmembrane domains and the distal C-terminus.

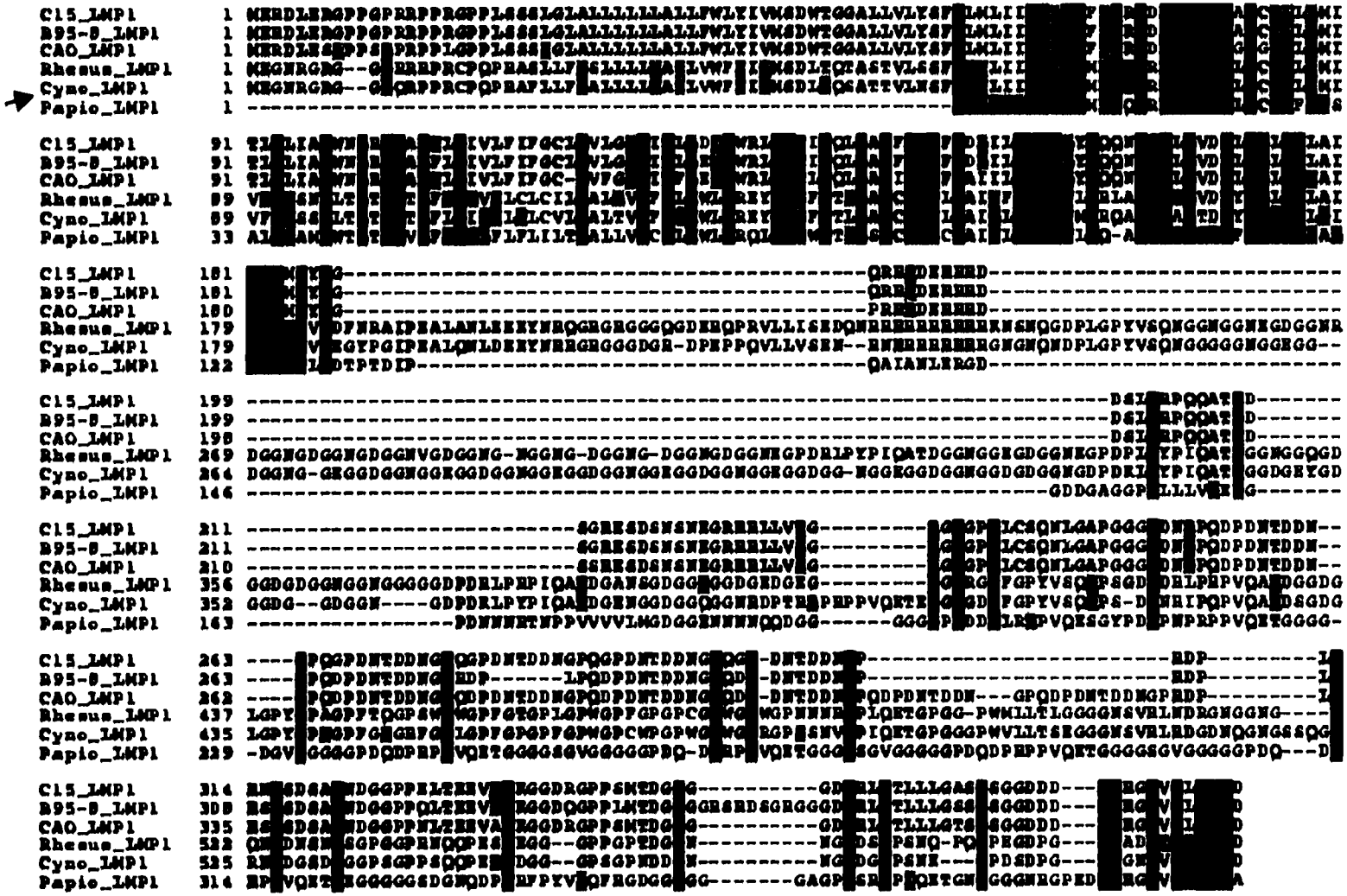
C15_LMP1
B95-8_LMP1
CAO_LMP1
Rhesus_LMP1
Cyno_LMP1
Papio_LMP1

APPENDIX V. TRAF binding motifs and their flanking sequences.

Comparison of TRAF binding motifs of Cyno-EBV LMP1 to other LMP1 and CD30 TRAF motifs. Residues flanking the core motif PXQXT have been shown to play a role in defining binding of TRAF core motif to TRAF3 (Franken et al. 1996). From these sequence comparisons, 4 of the 6 motifs expressed in Cyno-EBV LMP1 are predicted to share TRAF3 binding properties. These 4 TRAF binding motifs are located at a.a. 338, 369, 396 and 425. The other two TRAF motifs (a.a. 485 and 581) corresponded to the two most C-term. motifs.

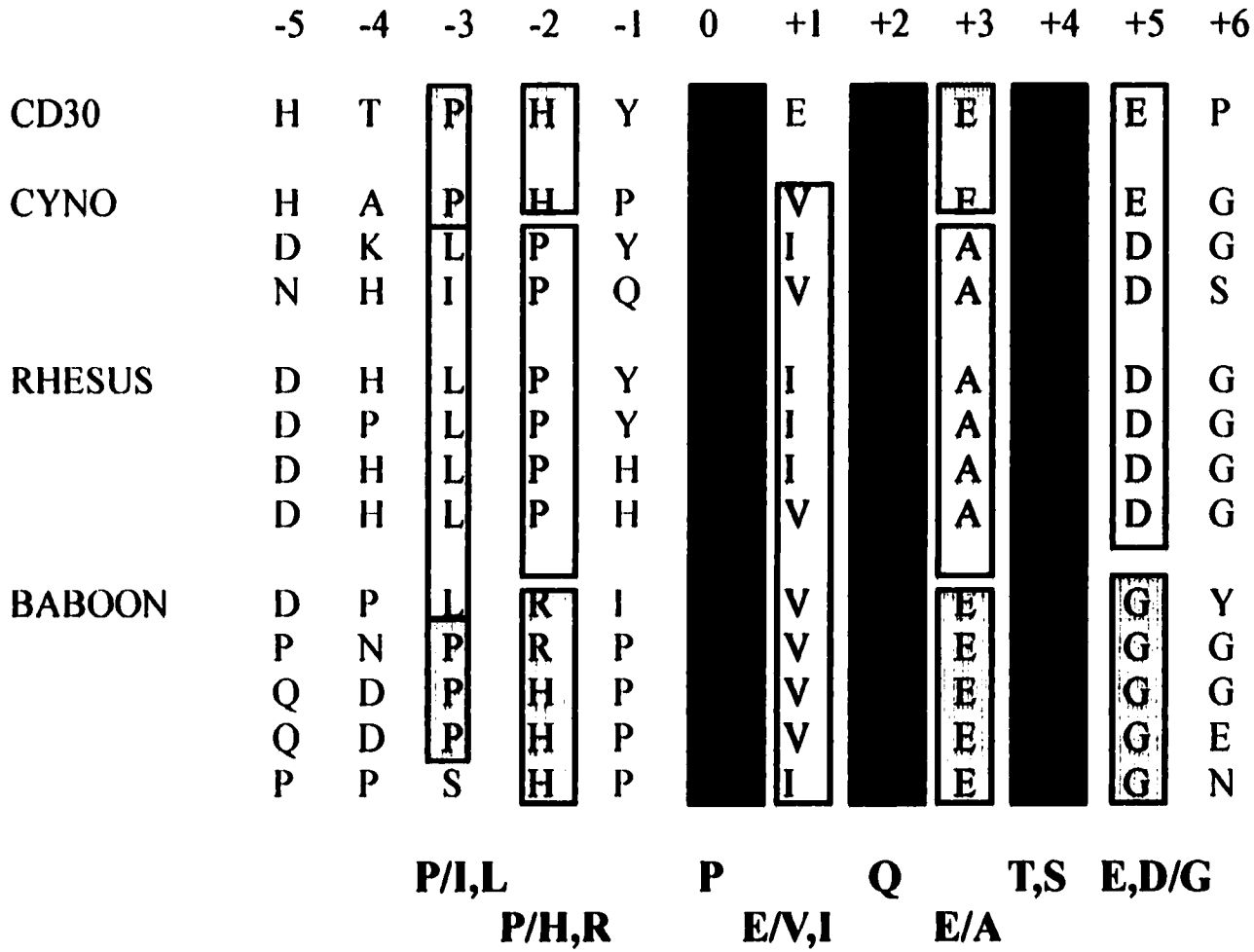
-5 -4 -3 -2 -1 0 +1 +2 +3 +4 +5 +6
CD30 H T P H Y E E E P
CYNO H A P H P V E E G
D K L P Y I A D G
N H I P Q V A D S
RHESUS D H L P Y I A D G
D P L P Y I A D G
D H L P H I A D G
D H L P H V A D G
BABOON D P L R I V E G Y
P N P R P V E G G
Q D P H P V E G G
Q D P H P V E G E
P P S H P I E G N
P/I,L
P/H,R
P
E/V,I
Q
E/A
T,S
E,D/G

APPENDIX VI. Conservation of the sequence $GPXXPX_6$ in human, rhesus and cynomolgus monkey LMP1s.

Both human and macaque LMP1 proteins express series of the proline-rich sequence $GPXXPX_6$ in their carboxy tail (where X represents any amino acid) (shown in green). Cyno-EBV harbors a series of 3 $GPXXPX_6$ located downstream from the repeat regions and two individual sequences $GPXXPX_6GPXXP$ closer to the carboxy terminus. Rhesus-EBV LMP1 shares the same series of 3 $GPXXPX_6$ as well as the two individual sequences. In Cyno-EBV and Rhesus-EBV LMP1s, the patterns were not found within a region of repeats whereas EBV LMP1s contain various numbers of these sequences as part of the 11 a.a.-repeat region PQDPDNTDDNG. The B95-8 LMP1 expresses a series of 4 $GPXXPX_6$ interrupted by a 5 a.a. insertion. The CAO and C15 LMP1s contain uninterrupted series of 7 and 4 $GPXXPX_6$ respectively. The JAK3 binding motifs, PXXPXP, located near or within these series of proline rich sequences are indicated in bold characters. Notice, the presence of one additional potential JAK binding motif in the amino terminal regions of Cyno-EBV and Rhesus-EBV LMP1.

>Cyno_LMP1

MEGNRGRGGGQRP**PRCPQP**HAFLLFGALLLLVAILVWFFIIMSDLSQSATTVLNSFAVVLIIIIIIIMLF
KRRLLCPLGLLCIILIMIVFLVSSLLTLTGQTLFLGILILVLCVLLALTVWFYIMWLLREYGASFWTLLA
FCLAFLLAILLLIIAVMLHQAWFTALTDLYWLMLFLGILIWLYVHEGYPGIPEALQNLDEEYNHHGHGGG
DGHDPEPPQVLLVSENHNHHHHHHHHGNGNQNDPLGPYVSQNGGGGGNGGEGGDGGNGGEGGDGGNGGEG
GDGGNGGEGGDGGNGGEGGDGGNGGEGGDGGNGGEGGDGGNGGDGDGGNGDPDKLPYPIQATDGGDGEYG
DGGDGGDGGNGDPDKLPYPIQATDGENGGDGGQGGNHDPTHAPHPPVQETEGGDGDPFGPYVSQGPSDPN
HIPQPVQASDSGDGLGPY**PFGPGP****PCWPGP**RGPSSNVGPIQE
TGPGGGPWVLLTSEGGGNSVHLHDGDNQGNGSSQ PSQQPEDNDGG
PSNEGPDSDPGDPGNPVQMSYYD

>Rhesus_LMP1

MEGNRGRGGGHRH**PRCPQP**HASLLFGSLLLLVAILVWFFIIMSDLTQTASTVLSSFAVVLIIIIIIIMLF
KRRLLCPLGLLCIILIMIVILVSNLLTLTGQTLFVGLVILCLCILLALAVWFYLMWLLREYGASFWTILA
FCLAFLLAIVFLIIAVLLHLAWFTVLVDLYWLLLFLAILIWIYVHDFNRAIPEALANLEEEYNHQGHGHG
GGQGDEHQPRVLLISEDQNHHHHHHHHHHKNSNQGDPLGPYVSQNGGNGGNEGDGGNRDGGNGDGGNGDG
GNVGDGGNGNGGNGDGGNGDGGNGDGGNEGPDHLPYPIQATDGGNGGEGDGGNEGPDPLPYPIQATDGGN
GGQGDGGDGDGGNGGNGGGGGDPDHLPHPIQATDGANSGDGGDGGDGEDGEGGGDRGPFGPYVSQGPSGD
PDHLPHPVQASDGGDGL **PFGPGP** WGPWGPNNNHGPLQE
TGPGGPWMLLTLGGGGNSVHLNDRGNGGN HNQQPESNEGG
PSNQPQGPEGDPGDPADPIQISYYD

>B95-8_LMP1

MEHDLERGPPGPRRPPRGPPLSSSLGLALLLLLLALLFWLYIVMSDWTGGALLVLYSFALMLIIIILIIF
IFRRDLLCPLGALCILLLMITLLLIALWNLHGQALFLGIVLFIFGCLLVLGIWIYLLEMLWRLGATIWQL
LAFFLAFFLDLILLIIALYLQQNWWTLLVDLLWLLLFLAILIWMYYHGQRHSDEHHHDDSLPHPQQATDD
SGHESDSNSNEGRHHLLVSGAGDGPPLCSQNLGAPGGGPDN **PHDPLP**
QDP **PHDPLP**HSPSDSAGNDGGPPQLTEEVENKGGDQGPPLMTDGGGGHSHDS
GHGGGDPHLPTLLLGSSGSGGDDDDPHGPVQLSYYD

>CAO_LMP1

MERDLESAPPSAPRPPLGPPLSSSIGLALLLLLLALLFWLYIVMSDWTGGALLVLYSFALMLIIIILIIF
IFRRDLLCPLGGLGLLLLMITLLLIALWNLHGQALYLGIVLFIFGCLVFGIWIYFLEILWRLGATLWQLL
AFILAFFLAIILLIIALYLQQNWWTLLVDLLWLLLFMAILIWMYYHGPRHTDEHHHDDSLPHPQQATDDS
SHESDSNSNEGRHHLLVSGAGDGPPLCSQNLGAPGGGPDN
PHDPLPHSPSDSAGNDGGPPN
LTEEVANKGGDRGPPSMTDGGGGDPHLPTLLLGTSGSGGDDDDPHGPVQLSYYD

>C15_LMP1

MEHDLERGPPGPRRPPRGPPLSSSLGLALLLLLLALLFWLYIVMSDWTGGALLVLYSFALMLIIIILIIF
IFRRDLLCPLGALCLLLLMITLLLIALWNLHGQALYLGIVLFIFGCLLVLGLWIYLLDILWRLGATIWQL
LAFFLAFFLDLILLIIALYLQQNWWTLLVDLLWLLLFLAILIWMYYHGQRHSDEHHHDDSLPHPQQATDD
SGHESDSNSNEGRHHLLVTGAGDGPPLCSQNLGAPGGGPDNAPQDPDNTDDN
PHDPLPHNPSDSAGNDGGPPELTEEVENKGGDRGPPSMTDGGG
GDPHLPTLLLGASGSGGDDDDPHGPVQLSYYD

APPENDIX VII. Multialignment of N-term. domains of LMP1 of Cyno-EBV, Rhesus-EBV, EBV and MyoD.

The predicted primary sequence of the N-term. domains of LMP1 of Cyno-EBV, Rhesus-EBV, EBV (CAO, C15, B95-8) and MyoD, a transcriptional activator, target of ubiquitin conjugation at the N-term., were aligned using the ClustalW program at http://workbench.sdsc.edu (Higgins et al. 1992; Thompson et al. 1994). The weigth matrix used was the gonnet series with a gap open penalty of 10 and a gap extension penalty of 0.2. Completely conserved residues are shown in magenta, identical residues, in yellow, similar residues, in grey and different residues in white. Conserved residues were observed in all proteins at position 2 (glutamic acid) and position 16 (14 in the monkey LMP1). Proline doublets (shown in circles) were also present in all proteins except for the Rhesus-EBV LMP1.

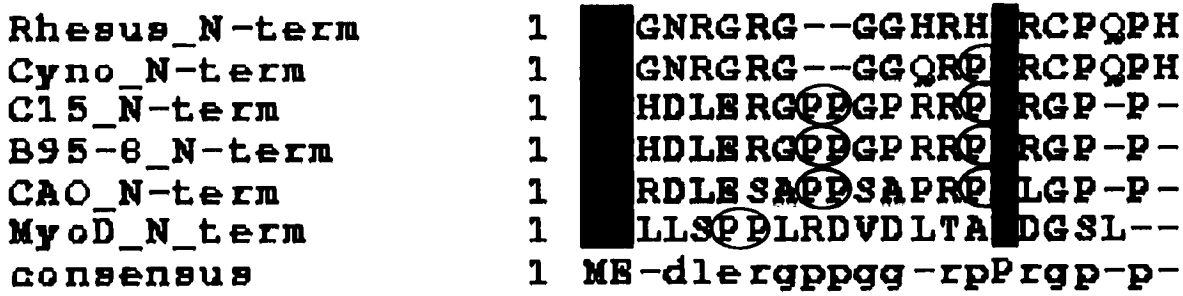
Rhesus_N-term 1 GNRGRG--GGHRH RCPQPH
Cyno_N-term 1 GNRGRG--GGQRP RCPQPH
C15_N-term 1 HDLERGPPGPRRP RGP-P-
B95-8_N-term 1 HDLERGPPGPRRP RGP-P-
CAO_N-term 1 RDLESAPPSAPRP LGP-P-
MyoD_N_term 1 LLSPPLRDVDLTA DGSL--
consensus 1 ME-dlergppgg-rpPrgp-p-